

University of New Mexico

UNM Digital Repository

Civil Engineering ETDs

Engineering ETDs

Fall 11-24-2020

Chemical interfacial reactions affecting the speciation and solubility of uranium in organic-rich environments

Carmen A. Velasco

Follow this and additional works at: https://digitalrepository.unm.edu/ce_etds



Part of the [Environmental Engineering Commons](#)

Recommended Citation

Velasco, Carmen A.. "Chemical interfacial reactions affecting the speciation and solubility of uranium in organic-rich environments." (2020). https://digitalrepository.unm.edu/ce_etds/253

This Dissertation is brought to you for free and open access by the Engineering ETDs at UNM Digital Repository. It has been accepted for inclusion in Civil Engineering ETDs by an authorized administrator of UNM Digital Repository. For more information, please contact disc@unm.edu.

Carmen A. Velasco Rivera

Candidate

Civil, Construction and Environmental Engineering

Department

This dissertation is approved, and it is acceptable in quality and form for publication:

Approved by the Dissertation Committee:

José M. Cerrato, Chairperson

Abdul-Mehdi S. Ali

Adrian J. Brearley

Stephen E. Cabaniss

Bruce M. Thomson

.....

**CHEMICAL INTERFACIAL REACTIONS AFFECTING THE
SPECIATION AND SOLUBILITY OF URANIUM
IN ORGANIC-RICH ENVIRONMENTS**

by

CARMEN A. VELASCO

B. S., Chemical Engineering, Universidad San Francisco de Quito,
2005

M.S., Chemical Engineering, Oregon State University, 2007

DISSERTATION

Submitted in Partial Fulfillment of the
Requirements for the Degree of

**Doctor of Philosophy
Engineering**

The University of New Mexico
Albuquerque, New Mexico

December, 2020

Acknowledgements

I am grateful to my mentor and friend, Professor Jose M. Cerrato, for trusting me with the great opportunity of doing research under his supervision and for his guidance, support, patience, and encouragement.

I am also thankful to my committee members, Dr. Mehdi Ali, Dr. Adrian Brearley, Dr. Stephen Cabaniss, and Dr. Bruce Thomson for their valuable recommendations, encouragement, and data analysis that are a basic component of my dissertation.

Special thanks to Dr. Christopher L. Osburn and Dr. Kateryna Artyushkova for their incredible knowledge, expertise, and assistance, which was the groundwork of this research. I want to sincerely acknowledge Dr. Jorge González, Dr. Juan Lezama-Pacheco, Dr. Omar Holguin, Dr. Jacqueline Jarvis, and Dr. Malak Tfaily for their input and guidance on my research, manuscript writing, and data interpretation.

I want to extend my gratitude to the E-H₂O Research family for their support and feedback throughout all stages of my Ph.D. career. I appreciate the input and help provided by my fellow students in the E-H₂O research group, with experimental designs, presentations, and manuscripts.

Finally, I wish to acknowledge the support and inspiration of family and friends. There are too many to mention individually. Special thanks to Isabel and Amelie for their love and understanding. I dedicate this dissertation and years of hard work to my brave mother, Zoila, who always believed in me. Even though we have been far away physically, I was always blessed with her wisdom and love. Her sacrifice and support are the reasons I made it. I could not have done this without you, Mami!

**CHEMICAL INTERACTIONS AFFECTING THE SPECIATION AND
PRECIPITATION OF URANIUM
IN ORGANIC-RICH MINERALIZED DEPOSITS**

by

Carmen A. Velasco

B. S. in Chemical Engineering, 2005

M.S. in Chemical Engineering, 2007

Ph.D. in Engineering, 2020

Abstract

The aim of this dissertation was to investigate the interfacial reactions between uranium (U) and natural organic matter (NOM) affecting the solubility, adsorption, and precipitation of U in organic-rich environments. The chemical interactions between U and NOM are not well understood, which justified the following research objectives: 1) Identify the effect of pH on U speciation and the organic functional chemistry in mineralized deposits from the Jackpile Mine.; 2) Identify the precipitation of U(VI) and NOM as a function of pH (2, 4 and 7); 3) Identify changes in DOM chemistry due to the reaction of NOM and U at acidic and neutral pH. Field and laboratory approaches used in this work contribute novel information about U speciation and reactivity in organic-rich environments. Fundamental knowledge from this work will be useful to identify future strategies towards remediation for contaminated sites.

TABLE OF CONTENTS

Acknowledgements	iii
Abstract.....	iv
TABLE OF CONTENTS	v
List of Figures.....	ix
Chapter 1: Introduction	1
Chapter 2: Literature Review.....	3
2.1 Uranium Mining in the US and legacy.....	3
2.2 Natural Organic Matter.	3
2.3 Gaps and Limitations in Existing Literature.	5
2.4. Research Objectives.....	7
2.5 References	9
Chapter 3. Organic Functional Group Chemistry in Mineralized Deposits	
Containing U(IV) and U(VI) from the Jackpile Mine in New Mexico.....	18
Abstract.....	19
3.1 Introduction.....	20
3.2 Materials and Methods.....	22
3.2.1 Sample Collection.....	22
3.2.2 Solid Analyses.	22
3.2.3 Acid Digestion and Dolution Metal Analyses.	23

3.2.4 Thermal Analyses for Solids.....	23
3.2.5 Extraction of Natural Organic Matter.....	23
3.2.6 Excitation Emission Matrix Spectroscopy (EEMS) Analyses.....	24
3.2.7 Effect of pH on Organic Functional Chemistry and U Species.....	25
3.3 Results and Discussion.....	26
3.3.1 Uranium in Unreacted Mineralized Deposit Solid Samples from the Jackpile Mine.....	26
3.3.2 Natural Organic Matter in Mineralized Deposits from the Jackpile Mine.....	27
3.3.3 Effect of pH on Organic Functional Group Chemistry.....	29
3.3.4 Effect of pH on U Species.....	30
3.4 Environmental Implications	32
3.5 Acknowledgments	33
3.6 References.....	39
Chapter 4. From Adsorption to Precipitation of U(VI) in the Presence of Natural Organic Matter	48
Abstract.....	49
4.1 Introduction.....	49
4.2 Materials and Methods.....	52
4.2.1 Chemicals.....	52
4.2.2 Batch Experiments.....	52
4.2.3 Aqueous Analyses.....	53
4.2.4 Solid Analyses.....	54

4.3 Results and Discussion.....	56
4.3.1 Effect of NOM on U Solubility.	56
4.3.2 Solid Analyses: From Adsorption to Precipitation.	60
4.4 Mechanistic Insights	66
4.5 Environmental Implications	68
4.6 Acknowledgments	68
4.7 References.....	74
Chapter 5. Changes in dissolved natural organic matter chemistry resulting from reaction with U(VI).....	87
Abstract.....	88
5.1 Introduction.....	88
5.2 Materials and Methods.....	90
5.2.1 Chemicals.....	90
5.2.2 Batch Experiments.	91
5.2.3 Microscopy and spectroscopy analyses.	92
5.2.4 DOM analyses.....	93
5.2.5 Aqueous Inorganic Analyses.	95
5.3. Results and Discussion.....	95
5.3.1 Uranium and NOM Chemistry on Unreacted and Reacted Solids.	95
5.3.2 Effect of U and pH on DOM Chemistry.....	97
5.4 Considerations about U-NOM Reactions.	101
5.5. Environmental Implications.	102

5.6. Acknowledgments.....	103
5.7. References.....	109
Chapter 6. Conclusions and Implications.....	117
6.1 Overall Conclusions.....	117
6.2 Environmental Implications and Future Research.	118
Appendix A	
Supplementary Information from Chapter 3: Organic Functional Group	
Chemistry in Mineralized Deposits Containing U(IV) and U(VI) from the	
Jackpile Mine in New Mexico	
	120
Appendix B	
Supplementary Information from Chapter 4: From Adsorption to Precipitation	
of U(VI) in the Presence of Natural Organic Matter	
	134
Figure S5.....	144
Figure S7.....	146
References.....	147
Appendix C	
Supplementary Information from Chapter 5: Changes on dissolved natural	
organic matter resulting from the reaction with U(VI) at acidic and neutral pH	
.....	
	148

List of Figures

Chapter 2

Figure 1. Research Summary - Schematic of interfacial reactions between U and NOM at environmentally relevant pH.....8

Chapter 3

Figure 1. Fitting of high resolution XPS Carbon (C 1s) and Uranium (U 4f) spectra of A) unreacted Jackpile Mine solids. Fitting of high resolution XPS Carbon (C 1s) and Uranium (U 4f) spectra of supernatant from batch extraction reactors at: B) pH 13; C) pH 7; and D) pH 2; and E) Percent composition of C 1s and U 4f spectra. 35

Figure 2. X-ray Absorption Spectroscopy (XAS) of unreacted and reacted solids (after LOI, pH 2 and pH 13) from the Jackpile Mine (JP₂). A) U-L_{III} edge EXAFS of the Jackpile Mine solid samples using the following references: uraninite, coffinite, and monomeric U(IV) for U(IV) and uranyl-adsorbed ferrihydrite as reference for U(VI).; B) Normalized bulk U-L_{III} edge XANES spectra using uraninite (nano-UO₂) as reference for U(IV) and U(VI) adsorbed ferrihydrite as reference for U(VI).; and C) Linear combination fitting of the U-L_{III} edge EXAFS spectra of U(VI) and U(IV) species in the Jackpile Mine solid samples..... 36

Figure 3. Thermal Analyses (Thermogravimetric Analysis, TGA, and Loss on Ignition, LOI) to estimate organic matter content in solid samples from the Jackpile Mine mineralized deposits: A) Change in mass content as a function of temperature (TGA) for unreacted solid samples JP₁ and JP₂.; and B) Mass loss comparison between TGA and LOI..... 37

Figure 4. Excitation-emission matrix spectroscopy (EEMS) from supernatant of batch extraction reactors at pH 7 and pH 2 from the Jackpile Mine samples: A) JP₁; and B) JP₂. Note QSE scaling differences on the color bar for each EEM. 38

Chapter 4

Figure 1. Soluble U concentration in batch experiments containing NOM, U in 4% HNO₃ and KCl (purple) and U control experiment containing U in 4% HNO₃ (yellow) at (A) 0.5 h, (B) 24 h, and (C) Soluble U concentration summary results. Initial concentrations used are 200 mgL⁻¹ NOM and 100 μM-UO₂(NO₃)₂ in 0.01 M KCl..... 70

Figure 2 X-ray absorption fine structure spectroscopy (XAFS) of solids collected from U-KCl-NOM and U-NOM batch experiments at pH 4 after 24 h reaction. (A) U L_{III}-edge EXAFS, (B) EXAFS Fourier transform and shell by shell fits indicate the presence of U likely bound to organic functional groups from POM through adsorption and U-U due to presence of crystalline solid phases only in sample from U-KCl-NOM experiment. (C) Results table for shell by shell fits of the EXAFS signal. 71

Figure 3 Bright-field TEM (TEM) and dark-field scanning transmission electron microscope (STEM) images, energy dispersive X-ray spectroscopy (EDS) spectra, and selected area electron diffraction (SAED) patterns for solids collected from batch reactions of U-KCl-NOM after 24 at pH 2 (A, B, C) and pH 4 (D, E, F, G, H, I). TEM image and SAED pattern (A, C) show the adsorption of U onto amorphous POM at pH 2, indicated by the presence of a distinct U X-ray peaks in the EDS

spectrum (B). EDS indicates low concentrations of U adsorbed onto POM (E), SAED shows diffuse diffraction rings characteristic of an amorphous phase (F) at pH 4 that contains lower concentrations of U than at pH 2. Crystallites of U- and K-bearing solids with minor Na were identified at pH 4 (G, H) and slightly tilted SAED pattern is consistent with the [010] zone axis of grimselite (I). 72

Figure 4 Electron energy loss spectra (EELS) (A), dark-field scanning transmission electron microscope (DF-STEM) image (B) and energy dispersive spectroscopy (STEM-EDS) X-ray spectra (C, D). Two EEL spectra for grimselite are shown in red and green showing the presence of the K L₃ and L₂ edges at 294 and 296 eV, respectively. A distinct shoulder is present on the lower energy side of the K edge at 289 eV, which could be attributable to either carbonate or carboxylic groups. The lower spectrum (brown) is from the amorphous holey carbon film support with a distinct 284 eV edge that can be assigned to the C π* peak. This feature is also apparent in the grimselite spectra because the crystallites occur directly on the holey carbon film support. The 289 eV feature is not present in the amorphous carbon substrate. Right hand images show a Dark-Field STEM image of the crystallites and X-ray maps of U and C, demonstrating that the crystallites contain C associated with U. An X-ray signal from the amorphous holey carbon film is clearly apparent in the lower right and upper left of the carbon X-ray map. 73

Chapter 5

Figure 1 X-ray absorption fine structure spectroscopy (XAFS) of solids collected from U-NOM experiments conducted for 24 h reaction. U L_{III}-edge EXAFS of sample at A) pH 2 and B) pH 4. C) Results table for shell by shell fits of the EXAFS signal. ... 104

Figure 2. A) Dissolved organic matter (DOM) and B) soluble U concentration after 24 h reaction of NOM and U in 4% NO₃ (purple), control experiments containing only NOM (brown) and only U in 4% NO₃ (yellow). 105

Figure 3. Fitting of high resolution XPS Carbon (C1s) of NOM control reactors and U+NOM as a function of pH of supernatant samples after 24 h reaction A) pH 2, B) pH 4, C) pH 7 and D) percent composition of C 1s..... 106

Figure 4. Recovery from solid phase extraction (SPE) using a styrene-divinylbenzene copolymer (PPL, Varian Bond Elut) PPL of batch experiments containing NOM and U in 4% NO₃ (purple) and Control NOM (brown) conducted at pH 2, pH 4 and pH 7: A) Dissolved organic carbon (DOC) and B) soluble uranium (U) concentration, and C) Summary of percent DOC and U recovery from SPE. Initial concentration of DOC 87 mgL⁻¹ and 100 μM U..... 107

Chapter 1: Introduction

The legacy of mining activities has resulted in numerous sites with elevated metal concentrations in water and soil.^{1,2} The western part of the United States has a legacy of over 160,000 abandoned mines and represents a particular extensive area of exposure to mine wastes.³ Uranium (U), and other metals concentrations in drinking water sources exceed United States Environmental Protection Agency (EPA) and World Health Organization (WHO) standards in the U.S.⁴⁻⁷ The problem is particularly important in regions where U mining has occurred. Several Native American tribes or pueblos in the southwestern US have had large U mines located on their lands. Studies have reported U concentrations of 35.3-772 $\mu\text{g L}^{-1}$ in surface waters near the Pueblo of Laguna, New Mexico (NM), neighboring the Jackpile Mine.¹ Metal concentrations that may impact human health for Native American people were also found to be correlated to mine source distance.⁴

The goal of this dissertation was to understand the chemical interfacial reactions between U and natural organic matter (NOM) affecting the solubility of U and changes in the molecular composition of NOM at environmentally relevant pH. This dissertation has been divided into 5 chapters and 3 appendixes. Chapter 2 is a literature review on the topics covered by this dissertation, including a background on uranium occurrence, chemistry, and mining, and natural organic matter (NOM) chemistry, the occurrence of U and NOM in the environment, and their interactions with each other, ending with a review of knowledge gaps. Chapters 3, 4, and 5 are the main body of work of the dissertation, formatted as research articles.

Chapter 3 has been published in *Environmental Science and Technology*: (<https://doi.org/10.1021/acs.est.9b00407>) and relates to the investigation of the functional group chemistry of natural organic matter (NOM) associated with both U(IV) and U(VI) in solids from mineralized deposits exposed to oxidizing conditions from the Jackpile Mine, Laguna Pueblo, NM using spectroscopic and aqueous chemistry techniques. Chapter 3 includes a discussion of the spectroscopy and aqueous chemistry results and provides potential mechanistic explanations of the interactions between U and NOM in samples from the Jackpile Mine.

Chapter 4 of this study focuses on the adsorption and precipitation of U due to the reaction with NOM at pH 2, pH 4, and pH 7. This chapter includes a discussion of the results from aqueous analyses, microscopy, and spectroscopy measurements on the solids collected at pH 2, pH 4, and pH 7. A discussion of the findings include: i) precipitation of U- and K-bearing crystalline solids detected at pH 4, ii) adsorption of U onto POM identified in the bulk at pH 2 and pH 4, and iii) the precipitation of inorganic, U-bearing solids at pH 7 detected in the absence of NOM.

Chapter 5 builds on our understanding of the adsorption and precipitation of U in the presence of NOM and focusses on identifying changes in dissolved organic matter (DOM) functional group chemistry resulting from the reaction with U(VI) at acidic and neutral pH in batch experiments. Spectroscopy and ultrahigh-resolution mass spectrometry were used to identify changes in the molecular composition of DOM resulting from the reaction with U. This chapter provides insights into the possible molecular changes in the organic functional chemistry due to reactions between U and NOM at pH conditions relevant to acid mine drainage and surface waters neighboring organic-rich environments. The manuscripts resulting from chapter 4 and chapter 5 are being prepared for submittal for publication. Appendices A, B and C contain supplementary information for chapters 3, 4, and 5, respectively.

Chapter 2: Literature Review

2.1 Uranium Mining in the US and legacy.

The legacy of operations for uranium (U) mining in the USA is distributed across several states, and many of these sites were located close to Native American communities. Studies have reported U concentrations of 35.3-772 $\mu\text{g L}^{-1}$ in surface waters near the Pueblo of Laguna, New Mexico (NM) neighboring the Jackpile Mine, one the largest uranium mines in the US.² These concentrations exceed the US Environmental Protection Agency maximum contaminant level of 30 $\mu\text{g L}^{-1}$.⁵ Additionally, the U concentration detected in solid samples from the Jackpile Mine, adjacent to the Rio Paguete, was 9300 mg kg^{-1} .² The Jackpile Mine has been listed in the EPA National Priorities List for the Comprehensive Environmental Response, Compensation, and Liability Act (CERCLA) cleanup.⁶ Uranium (U) is regulated because it can cause cancer, kidney toxicity, miscarriages, birth defects and heart diseases.^{3, 8, 9} Recent evidence suggests that residential proximity to abandoned mine-sites results in increased serum cumulative inflammatory potential, independent of metals-intake via drinking water. A study in the Grants Mining District located in western NM reports that U-bearing dust affects the extent of U dissolution in simulated lung fluids, which could have potential health implications.¹⁰

2.2 Natural Organic Matter.

Natural organic matter (NOM) is a complex combination of heterogeneous organic molecules, resulting from the decomposition of animal and plant matter.⁸ NOM consist of and extraordinarily complex mixture of compounds including carbohydrates, amino acids, and protein.⁹ Because of the molecular heterogeneity and complexity of NOM, it is often is characterized based on its solubility. Natural organic matter is most abundant in litter layers and upper mineral horizons, of soils and is transported to subsoils by water as dissolved molecules and

fine suspended colloids or dissolved organic matter (DOM)^{10, 11} Dissolved organic matter is the organic matter fraction that passes through a 0.45- μm filter; while particulate organic matter (POM) refers to the organic particles remaining on a 0.45 μm filter.¹²⁻⁸ DOM affects biogeochemical processes, particle stability and transport, metal complexation, and production of disinfection byproducts (DBPs) during water and wastewater treatment.²¹⁻²⁵

The dissolved organic matter (DOM) fraction of NOM is closely associated with the mineral matrix of soil due to the strong complexation between surface metals and acidic organic ligands, particularly with those associated with aromatic structures.¹⁰ Changes in pH and reactions with metals affect the molecular composition of DOM and POM.

Natural organic matter can also be operationally defined as a mixture of humic and nonhumic substances. The recognizable plant debris and organic compounds, such as polysaccharides, lignin, proteins, and polypeptides, are categorized as nonhumic substances.¹³ The remaining high-molecular-weight, highly transformed, brown- to black-colored materials are considered humic substances (HS).¹⁴ Humic substances are often described as coiled, long-chain molecules or two- or three-dimensional cross-linked macromolecules with a wide range of organic functional groups. The molecular structure and chemistry of HS are still not well understood because of intrinsic chemical heterogeneity, geographical variability.¹⁵ Thus, HS are also operationally fractionated based on their solubility.¹⁶ Fulvic acid (FA) are soluble at all pH values, humic acids (HA) are insoluble at $\text{pH} < 2$ but soluble at higher pH, whereas humins are insoluble in water at all pH values.^{17, 18} Despite the arbitrary nature of this separation method, it is mostly used to achieve a segregation of humic substances according to their chemical properties, which chiefly depend on surface functional groups and macromolecular structure.

The major constituents of NOM are C, O, H, and N; other elements are P and S. The elemental compositions are more distinguishable according to fractionation (FA vs HA) than to sources and geographical areas. Fulvic acid have lower contents of C and N but higher contents of O and S than HA. Based on elemental compositions, the mole ratios of O/C, H/C, or N/C are calculated to indicate the degree of polarity/ aromaticity and unsaturation of carbon chains. The O/C ratios are about 0.5 for HA and about 0.7 for FA. The H/C ratios, which have a larger variation, are about 1.0 for HA and about 1.4 for FA. In general, FA has greater aliphatic character, while HA is of higher aromaticity and hydrophobicity. Insoluble humin is believed to be similar HA, with slightly less aromatic groups and acidity but higher contents of polysaccharide and alcoholic OH.^{13, 15, 16}

Suwannee River natural organic matter (SRNOM) is a well-known end member of NOM from an aquatic system and is a reference material of the International Humic Substances Society. The SRNOM was acquired from 36,890 L of filtered river water that was concentrated 40-fold on-site using reverse osmosis (RO) systems. After RO, the concentrated sample was desalted by cation exchange (CEX), freeze dried, and homogenized. The overall yield of dissolved organic carbon (DOC) was 84.2%. The final NOM sample supplied to the IHSS, which is designated 2R101N, contains only 3.89% inorganic ash, which reasonably allows most chemical analyses.¹⁹⁻²¹

2.3 Gaps and Limitations in Existing Literature.

This dissertation work addresses a current gap in the literature related to understanding the chemical interactions between NOM, and U which affect U adsorption, precipitation, and dissolution in organic-rich environments at environmentally relevant pH. While the presence of NOM in sandstone formations is well established, the effects of uranium interaction with NOM on the organic group functional chemistry has not been identified.^{2, 53-55} Improving the current

understanding on the organic functional group chemistry found in sandstone formations and mineralized U deposits will help to identify the binding mechanisms influencing the interactions of U and NOM. These interactions may ultimately affect the reactive transport of U in soils, surface water and groundwater, and uptake in plants. Although several methods have been used to understand the mineralogy of sandstone formations and U mineralized deposits, the analysis of particulate NOM is challenging.¹² The application of X-ray photoelectron spectroscopy (XPS) to observe changes of organic functional groups in U mineralized deposits as a result of pH changes has not been widely used.^{56, 57}

The effect of pH on the precipitation of U in the presence of NOM needs to be further investigated given the effect it has on U and NOM chemistry. One approach has been modelling the reactivity of U with specific functional groups (e.g. carboxyl or phenolic) for fulvic acid (FA) and humic acid (HA).^{2, 10, 23} Few experimental studies have been conducted to understand the influence of pH on the precipitation of U in the presence of NOM.^{18, 35, 58-60} Laboratory experiments conducted in a previous study showed that the complexation of uranyl with carboxyl groups of NOM is possible by forming uranyl-carboxyl compounds.⁶¹ Despite previous efforts, the role of pH on U and NOM reactions which ultimately influences U solubility in the environment needs to be better understood.

While there are several studies of the interactions between DOM and U, there is limited information about the reactions of U-DOM that control the complexation chemistry and its effect on U solubility in the environment.^{29, 30, 32, 35} Dissolved organic matter contains metal-binding functional groups (such as carboxylates, phenols, amines, thiols) with binding affinities and ligand densities spanning many orders of magnitude.⁶² Binding of U by DOM remains poorly understood at the molecular scale under environmentally relevant conditions.⁶² Understanding the reaction

mechanisms between U and DOM continue to be challenging at the molecular scale by the intrinsic complexity of DOM and U chemistry, the lack of binding constants, and analytical limitations.⁶² Improving the current understanding of the influence of pH on U-DOM complexes will help to identify how the solubility of U changes in natural waters.^{30, 32, 63, 64} Although there is evidence that the hydrophobicity of DOM influences U mobility⁶⁵, the behavior of different functional groups as a function of pH and the reaction with U is still not well understood.

The integration of experiments using natural samples from mineralized deposits, laboratory-controlled experiments with advanced analytical techniques could provide new information about the effect of pH on interfacial reactions such as complexation, adsorption and precipitation between NOM, and U.

2.4. Research Objectives

This research sought to advance the understanding of the interfacial chemical reactions between U and NOM in organic-rich environments which are currently not well understood. Part of this work contributes to the state of the current knowledge by identifying the organic functional group chemistry and U species (i.e U(IV) and U(VI)) in mineralized deposits. Laboratory experiments aim to studying the effects of pH and NOM on the adsorption and precipitation, as well as the changes on the organic functional group chemistry of DOM due to these reactions.

The overarching objective of this dissertation is to combine experiments using natural samples from an organic-rich mineralized U deposit and laboratory-controlled conditions to investigate the chemical reactions affecting the speciation of U(IV), U(VI) and the organic functional group chemistry in organic-rich environments using aqueous analyses, advanced spectroscopy, microscopy and, ultrahigh-resolution mass spectrometry.

The specific objectives and hypotheses of this work are (Figure 1):

Objective 1: Identify the effect of pH on U speciation and the organic functional chemistry in mineralized deposits from the Jackpile Mine.

Hypothesis 1: Changes in pH affect the binding of carboxylic functional groups in NOM and the speciation of U(IV) and U(VI) in mineralized deposits.

Objective 2: Identify the precipitation of U(VI) and NOM as a function of pH (2, 4 and 7)

Hypothesis 2: Natural organic matter at pH 4 enhances the co-precipitation of U(VI)-NOM compared to pH 2 and pH 7.

Objective 3: Identify changes in DOM chemistry due to the reaction of NOM and U at acidic and neutral pH.

Hypothesis 3: The aqueous complexation between U and DOM at pH 4 affects the organic functional group chemistry and the molecular structure of DOM.

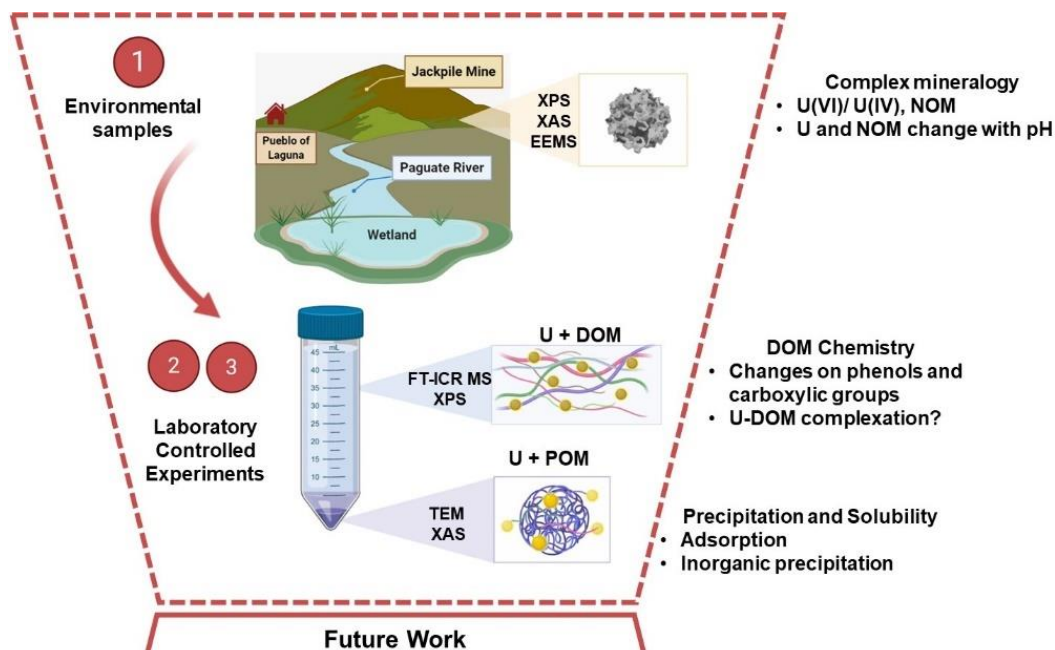


Figure 1: Research Summary - Schematic of interfacial reactions between U and NOM at environmentally relevant pH

2.5 References

1. Blake, J. M.; De Vore, C. L.; Avasarala, S.; Ali, A.-M.; Roldan, C.; Bowers, F.; Spilde, M. N.; Artyushkova, K.; Kirk, M. F.; Peterson, E.; Rodriguez-Freire, L.; Cerrato, J. M., Uranium mobility and accumulation along the Rio Paguete, Jackpile Mine in Laguna Pueblo, NM. *Environ. Sci-Proc. Imp.* **2017**, *19*, (4), 605-621.
2. USEPA, Radionuclides Rule: A Quick Reference Guide. Office of Water (4606). In EPA 816-F-01-003: 2001.
3. USEPA, Jackpile-Paguete Uranium Mine Laguna Pueblo, NM. In EPA 2018.
4. Zychowski, K. E.; Kodali, V.; Harmon, M.; Tyler, C. R.; Sanchez, B.; Ordonez Suarez, Y.; Herbert, G.; Wheeler, A.; Avasarala, S.; Cerrato, J. M.; Kunda, N. K.; Muttill, P.; Shuey, C.; Brearley, A.; Ali, A.-M.; Lin, Y.; Shoeb, M.; Erdely, A.; Campen, M. J., Respirable Uranyl-Vanadate-Containing Particulate Matter Derived From a Legacy Uranium Mine Site Exhibits Potentiated Cardiopulmonary Toxicity. *Toxicological Sciences* **2018**, *164*, (1), 101-114.
5. Lewis, J.; Hoover, J.; MacKenzie, D., Mining and Environmental Health Disparities in Native American Communities. *Curr Environ Health Rep* **2017**, *4*, (2), 130-141.
6. Harmon, M. E.; Lewis, J.; Miller, C.; Hoover, J.; Ali, A. S.; Shuey, C.; Cajero, M.; Lucas, S.; Zychowski, K.; Pacheco, B.; Erdei, E.; Ramone, S.; Nez, T.; Gonzales, M.; Campen, M. J., Residential proximity to abandoned uranium mines and serum inflammatory potential in chronically exposed Navajo communities. *J Expo Sci Environ Epidemiol* **2017**, *27*, (4), 365-371.
7. Hettiarachchi, E.; Paul, S.; Cadol, D.; Frey, B.; Rubasinghe, G., Mineralogy Controlled Dissolution of Uranium from Airborne Dust in Simulated Lung Fluids (SLFs) and Possible Health Implications. *Environ. Sci. Technol. Let.* **2018**.

8. MacCarthy, I. H. S. a. P., *Aquatic Humic Substances: Influence on Fate and Treatment of Pollutants*. American Chemical Society: Washington, DC, 1988.
9. Aiken, G. R.; McKnight, D. M.; Wershaw, R. L.; MacCarthy, P., Humic Substances in Soil, Sediment, and Water. 1985. *Soil Science* **1986**, *142*, (5), 323.
10. Kaiser, K.; Kalbitz, K., Cycling downwards – dissolved organic matter in soils. *Soil Biology and Biochemistry* **2012**, *52*, 29-32.
11. Nebbioso, A.; Piccolo, A., Molecular characterization of dissolved organic matter (DOM): a critical review. *Anal Bioanal Chem* **2013**, *405*, (1), 109-24.
12. Potter, B., Washington, DC, 2005., Method 415.3 - Measurement of total organic carbon, dissolved organic carbon and specific UV absorbance at 254 nm in source water and drinking water. U.S. **2005**.
13. Tsang, D., Chapter 2 - Influence of Natural Organic Matter on Contaminant Removal by Permeable Reactive Barrier. In *The Role of Colloidal Systems in Environmental Protection*, Fanun, M., Ed. Elsevier: Amsterdam, 2014; pp 19-40.
14. Sparks, D. L., Soil physical chemistry, 2nd ed. CRC Press, New York. **1999**.
15. Sutton, R. S., Molecular structure in soil humic substances: the new view. *Environ. Sci. Technol.* **2005**, (39), 9009–9015.
16. Tipping, E., Cation binding by humic substances. Cambridge University Press, London. **2002**.
17. Darko, B.; Jiang, J.-Q.; Kim, H.; Machala, L.; Zboril, R.; Sharma, V. K., 8 - Advances Made in Understanding the Interaction of Ferrate(VI) with Natural Organic Matter in Water. In *Water Reclamation and Sustainability*, Ahuja, S., Ed. Elsevier: Boston, 2014; pp 183-197.

18. de Melo, B., Motta, F. L.; Santana, M. H. A., Humic acids: Structural properties and multiple functionalities for novel technological developments. *Materials Science and Engineering: C* **2016**, *62*, 967-974.
19. Averett, R. C.; Leenheer, J.; McKnight, D.; Thorn, K. In *Humic substances in the Suwannee River, Georgia; interactions, properties, and proposed structures*, 1994; 1994.
20. Green, N.; McInnis, D.; Hertkorn, N.; Maurice, P.; Perdue, E., Suwannee River Natural Organic Matter: Isolation of the 2R101N Reference Sample by Reverse Osmosis. *Environ. Eng. Sci.* **2015**, *32*, 38-44.
21. Li, Y.; Harir, M.; Lucio, M.; Kanawati, B.; Smirnov, K.; Flerus, R.; Koch, B. P.; Schmitt-Kopplin, P.; Hertkorn, N., Proposed Guidelines for Solid Phase Extraction of Suwannee River Dissolved Organic Matter. *Analytical Chemistry* **2016**, *88*, (13), 6680-6688.
22. Spirakis, C. S., The roles of organic matter in the formation of uranium deposits in sedimentary rocks. *Ore Geol. Rev.* **1996**, *11*, (1), 53-69.
23. Cumberland, S. A.; Douglas, G.; Grice, K.; Moreau, J. W., Uranium mobility in organic matter-rich sediments: A review of geological and geochemical processes. *Earth-Sci. Rev.* **2016**, *159*, 160-185.
24. Birdseye, H. S., Uranium deposits in northern Arizona. In *Black Mesa Basin (Northeastern Arizona)*, Anderson, R. Y.; Harshbarger, J. W., *New Mexico Geological Society 9th Annual Fall Field Conference Guidebook*, 1958; pp 161-163.
25. Deditius, A. P., Utsunomiya, S., Ewing, R.C., The chemical stability of coffinite, $USiO_4 \cdot nH_2O$; $0 < n < 2$, associated with organic matter: a case study from Grants uranium region, New Mexico, USA. *Chem. Geol.* **2008**, *1-4*, (251), 33-49.

26. Hansley, P. L.; Spirakis, C. S., Organic matter diagenesis as the key to a unifying theory for the genesis of tabular uranium-vanadium deposits in the Morrison Formation, Colorado Plateau. *Econ. Geol.* **1992**, *87*, (2), 352-365.
27. Leventhal, J. S.; Daws, T. A.; Frye, J. S., Organic geochemical analysis of sedimentary organic matter associated with uranium. *Appl. Geochem.* **1986**, *1*, (2), 241-247.
28. USEPA, Technical Report on Technologically Enhanced Naturally Occurring Radioactive Materials from Uranium Mining Vol. 1: Mining and Reclamation Background. In Office of Radiation and Indoor Air EPA 402-R-08-005: 2008.
29. Ellsworth, H. V., Thucholite and uraninite from the Wallingford mine near Buckingham, Quebec. *Am. Mineral.* **1928**, *13* (8), 442-448.
30. Cumberland, S. A.; Etschmann, B.; Brugger, J.; Douglas, G.; Evans, K.; Fisher, L.; Kappen, P.; Moreau, J. W., Characterization of uranium redox state in organic-rich Eocene sediments. *Chemosphere* **2018**, *194*, 602-613.
31. Velasco, C. A.; Artyushkova, K.; Ali, A.-M. S.; Osburn, C. L.; Gonzalez-Estrella, J.; Lezama-Pacheco, J. S.; Cabaniss, S. E.; Cerrato, J. M., Organic Functional Group Chemistry in Mineralized Deposits Containing U(IV) and U(VI) from the Jackpile Mine in New Mexico. *Environmental Science & Technology* **2019**, *53*, (10), 5758-5767.
32. Regenspurg, S.; Margot-Roquier, C.; Harfouche, M.; Froidevaux, P.; Steinmann, P.; Junier, P.; Bernier-Latmani, R., Speciation of naturally-accumulated uranium in an organic-rich soil of an alpine region (Switzerland). *Geochimica et Cosmochimica Acta* **2010**, *74*, (7), 2082-2098.
33. Gorman-Lewis, D.; Burns, P. C.; Fein, J. B., Review of uranyl mineral solubility measurements. *The Journal of Chemical Thermodynamics* **2008**, *40*, (3), 335-352.

34. Finch, R.; Murakami, T., Systematics and Paragenesis of Uranium Minerals. In 1999; Vol. 38, pp 91-180.
35. Kim, K.-W.; Kim, Y.-H.; Lee, S.-Y.; Lee, J.-W.; Joe, K.-S.; Lee, E.-H.; Kim, J.-S.; Song, K.; Song, K.-C., Precipitation Characteristics of Uranyl Ions at Different pHs Depending on the Presence of Carbonate Ions and Hydrogen Peroxide. *Environmental Science & Technology* **2009**, *43*, (7), 2355-2361.
36. Chang, P.; Yu, S.; Chen, T.; Ren, A.; Chen, C.; Wang, X., Effect of pH, ionic strength, fulvic acid and humic acid on sorption of Th(IV) on Na-rectorite. *Journal of Radioanalytical and Nuclear Chemistry* **2007**, *274*, (1), 153-160.
37. Du, L.; Li, S. C.; Li, X. L.; Wang, P.; Huang, Z. Y.; Tan, Z. Y.; Liu, C. L.; Liao, J. L.; Liu, N., Effect of humic acid on uranium(VI) retention and transport through quartz columns with varying pH and anion type. *J. Environ. Radioact.* **2017**, *177*, 142-150.
38. Luo, W.; Gu, B., Dissolution and Mobilization of Uranium in a Reduced Sediment by Natural Humic Substances under Anaerobic Conditions. *Environ. Sci. Technol.* **2009**, *43*, (1), 152-156.
39. Tinnacher, R. M.; Nico, P. S.; Davis, J. A.; Honeyman, B. D., Effects of Fulvic Acid on Uranium(VI) Sorption Kinetics. *Environ. Sci. Technol.* **2013**, *47*, (12), 6214-6222.
40. Bone, S. E.; Dynes, J. J.; Cliff, J.; Bargar, J. R., Uranium(IV) adsorption by natural organic matter in anoxic sediments. *P. Natl. Acad. Sci. Usa* **2017**, (4), 711.
41. Bone, S. E.; Cahill, M. R.; Jones, M. E.; Fendorf, S.; Davis, J.; Williams, K. H.; Bargar, J. R., Oxidative Uranium Release from Anoxic Sediments under Diffusion-Limited Conditions. *Environ. Sci. Technol.* **2017**, *51*, (19), 11039-11047.
42. Lenhart, J. J.; Cabaniss, S. E.; MacCarthy, P.; Honeyman, B. D., Uranium(VI) complexation with citric, humic and fulvic acids. *Radiochim. Acta* **2000**, *88*, (6), 345-353.

43. von der Heyden, B. P.; Roychoudhury, A. N.; Mtshali, T. N.; Tyliczszak, T.; Myneni, S. C. B., Chemically and Geographically Distinct Solid-Phase Iron Pools in the Southern Ocean. *Science* **2012**, *338*, (6111), 1199-1201.
44. Daugherty, E. E.; Gilbert, B.; Nico, P. S.; Borch, T., Complexation and Redox Buffering of Iron(II) by Dissolved Organic Matter. *Environ. Sci. Technol.* **2017**, *51*, (19), 11096-11104.
45. Tan, L.; Wang, X.; Tan, X.; Mei, H.; Chen, C.; Hayat, T.; Alsaedi, A.; Wen, T.; Lu, S.; Wang, X., Bonding properties of humic acid with attapulgite and its influence on U(VI) sorption. *Chem. Geol.* **2017**, *464*, 91-100.
46. Bordelet, G.; Beaucaire, C.; Phrommavanh, V.; Descostes, M., Chemical reactivity of natural peat towards U and Ra. *Chemosphere* **2018**, *202*, 651-660.
47. Omar, H. A.; Aziz, M.; Shakir, K., Adsorption of U(VI) from dilute aqueous solutions onto peat moss. *Radiochim. Acta* **2007**, *95*, (1), 17-24.
48. Mikutta, C.; Langner, P.; Bargar, J. R.; Kretzschmar, R., Tetra- and Hexavalent Uranium Forms Bidentate-Mononuclear Complexes with Particulate Organic Matter in a Naturally Uranium-Enriched Peatland. *Environ. Sci. Technol.* **2016**, *50*, (19), 10465-10475.
49. Li, D. E.; Kaplan, D. I.; Chang, H. S.; Seaman, J. C.; Jaffe, P. R.; van Groos, P. K.; Scheckel, K. G.; Segre, C. U.; Chen, N.; Jiang, D. T.; Newville, M.; Lanzirrotti, A., Spectroscopic Evidence of Uranium Immobilization in Acidic Wetlands by Natural Organic Matter and Plant Roots. *Environ. Sci. Technol.* **2015**, *49*, (5), 2823-2832.
50. Noller, B. N.; Watters, R. A.; Woods, P. H., The role of biogeochemical processes in minimising uranium dispersion from a mine site. *Journal of Geochemical Exploration* **1997**, *58*, (1), 37-50.

51. Ho, C. H.; Miller, N. H., Effect of humic acid on uranium uptake by hematite particles. *Journal of Colloid and Interface Science* **1985**, *106*, (2), 281-288.
52. Lenhart, J. J.; Honeyman, B. D., Uranium(VI) sorption to hematite in the presence of humic acid. *Geochimica et Cosmochimica Acta* **1999**, *63*, (19), 2891-2901.
53. Cumberland, S. A.; Douglas, G.; Grice, K.; Moreau, J. W., Uranium mobility in organic matter-rich sediments: A review of geological and geochemical processes. *Earth Sci. Rev.* **2016**, *159*, 160-185.
54. Blake, J. M.; De Vore, C. L.; Avasarala, S.; Ali, A.-M.; Roldan, C.; Bowers, F.; Spilde, M. N.; Artyushkova, K.; Kirk, M. F.; Peterson, E.; Rodriguez-Freire, L.; Cerrato, J. M., Uranium mobility and accumulation along the Rio Paguete, Jackpile Mine in Laguna Pueblo, NM. *Environ. Sci. Process. Impacts* **2017**, *19*, (4), 605-621.
55. El Hayek, E.; Torres, C.; Rodriguez-Freire, L.; Blake, J. M.; De Vore, C. L.; Brearley, A. J.; Spilde, M. N.; Cabaniss, S.; Ali, A.-M. S.; Cerrato, J. M., Effect of Calcium on the Bioavailability of Dissolved Uranium(VI) in Plant Roots under Circumneutral pH. *Environ. Sci. Technol.* **2018**, *52*, (22), 13089-13098.
56. Lu, G.; Haes, A. J.; Forbes, T. Z., Detection and identification of solids, surfaces, and solutions of uranium using vibrational spectroscopy. *Coord. Chem. Rev.* **2018**, *374*, 314-344.
57. Yang, J. B.; Volesky, B., Modeling uranium-proton ion exchange in biosorption. *Environmental Science & Technology* **1999**, *33*, (22), 4079-4085.
58. Trenfield, M. A.; Ng, J. C.; Noller, B.; Markich, S. J.; van Dam, R. A., Dissolved organic carbon reduces uranium toxicity to the unicellular eukaryote *Euglena gracilis*. *Ecotoxicology* **2012**, *21*, (4), 1013-1023.

59. Lavoie, M.; Sabatier, S.; Garnier-Laplace, J.; Fortin, C., Uranium accumulation and toxicity in the green alga *Chlamydomonas reinhardtii* is modulated by pH. *Environ. Toxicol. Chem.* **2014**, *33*, (6), 1372-1379.
60. Granger H. C, S. E. S., Dean B. G., And Moore F. B. , Sandstone-type uranium deposits at Ambrosia Lake, New Mexico; an interim report. *Econ. Geol.* **1961**, *56*, (7), 1179-1210.
61. Nash, J. T., Uranium deposits in the Jackpile Sandstone, New Mexico. *Econ. Geol.* **1968**, *63* (7), 737–750.
62. S. S. Adams, H. S. C., P. L. Hafen, H. Salek-Nejad, Interpretation of postdepositional processes related to the formation and destruction of the Jackpile-Paguate uranium deposit, Northwest New Mexico. *Econ. Geol.* **1978**, *73*, (8), 1635-1654.
63. Yang, Y.; Saiers, J. E.; Barnett, M. O., Impact of Interactions between Natural Organic Matter and Metal Oxides on the Desorption Kinetics of Uranium from Heterogeneous Colloidal Suspensions. *Environ. Sci. Technol.* **2013**, *47*, (6), 2661-2669.
64. Yang, Y.; Saiers, J. E.; Xu, N.; Minasian, S. G.; Tyliszczak, T.; Kozimor, S. A.; Shuh, D. K.; Barnett, M. O., Impact of Natural Organic Matter on Uranium Transport through Saturated Geologic Materials: From Molecular to Column Scale. *Environ. Sci. Technol.* **2012**, *46*, (11), 5931-5938.
65. Volkov, I. V.; Polyakov, E. V., Interaction of Humic Acids with Microelements/Radionuclides in Sorption Systems. *Radiochemistry* **2020**, *62*, (2), 141-160.
66. Tomažič, B.; Branica, M., Precipitation and hydrolysis of uranium(VI) in aqueous solutions—VII: Boundary conditions for precipitation from solutions of $\text{UO}_2(\text{NO}_3)_2\text{-KOH-K}$, Ba, La and Eu nitrate. *Journal of Inorganic and Nuclear Chemistry* **1972**, *34*, (4), 1319-1332.

67. Tomažič, B.; Samaržija, M.; Branica, M., Precipitation and hydrolysis of uranium (VI) in aqueous solutions-VI. *Journal of Inorganic and Nuclear Chemistry* **1969**, *31*, 1771.
68. Rallakis, D.; Michels, R.; Brouand, M.; Parize, O.; Cathelineau, M., The Role of Organic Matter on Uranium Precipitation in Zoovch Ovoo, Mongolia. *Minerals* **2019**, *9*, 310.
69. Aiken, G. R.; Hsu-Kim, H.; Ryan, J. N., Influence of Dissolved Organic Matter on the Environmental Fate of Metals, Nanoparticles, and Colloids. *Environmental Science & Technology* **2011**, *45*, (8), 3196-3201.
70. Manaka, M.; Seki, Y.; Okuzawa, K.; Kamioka, H.; Watanabe, Y., Natural attenuation of dissolved uranium within a small stream of central Japan. *Limnology* **2007**, *8*, (2), 143-153.
71. Manaka, M.; Seki, Y.; Okuzawa, K.; Watanabe, Y., Uranium sorption onto natural sediments within a small stream in central Japan. *Limnology* **2008**, *9*, (3), 173-183.
72. Novotnik, B.; Chen, W.; Evans, R. D., Uranium bearing dissolved organic matter in the porewaters of uranium contaminated lake sediments. *Applied Geochemistry* **2018**, *91*, 36-44.

Chapter 3. Organic Functional Group Chemistry in Mineralized Deposits

Containing U(IV) and U(VI) from the Jackpile Mine in New Mexico

Carmen A. Velasco¹, Kateryna Artyushkova², Abdul-Mehdi S. Ali³, Christopher L. Osburn⁴,
Jorge Gonzalez-Estrella¹, Juan S. Lezama Pacheco⁵, Stephen E. Cabaniss⁶, and José M. Cerrato^{1*}

¹ Department of Civil, Construction & Environmental Engineering, MSC01 1070, University of New Mexico, Albuquerque, New Mexico 87131, USA

² Department of Chemical and Biological Engineering, MSC01 1120, University of New Mexico, Albuquerque, New Mexico 87131, USA

³ Department of Earth and Planetary Sciences, MSC03 2040, University of New Mexico, Albuquerque, New Mexico 87131, USA

⁴ Department of Marine, Earth, and Atmospheric Sciences, North Carolina State University, Raleigh, North Carolina, United States

⁵ Department of Environmental Earth System Science, Stanford University, California 94305

⁶ Department of Chemistry and Chemical Biology, University of New Mexico, Albuquerque, New Mexico 87131, USA

Abstract.

We investigated the functional group chemistry of natural organic matter (NOM) associated with both U(IV) and U(VI) in solids from mineralized deposits exposed to oxidizing conditions from the Jackpile Mine, Laguna Pueblo, NM. The Uranium (U) content in unreacted samples was 0.44% to 2.6% by weight determined by X-ray fluorescence (XRF). In spite of prolonged exposure to ambient oxidizing conditions, $\approx 49\%$ of U(IV) and $\approx 51\%$ of U(VI) were identified on U-L_{III} edge extended X-ray absorption fine structure (EXAFS) spectra. Loss on ignition and thermogravimetric analyses (TGA) identified between 13% and 44% of NOM in the samples. Carbonyl, phenolic and carboxylic functional groups in the unreacted samples were identified by fitting of high-resolution X-ray photoelectron spectroscopy (XPS) C 1s and O 1s spectra. Peaks corresponding to phenolic and carbonyl functional groups had higher intensity than those corresponding to carboxylic groups in samples from the supernatant from batch extractions conducted at pH 13, 7 and 2. U(IV) and U(VI) species were detected in the supernatant after batch extractions conducted under oxidizing conditions by fitting of high-resolution XPS U 4f spectra. The outcomes from this study highlight the importance of pH on the organic functional group chemistry and U speciation in mineralized deposits.

3.1 Introduction

The legacy of operations for uranium (U) mining in the USA has impacted several sites, many of which are located near Native American communities. For example, studies have reported U concentrations of 35.3-772 $\mu\text{g L}^{-1}$ in surface waters near the Pueblo of Laguna, New Mexico (NM) neighboring the Jackpile Mine.¹ These concentrations exceed the US Environmental Protection Agency maximum contaminant limit of 30 $\mu\text{g L}^{-1}$.² Additionally, the U concentration detected in solid samples from the Jackpile Mine, adjacent to the Rio Paguete, was 9300 mg kg^{-1} .¹ A recent study in the Grants Mining District in NM reports that U-bearing dust affects the extent of U dissolution in simulated lung fluids, which could have potential health implications.³ The Jackpile Mine has been listed in the EPA National Priorities List for CERCLA cleanup.⁴

Natural organic matter (NOM) and U co-occur in the Jackpile Sandstone Member of the Morrison Formation. Sandstone formations are characterized by varied sizes of sorted pebbles and sands, and lenses of concentrated NOM.⁵ Uranium is trapped within the NOM-layers of detritus and humus, leading to the formation of NOM-U rich deposits.⁶ Natural organic matter may enhance the preservation of U(IV) phases for more than 30 million years exposed to oxidizing fluids.^{5, 12}

Organic functional groups play a key role in the chemical speciation and reactivity of U and other metals in the environment. Dissolved humic substances facilitate the transport of U and other metals as a function of pH by affecting the sorption on mineral surfaces.¹³⁻¹⁶ Soluble U complexes with humic substances in peats.¹⁷ The formation of U(VI)-humate complexes between pH 4 and 6 can influence sorption of U on NOM.^{17, 18} Previous studies found that U is predominantly bound in bidentate-mononuclear complexes to carboxyl ligands in natural NOM,

inhibiting the precipitation of U minerals.¹⁹⁻²² Furthermore, U(IV) can complex with NOM functional groups, resulting in the formation of monomeric U(IV) species that have been observed in anoxic sediments and ore deposits together with other crystalline U(IV) phases such as uraninite.²³⁻²⁶ Other studies reported NOM complexation influences the abiotic oxidation rate of Fe(II) by O₂.^{27, 28, 29} For example, functional groups such as quinones act as terminal electron acceptors in anaerobic microbial respiration, while phenols serve as electron donors for the reduction of electron acceptors, such as Fe(III), Mn(IV), arsenate, Cr(VI), and U(IV).³⁰⁻³² Despite these findings, the influence of pH on the organic functional group chemistry and U(IV) and U(VI) co-occurring in U mine sites remained unknown.

While the presence of NOM in sandstone formations is well established, the functional groups have not been identified.^{1, 33-35} Improving the understanding of the organic functional group chemistry found in sandstone formations and mineralized U deposits will help to identify the binding mechanisms influencing the interactions of U and NOM. These interactions may ultimately affect the reactive transport of U in soils, surface water and groundwater, and uptake in plants.³⁶ Although several methods have been used to understand the mineralogy of sandstone formations and U mineralized deposits, the analysis of particulate NOM is challenging.⁶ The application of X-ray photoelectron spectroscopy (XPS) to observe changes of organic functional groups in U mineralized deposits as a result of pH changes is not well documented.^{37, 38} Integrating XPS analyses with other physical and chemical methods could provide new information about NOM functional chemistry in U samples from mineralized deposits.

The objective of this study was to identify the organic functional group chemistry in U mineralized deposits from the Jackpile Mine. We integrated excitation emission matrix spectroscopy (EEMS), XPS, XAS, thermal analyses and batch extraction experiments. A novel

aspect of this investigation is identifying the influence of pH on the organic functional group chemistry, U(IV) and U(VI) co-occurring in samples of complex mineralogy from a sandstone geological formation through the integration of a variety of analytical techniques with laboratory experiments. The results of this study provide insights about the reactions between NOM and U in mineralized deposits which are relevant for risk assessment and remediation strategies.

3.2 Materials and Methods

3.2.1 Sample Collection.

Two solid samples (JP₁ and JP₂) from mineralized deposits from the Jackpile Mine (35° 8'28.09"N, 107°20'19.67"W) were collected from a location described in a previous study.¹ Samples were collected in the summer of 2017, crushed, and sieved with a US Standard #230 mesh (63 μm). We referred as “unreacted samples” to the crushed and sieved solids before any treatment was applied to them.

3.2.2 Solid Analyses.

Solid phase analyses were conducted on unreacted samples by X-ray Fluorescence (XRF); and C, H, N, and O elemental analysis. X-ray absorption spectroscopy (XAS) and XPS were performed on unreacted samples, on reacted solids after loss-on-ignition (LOI), and on solids remaining from batch extraction experiments. X-ray absorption spectroscopy measurements were conducted at Beamline 7-3 at the Stanford Synchrotron Radiation Laboratory (SSRL) at the U L_{III} edge in fluorescence mode. Data was collected at room temperature in a He purged environmental chamber. Linear combination fitting was performed using the following reference materials as end-members as measured from other studies: monomeric U(IV),³⁹ uraninite,⁴⁰ U(VI) adsorbed with ferrihydrite,⁴¹ and the coffinite reference

was obtained from the Mineral Collection in the Department of Earth and Planetary Sciences, University of New Mexico. References and standards were pulverized and pressed into the slots of aluminum holders and sealed with Kapton tape on both sides. Data processing and analyses for XAS was conducted using Athena and Artemis software.⁴² A Kratos Ultra DLD X-ray Photoelectron Spectrometer was used to acquire the near surface (<10 nm) atomic composition and oxidation states. Survey spectra were acquired at 80 eV and high resolution at 20 eV pass energy. Monochromatic Al source was used at 150 W power to obtain C 1s and U 4f high-resolution spectra from the top ~4-10 nm of the surface. Three areas per replicate were analyzed, average and standard deviations are reported. Shirley background subtraction was used to process the spectra using CasaXPS software. Additional details about these methods are included in the Supporting Information (SI).

3.2.3 Acid Digestion and Dolution Metal Analyses.

Acid digestions in triplicates were conducted to assess the U acid-extractable content from the mineralized surface deposit solids, by adding 2 mL HNO₃, 6 mL HCl, and 3 mL concentrated HF into 50 mL Teflon digestion tubes containing 2.000 ± 0.002 g of homogenized samples. Inductively coupled plasma optical emission spectroscopy (ICP-OES) and inductively coupled plasma mass spectrometry (ICP-MS) measured metal concentrations in solution. Additional description of these methods is in the SI.

3.2.4 Thermal Analyses for Solids.

..... The NOM content in the mineralized deposit solid samples was estimated by LOI and thermogravimetric analyses (TGA). Details of these methods are provided in the SI.

3.2.5 Extraction of Natural Organic Matter.

Natural organic matter from the mineralized deposit solid samples was identified by a modified approach of the Nagoya Method as described in a study conducted to characterize humic substances by EEMS and parallel factor analysis.^{43, 44} Detailed information about batch extractions is in the SI. Briefly, NOM from our samples was extracted with a 0.1 N NaOH solution at pH 13. Reactions were carried out in triplicate for 24 h at 4°C. A set of batch reactors was acidified from pH 13 to pH 7 with concentrated trace metal grade HCl. Exposing these samples to pH 7 is environmentally relevant because circumneutral pH conditions are characteristic of the Rio Paguate near the Jackpile Mine.¹ Another set of batch reactors was acidified from pH 13 to pH 2. Exposing these samples to pH 2 is relevant because acid drainage has been observed in mine waste sites.⁴⁵⁻⁴⁷ Subsequently, after adjusting pH, samples were centrifuged, decanted, and filtered using a 0.2 µm filter. Supernatant samples were stored at 4°C in the dark until EEMS analysis. Remaining solids (reacted solids) were stored for XAS and XPS analyses.

3.2.6 Excitation Emission Matrix Spectroscopy (EEMS) Analyses.

Excitation emission matrix spectroscopy was used as a rapid, nondestructive, and sensitive method to provide information of the fluorescing fraction of the NOM. Absorbance spectra of dissolved NOM solutions were measured from 200 nm to 800 nm on a Varian Cary 300UV spectrophotometer in 1-cm quartz cells. Fluorescence spectra were acquired on a Varian Eclipse spectrofluorometer. Excitation wavelengths were sampled from 240 nm to 450 nm at 5-nm intervals; emission wavelengths were sampled every 2 nm from 300 nm to 600 nm. A Milli-Q water blank was subtracted from each absorbance and fluorescence measurement. Milli-Q water was 18 MΩ resistivity and < 5 ppb TOC. Samples were diluted if the absorbance in a 1-cm

cell was greater than 0.4 at 240 nm. Corrections for fluorescence were made for lamp excitation intensity and detector emission responses, and afterward, corrections for inner filter effects were applied using standard approaches.⁴⁸ Finally, the results were calibrated first to the water Raman signal of each instrument and then in quinine sulfate units (QSU). Fluorescence results were processed with an in-house MATLAB script (Math-Works, MA). Dissolved NOM was quantified by measuring the dissolved organic carbon (DOC) via automated heated-persulfate oxidation following an additional filtration through a 0.45 μ m PVDF filter.

3.2.7 Effect of pH on Organic Functional Chemistry and U Species.

.....Batch extraction experiments assessed the effect of pH on the organic functional groups in the NOM from the mineralized deposit solids from the Jackpile Mine. For this set of reactions, we used the sample with the highest NOM content (JP₂) as determined by LOI and TGA. Natural organic matter was extracted by using 0.1 N NaOH and after 24 h of reaction, the pH was acidified from pH 13 to pH 7 and from pH 13 to pH 2 with metal trace grade HCl. After reaching the target pH, the supernatant was decanted and filtered through a 0.45 μ m filter. Drops of the decanted and filtered supernatant at pH 13 (control), pH 7 and pH 2 were drop-cast on a freshly cleaved mica surface and allowed to dry. Dried supernatants and reacted solids from batch extraction experiments were then analyzed by XPS to obtain high-resolution spectra for C 1s, O 1s, and U 4f. A high-resolution C 1s and O1s spectrum from fresh cleaved mica was obtained to account for the adventitious carbon present on the mica surface. Out of the total carbon detected, less than 10% was due to adventitious carbon on the surface of freshly cleaved mica (Figure S1). The rest of the carbon corresponded to the NOM in the supernatant. Five peaks have been used to fit the high-resolution C 1s spectra to specific functional groups: aliphatic C-C at 285 eV, secondary carbon

(C*-C-OH/C*-C=O) at 285.8 eV, phenol carbon at 286.5 eV, carbonyl carbon at 288.0 eV and carboxylic C at 289.2 eV. Details about sample preparation for XPS analyses are provided in the SI. Metal concentrations in the supernatant from each batch extraction reactor were analyzed by ICP-OES/ICP-MS. All reactions were carried out on triplicates.

3.3 Results and Discussion

3.3.1 Uranium in Unreacted Mineralized Deposit Solid Samples from the Jackpile Mine.

Samples contained $0.44 \pm 0.03\%$ (JP₁) and $2.61 \pm 0.09\%$ (JP₂) U by weight according to acid digestions and ICP-OES results. XRF analyses detected 1.02% (JP₁) and 8.22% (JP₂) by weight U. XRF and acid digestions are different approaches to measure the concentration of U in the solid samples. XRF measures the total bulk concentration of a particular element, while acid digestions determine the total acid extractable elemental concentration. Both techniques measure the elemental content in a sample and the results complement each other. The concentrations of U found in our samples are 3 to 4 orders of magnitude higher than the crustal U average of 2.78 mg kg^{-1} .¹¹ Previous studies have found co-occurrence of U and other elements in mine wastes and wetlands adjacent to the Jackpile Mine.^{1,35}

.....Unreacted sample JP₂ showed 19.4 rel% U(IV) and 80.6 rel% U(VI) relative (rel) to the total U detected in the near surface by high-resolution U 4f XPS spectra (Figure 1A). Spectra from U-L_{III} edge XANES on sample JP₂ also suggests that the unreacted solid samples contained a mixture of U(IV) and U(VI) (Figure 2). Unreacted samples averaged $\approx 49\%$ of U(IV) and $\approx 51\%$ of U(VI) according to the linear combination fitting of the U-L_{III} edge EXAFS spectra. Linear combination fits of the EXAFS spectra suggested samples contained more monomeric U(IV) (29%) than coffinite (19%) and also lacked uraninite (Figure 2C and Table S1). Previous studies also found monomeric U, coffinite, and oxidized U in the Jackpile Mine and in an undisturbed U

roll-front ore deposit in Wyoming; and in the microbial reduction of U(VI) in subsurface systems.^{1, 24, 25, 39} The proportions of U species found by XPS (near surface) and XAS (bulk) are different due to the characteristics of each technique. However, both results complement each other and confirm the existence of U(IV) and U (VI) in the surface and bulk part of our samples. Additional analyses were pursued to investigate the physical and chemical characteristics of the NOM from the Jackpile Mine.

3.3.2 Natural Organic Matter in Mineralized Deposits from the Jackpile Mine.

Natural Organic Matter Content. LOI and TGA were used to estimate the NOM content in the unreacted samples (Figure 3). Sample JP₂ exhibited higher mass loss (44.8±0.22% by LOI and 43.19±0.74% by TGA) than JP₁ (13.6±0.26% by LOI and 13.84±0.99% by TGA). Volatilization of NOM caused the mass loss in the samples. Other research found lower content of NOM in Jackpile Mine samples, ranging from 0.07% to 21.8% by LOI at 550°C, and 1.2% to 2.8% by LOI at 850°C while wetlands adjacent to the Jackpile Mine contained 14% to 15% NOM by LOI.^{1, 33, 35, 49, 50} A recent study in the Mulga Rock U deposit in Western Australia found that the LOI at 550°C ranged between 1 to 57% by weight.⁵¹ U-L_{III} edge XANES analyses detected the oxidation of U in the solid samples after LOI (Figure 2B). The heat treatment (550 °C) likely oxidized the amorphous U(IV), while coffinite remained stable at this temperature. Other literature has also reported U oxidation when solids are exposed to high temperatures.⁵²

Elemental Analysis. For this analysis, we used the sample with the highest NOM content (JP₂) as determined by LOI and TGA. Unreacted samples showed 33.2% C, 10.8% O, 1.4% H and 0.16% N by weight for sample JP₂. These findings are within range of another study in the Grants Belt.⁴⁹ The low H/C ratio (0.513) indicates high aromaticity as suggested in other studies.^{53, 54} Moreover,

low O/C (0.243) and (O+N)/C (0.247) ratios indicate low hydrophilicity and polarity.^{53, 54, 55, 56} Elemental analyses require a pure organic sample to avoid accounting for the C, O, H, and N from the minerals contained in the sample. The C detected with this technique is within the range identified by TGA and LOI.

Fluorescence Properties of Extracted Organic Matter from Mineralized Deposits from the Jackpile Mine. Excitation emission matrix spectroscopy (EEMS) was used to assess the chemical properties of the fluorescing fraction of the NOM from the mineralized deposits samples from the Jackpile Mine. Samples JP₁ and JP₂ showed two major peak regions corresponding to the macromolecular signature of humic substances (Figure 4). Peak A corresponds to the Ex/Em wavelengths of 260/380-460 nm, and peak C corresponds to 320-360/420-460 nm according to previous studies.^{44, 57} The change observed on EEMS at pH 2 is attributed to the precipitation of humic acids which are insoluble at low pH.^{15, 58} The dissolved organic carbon measured at pH 7 was 14.0±1.7 mg L⁻¹ for JP₁ and 8.7±0.9 mg L⁻¹ for JP₂.

Organic Functional Group Chemistry from Mineralized Deposits from the Jackpile Mine. Phenolic (18.3±2.5 rel%) and carbonyl (8.6±0.7 rel%) functional groups were more abundant while carboxylic groups (5.8±0.2 rel%) were the least abundant relative to the total carbon detected by high-resolution XPS C 1s and O 1s on the surface of unreacted solid samples (Figure 1 and Figure S2). Fitting of high-resolution XPS C 1s showed the characteristic peaks for phenolic (286.5 eV), carbonyl (288 eV) and carboxylic (289 eV) functional groups in the unreacted solid samples. The peak due to secondary carbon (all carbons bonded to phenolic, carbonyl and carboxylic carbon) was included in the fit at 285.6 eV. Contrary to what has been reported in previous studies on NOM, we found that carboxylic functional groups were less abundant than phenols or carbonyls.^{59,}

⁶⁰ This finding is likely due to the fact that our samples are highly aromatic as suggested by the

low H/C ratio. As suggested in other studies, the concentration of phenolic and carbonyl functional groups may affect the occurrence of U(IV) and U(VI), as both functional groups can influence the speciation of U found in our site.^{31, 59} Batch extraction experiments at pH 13, 7 and 2 were conducted to investigate changes in functional chemistry of NOM and U oxidation state as a function of solution pH.

3.3.3 Effect of pH on Organic Functional Group Chemistry.

Fitting of high resolution XPS C 1s and O 1s spectra show more changes in peak intensity corresponding to phenolic and carbonyl functional groups compared to carboxylic groups in the supernatant in response to pH changes from batch extractions (Figure 1 and Figure S2). For instance, the relative percent of phenolic groups in C 1s high resolution spectra increased with pH from 5.4 rel% at pH 13 to 14.4 rel% at pH 7 and to 11.0 rel% at pH 2. Likewise, the supernatant of reactor at pH 13 contained 1.5 rel% to 6.9 rel% fewer carbonyl groups than reactors at pH 7 and pH 2. In contrast to phenolic and carbonyl groups, the intensity of peaks corresponding to carboxylic groups in the supernatant of reactor at pH 13 were similar to reactor supernatants at pH 7 and pH 2 (within a range of 1.2 rel% to 1.7 rel%). Previous studies suggest that U in peat systems was coordinated to C atoms with carboxyl groups from particulate NOM through bidentate-mononuclear U(IV/VI) complexes.²⁶ Other studies found that U-phenolic bonds are prevalent at pH 6, while UO₂-carboxyl bonding is predominant at pH 3.5.⁶¹ Furthermore, research found that U(VI) was immobilized by natural NOM and reduced U(IV) was bound with carboxylic groups in plant roots.⁶² Our results suggest that carboxylic functional groups may help to stabilize U(IV) in these environments.

Our XPS data indicate a possible complexation at pH 13 between carboxylic functional groups with U or other elements found in the surface our samples such as K, Fe, or V (Table S2).

A peak located between carboxyl group (289 eV) and carbonyl group (288 eV) was observed at 23.5 ± 0.2 rel% only in the supernatant from reactor at pH 13 (Figure 1B). A previous study showed that the electrostatic interactions between different chemical moieties cause shifts in the binding energy detected by XPS.⁶³ For example, the formation of surface complexes (e.g. C-O-M) may cause a shift of the binding energy of carboxylic carbon (C(=O)-OH) to a lower value than the characteristic peak for carboxyl groups alone. Further research is necessary to study the mechanism of interaction between specific organic functional groups, U, and other metals occurring in mineralized deposits. Ongoing studies from our research group are assessing the binding of U and organic functional groups in more controlled laboratory environments using XPS; these include possible oxidation of NOM at high pH.

The peak intensity corresponding to phenolic, carbonyl, and carboxylic functional groups as a result of the batch extractions in the reacted solids compared to peaks observed on the unreacted samples decreased except for the carbonyl peak after the reaction at pH 13 (Figure S3). Further investigation about the mechanisms and interactions between these functional groups and U in our samples should be pursued.

3.3.4 Effect of pH on U Species.

A mixture of U(IV) and U(VI) was detected on the supernatant and reacted solids of all reactors. Fitting of high-resolution XPS U 4f spectra of the reacted solids indicates that U(IV) decreased for all reactors relative to the unreacted samples suggesting that U oxidation occurred in the solid sample surface as a result of the reaction conditions tested in our study (Figure S3). The surface concentration of U(VI) in the reacted solids increased by 14.0 rel% at pH 13, 4.4 rel% at pH 7 and 14.6 rel% at pH 2 when compared to the unreacted solids.

Analyses of U-L_{III} edge XANES spectra also identified a mixture of U(IV) and U(VI) in the reacted solid samples, as well as unreacted solids as discussed earlier (Figure 2). Linear combination fitting of the U-L_{III} edge EXAFS spectra detected similar proportions of U(IV) and U(VI) components on reacted solids from batch extraction reactors at pH 7 [46% U(IV) and 54% U(VI)] and pH 2 [49% U(IV) and 51%(VI)] (Table S3). The species of U in the reacted solids likely changed as a function of the pH conditions we investigated. Mineral forms of U such as uraninite and coffinite are stable in subsurface environments while biogenic uraninite and monomeric U(IV) oxidize more readily.^{64, 65, 66} Previous research has also found U(VI) with reduced U-bearing minerals such as coffinite in the Jackpile Mine.^{1, 8, 45} Similarly, other studies conducted on organic-rich subsurface sediments found U(IV), and U(VI).^{51, 67, 68}

A mixture of U(IV) and U(VI) was identified using high-resolution XPS U 4f spectra of the supernatant from all batch extractions. The peak intensity corresponding to U(IV) in the supernatant was higher for the reactor at pH 2 and lower for the reactor at pH 13 (Fig. 1). While we found U(IV) and U(VI) species in the reacted solids, it is interesting to observe U(IV) in the supernatant from the batch extractions conducted in oxidizing conditions. The U(IV) detected in solution may be U(IV)-NOM colloids, which have been observed in groundwater and wetlands.⁶⁹ However, the oxidation kinetics of U(IV) species in the supernatant and the mechanisms of formations need to be investigated.

The concentration of U measured in solution in reactors at pH 13 and pH 2 was similar (pH 13 = 34.5 ± 2.78 ; pH 2 = 40.2 ± 13.49 mg L⁻¹), while U in solution for the reactor at pH 7 was at least 15-fold lower (1.86 ± 1.28 mg L⁻¹, Figure S4). High U concentrations in solution found at pH 2 may be due to the weak adsorption with the solids at this pH. Higher concentrations of U in solution at pH 13 are likely due to the complexation of U with organic functional groups from the

NOM and possibly with inorganic ligands as well. These findings complement the XAS analysis which also indicated that the U-NOM binding decreased in reacted solids. The concentration of U in solution may depend on the co-precipitation of humic substances, and solubility of other U-bearing phases as a function of pH as suggested by other studies.^{6, 51} Specific mechanisms causing changes in the soluble U as a function of pH require further investigation in the context of the complex mineralogy of the Jackpile Mine.

3.4 Environmental Implications

The main findings of our study indicate that phenolic and carbonyl functional groups are more abundant than carboxyl functional groups in the NOM from the Jackpile Mine mineralized deposit samples, and show detectable changes on the XPS C 1s spectra after batch extraction at pH 13, pH 7 and pH 2. Contrary to what is commonly found in NOM^{59, 60}, carboxylic functional groups were the least abundant. Limited changes in the XPS C 1s peaks characteristic of the carboxylic groups were observed as a function of the pH conditions tested in this study. A unique finding of our study is that U(IV) was identified in unreacted solids, exposed to surface oxidizing conditions for several decades, as well as in reacted solids and in the supernatant collected from the batch reaction experiments conducted in oxidizing conditions. In addition to detecting U(IV) in supernatants from batch experiments at pH 13, 7 and 2; we observed noticeable differences in photoelectron peak intensities corresponding to phenolic- and carbonyl-, in comparison to those for carboxylic-functional groups. The organic functional groups in these mineralized deposit samples from the Jackpile Mine could affect the redox, complexation, and precipitation chemistry of U. These chemical reactions could be relevant to the mobilization of the dissolved, colloidal, and particulate forms of U(IV) and U(VI) as shown in other studies.^{26, 70} For instance, a recent investigation found high concentration of U(VI) in organic-rich layers as monodentate complexes

bound to carboxyl and phosphoryl groups of humic substances above a wetland redox boundary, and the complexation of U(IV) by NOM in reducing conditions.⁷¹ Understanding changes in organic functional chemistry at pH 7 and pH 2 is environmentally relevant due to their influence on chemical reactions that could impact U mobility and transport from the Jackpile Mine to surface waters and plants.^{1, 36} For example, circumneutral pH conditions are characteristic of surface waters adjacent to the Jackpile Mine, while lower pH is commonly observed in sites affected by acid mine drainage.^{1, 45, 47} Future research is necessary to identify specific mechanisms through which functional groups from the NOM found in our study control U reactivity in sites with complex mineralogy such as the Jackpile Mine, particularly the influence of NOM on U(IV) stabilization in oxic conditions. This information is essential for the development of risk assessment and remediation strategies in this site and other organic-rich uranium mineral deposits. These findings identify the need for further investigations related to the influence of organic functional groups on heavy metal transport and reactivity.

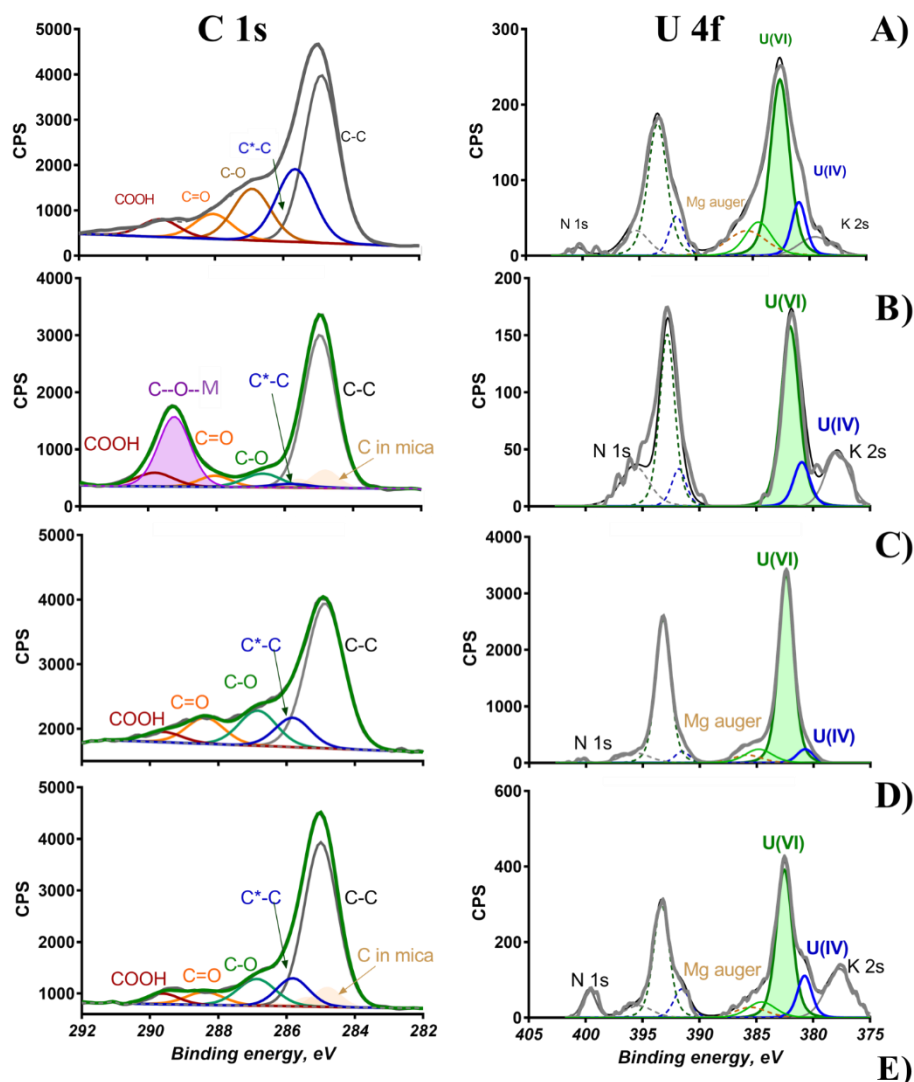
3.5 Acknowledgments

The authors would like to acknowledge the existing partnership with the Pueblo of Laguna Environment and Natural Resources Department. We also acknowledge the contributions of Dr. Johanna Blake and Dr. Viorel Atudorei for their support and thoughtful comments, which contributed to significantly improve this study. Part of this research was carried out at the Stanford Synchrotron Radiation Light source, a national user facility operated by Stanford University on behalf of the US DOE-OBER. Funding for this research was provided by the National Science Foundation (CAREER Award 1652619) and the National Institute of Environmental Health Sciences 472 Superfund Research Program (Award 1 P42 ES025589). Any opinions, findings, and conclusions or recommendations expressed in this publication are those of the author(s) and do

not necessarily reflect the views of the National Science Foundation or the National Institutes of Health.

Supporting Information Available

Additional materials and methods, four tables (S1, S2, S3 and S4), and four figures (S1, S2, S3 and S4) are available in SI. This material is available free of charge via the Internet at <http://pubs.acs.org>.



Sample	pH	Carbonyl (C=O)	Phenol (COH)	Carboxylic (COOH)	C-O-M	U (IV)	U (VI)
Unreacted Mine Wastes	as is	8.6%	18.3%	5.8%	0.0%	19.4%	80.6%
Supernatant	13	3.8%	5.4%	5.4%	23.5%	6.6%	93.4%
	7	10.7%	14.4%	4.2%	0.0%	22.1%	77.9%
	2	5.3%	11.0%	3.7%	0.0%	31.0%	69.0%
	13	10.3%	14.6%	5.3%	0.0%	5.4%	94.6%
Reacted Solids	7	5.7%	12.7%	3.6%	0.0%	15.0%	85.0%
	2	2.2%	5.9%	5.2%	0.0%	4.8%	95.2%

Figure 1. Fitting of high resolution XPS Carbon (C 1s) and Uranium (U 4f) spectra of A) unreacted Jackpile Mine solids. Fitting of high resolution XPS Carbon (C 1s) and Uranium (U 4f) spectra of supernatant from batch extraction reactors at: B) pH 13; C) pH 7; and D) pH 2; and E) Percent composition of C 1s and U 4f spectra.

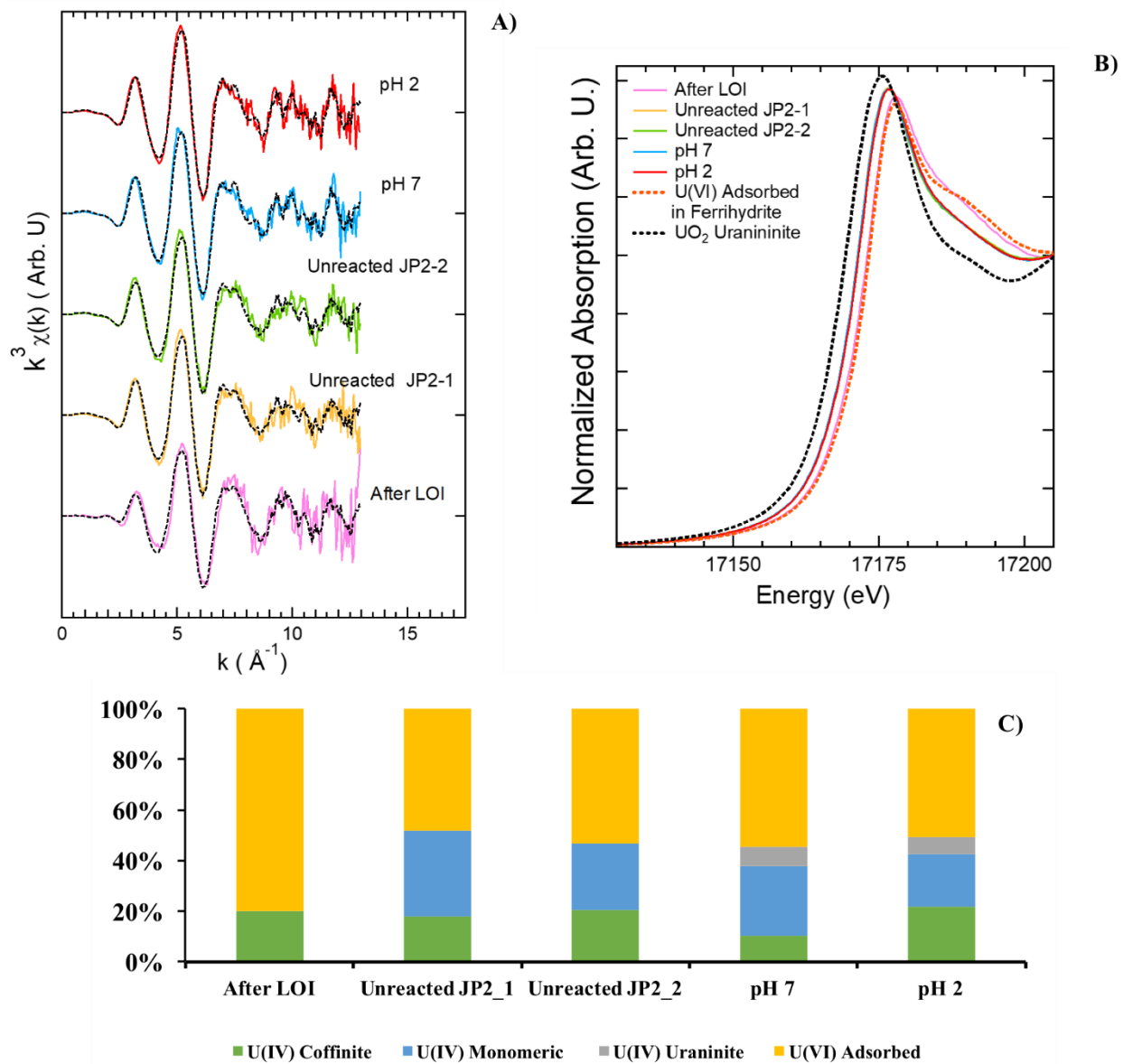


Figure 2. X-ray Absorption Spectroscopy (XAS) of unreacted and reacted solids (after LOI, pH 2 and pH 13) from the Jackpile Mine (JP₂). A) U-L_{III} edge EXAFS of the Jackpile Mine solid samples using the following references: uraninite, coffinite and monomeric U(IV) for U(IV) and uranyl-adsorbed ferrihydrite as reference for U(VI).; B) Normalized bulk U-L_{III} edge XANES spectra using uraninite (nano-UO₂) as reference for U(IV) and U(VI) adsorbed ferrihydrite as reference for U(VI).; and C) Linear combination fitting of the U-L_{III} edge EXAFS spectra of U(VI) and U(IV) species in the Jackpile Mine solid samples.

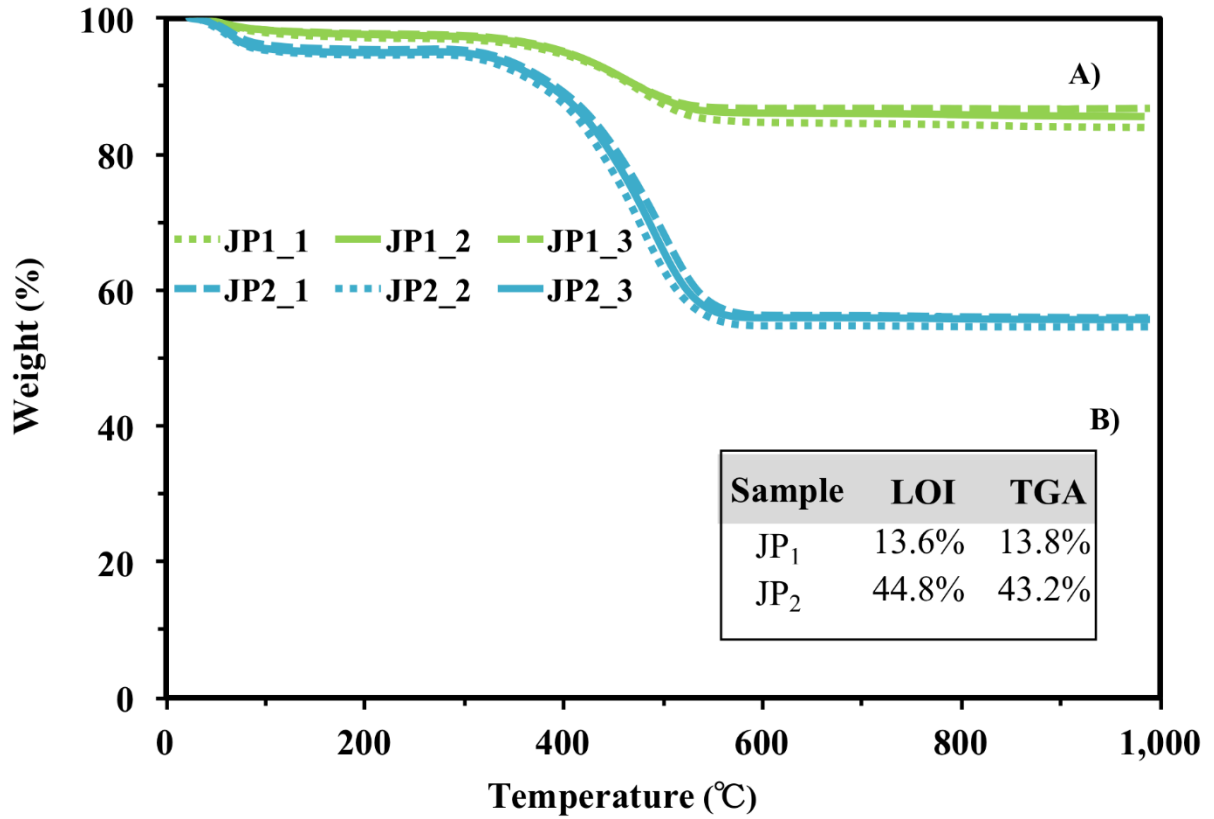


Figure 3. Thermal Analyses (Thermogravimetric Analysis, TGA, and Loss on Ignition, LOI) to estimate organic matter content in solid samples from the Jackpile Mine mineralized deposits: A) Change in mass content as a function of temperature (TGA) for unreacted solid samples JP₁ and JP₂; and B) Mass loss comparison between TGA and LOI.

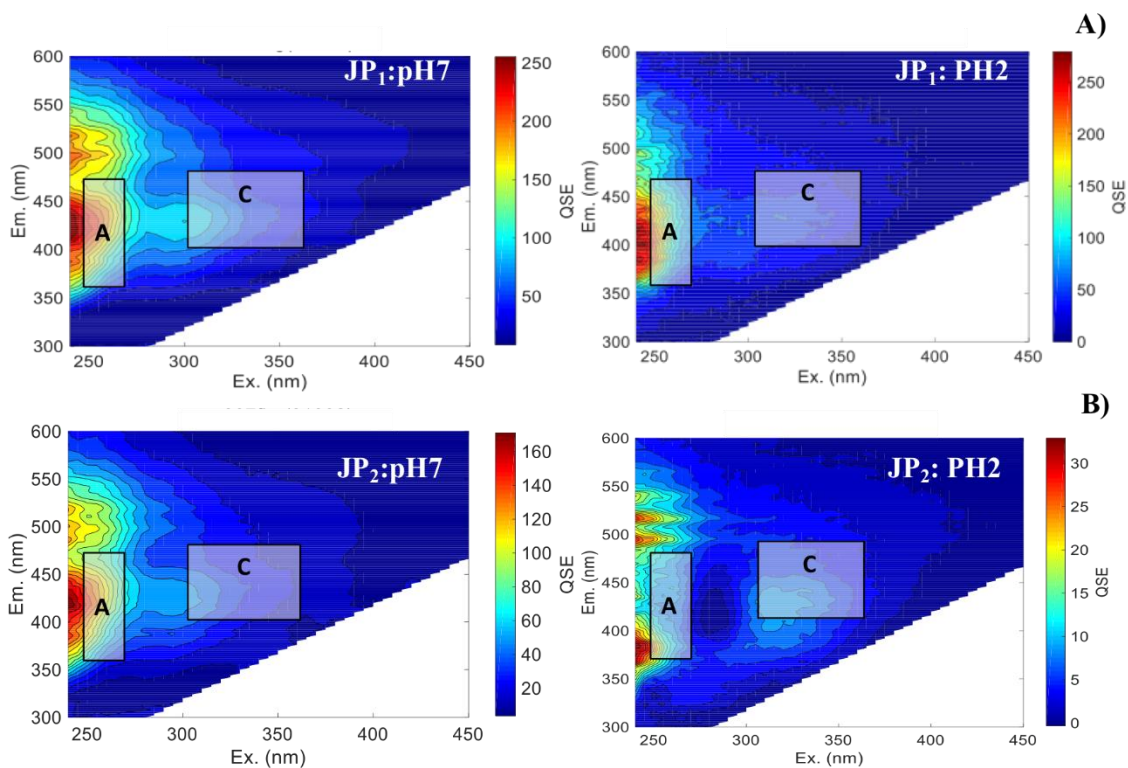


Figure 4. Excitation-emission matrix spectroscopy (EEMS) from supernatant of batch extraction reactors at pH 7 and pH 2 from the Jackpile Mine samples: A) JP₁; and B) JP₂. Note QSE scaling differences on the color bar for each EEM.

3.6 References.

- 1.Blake, J. M.; De Vore, C. L.; Avasarala, S.; Ali, A.-M.; Roldan, C.; Bowers, F.; Spilde, M. N.; Artyushkova, K.; Kirk, M. F.; Peterson, E.; Rodriguez-Freire, L.; Cerrato, J. M., Uranium mobility and accumulation along the Rio Paguete, Jackpile Mine in Laguna Pueblo, NM. *Environ. Sci. Process. Impacts* **2017**, *19*, (4), 605-621.
- 2.USEPA, Radionuclides Rule: A quick reference guide. Office of Water (4606). In EPA 816-F-01-003: 2001.
- 3.Hettiarachchi, E.; Paul, S.; Cadol, D.; Frey, B.; Rubasinghege, G., Mineralogy controlled dissolution of uranium from airborne dust in simulated lung fluids (SLFs) and possible health implications. *Environ. Sci. Technol. Let.* **2018**.
- 4.USEPA, Jackpile-Paguete uranium mine Laguna Pueblo, NM. In EPA 2018.
- 5.Spirakis, C. S., The roles of organic matter in the formation of uranium deposits in sedimentary rocks. *Ore Geol. Rev.* **1996**, *11*, (1), 53-69.
- 6.Cumberland, S. A.; Douglas, G.; Grice, K.; Moreau, J. W., Uranium mobility in organic matter-rich sediments: A review of geological and geochemical processes. *Earth Sci. Rev.* **2016**, *159*, 160-185.
- 7.Birdseye, H. S., Uranium deposits in northern Arizona. In *Black Mesa Basin (Northeastern Arizona)*, Anderson, R. Y.; Harshbarger, J. W., *New Mexico Geological Society 9th Annual Fall Field Conference Guidebook*, 1958; pp 161-163.
- 8.Deditius, A. P., Utsunomiya, S., Ewing, R.C., The Chemical Stability of Coffinite, $USiO_4 \cdot nH_2O$; $0 < n < 2$, Associated with Organic Matter: A Case Study From Grants Uranium Region, New Mexico, USA. *Chem. Geol.* **2008**, *1-4*, (251), 33-49.

9. Hansley, P. L.; Spirakis, C. S., Organic matter diagenesis as the key to a unifying theory for the genesis of tabular uranium-vanadium deposits in the Morrison Formation, Colorado Plateau. *Econ. Geol.* **1992**, *87*, (2), 352-365.
10. Leventhal, J. S.; Daws, T. A.; Frye, J. S., Organic geochemical analysis of sedimentary organic matter associated with uranium. *Appl. Geochem.* **1986**, *1*, (2), 241-247.
11. USEPA, Technical report on technologically enhanced naturally occurring radioactive materials from uranium mining Vol. 1: Mining and reclamation background. In Office of Radiation and Indoor Air EPA 402-R-08-005: 2008.
12. Ellsworth, H. V., Thucholite and uraninite from the Wallingford mine near Buckingham, Quebec. *Am. Mineral.* **1928**, *13* (8), 442-448.
13. Du, L.; Li, S. C.; Li, X. L.; Wang, P.; Huang, Z. Y.; Tan, Z. Y.; Liu, C. L.; Liao, J. L.; Liu, N., Effect of humic acid on uranium(VI) retention and transport through quartz columns with varying pH and anion type. *J. Environ. Radioact.* **2017**, *177*, 142-150.
14. Luo, W.; Gu, B., Dissolution and mobilization of uranium in a reduced sediment by natural humic substances under anaerobic conditions. *Environ. Sci. Technol.* **2009**, *43*, (1), 152-156.
15. Sutton, R. S., G., Molecular structure in soil humic substances: the new view. *Environ. Sci. Technol.* **2005**, (39), 9009-9015.
16. Tinnacher, R. M.; Nico, P. S.; Davis, J. A.; Honeyman, B. D., Effects of fulvic acid on uranium(VI) sorption kinetics. *Environ. Sci. Technol.* **2013**, *47*, (12), 6214-6222.
17. Bordelet, G.; Beaucaire, C.; Phrommavanh, V.; Descostes, M., Chemical reactivity of natural peat towards U and Ra. *Chemosphere* **2018**, *202*, 651-660.
18. Aziz, M.; Shakir, K., Adsorption of U(VI) from dilute aqueous solutions onto peat moss. *Radiochim. Acta* **2007**, *95*, (1), 17-24.

19. Bone, S. E.; Dynes, J. J.; Cliff, J.; Bargar, J. R., Uranium(IV) adsorption by natural organic matter in anoxic sediments. *P. Natl. Acad. Sci. U.S.A* **2017**, (4), 711.
20. Daugherty, E. E.; Gilbert, B.; Nico, P. S.; Borch, T., Complexation and redox buffering of iron(II) by dissolved organic matter. *Environ. Sci. Technol.* **2017**, *51*, (19), 11096-11104.
21. Lenhart, J. J.; Cabaniss, S. E.; MacCarthy, P.; Honeyman, B. D., Uranium(VI) complexation with citric, humic and fulvic acids. *Radiochim. Acta* **2000**, *88*, (6), 345-353.
22. von der Heyden, B. P.; Roychoudhury, A. N.; Mtshali, T. N.; Tyliszczak, T.; Myneni, S. C. B., Chemically and geographically distinct solid-phase iron pools in the Southern Ocean. *Science* **2012**, *338*, (6111), 1199-1201.
23. Alessi, D. S.; Lezama-Pacheco, J. S.; Janot, N.; Suvorova, E. I.; Cerrato, J. M.; Giammar, D. E.; Davis, J. A.; Fox, P. M.; Williams, K. H.; Long, P. E.; Handley, K. M.; Bernier-Latmani, R.; Bargar, J. R., Speciation and reactivity of uranium products formed during in situ bioremediation in a shallow alluvial aquifer. *Environ. Sci. Technol.* **2014**, *48*, (21), 12842-12850.
24. Bhattacharyya, A.; Campbell, K. M.; Kelly, S. D.; Roebbert, Y.; Weyer, S.; Bernier-Latmani, R.; Borch, T., Biogenic non-crystalline U(IV) revealed as major component in uranium ore deposits. *Nat. Commun.* **2017**, *8*, 15538.
25. Bone, S. E.; Cahill, M. R.; Jones, M. E.; Fendorf, S.; Davis, J.; Williams, K. H.; Bargar, J. R., Oxidative uranium release from anoxic sediments under diffusion-limited conditions. *Environ. Sci. Technol.* **2017**, *51*, (19), 11039-11047.
26. Mikutta, C.; Langner, P.; Bargar, J. R.; Kretzschmar, R., Tetra- and hexavalent uranium forms bidentate-mono-nuclear complexes with particulate organic matter in a naturally uranium-enriched peatland. *Environ. Sci. Technol.* **2016**, *50*, (19), 10465-10475.

27. Bargar, J. R.; Williams, K. H.; Campbell, K. M.; Long, P. E.; Stubbs, J. E.; Suvorova, E. I.; Lezama-Pacheco, J. S.; Alessi, D. S.; Stylo, M.; Webb, S. M.; Davis, J. A.; Giammar, D. E.; Blue, L. Y.; Bernier-Latmani, R., Uranium redox transition pathways in acetate-amended sediments. *P. Natl. Acad. Sci. U.S.A* **2013**, *110*, (12), 4506-4511.
28. Peng, C.; Sundman, A.; Bryce, C.; Catrouillet, C.; Borch, T.; Kappler, A., Oxidation of Fe(II) organic matter complexes in the presence of the mixotrophic nitrate-reducing Fe(II)-oxidizing bacterium *acidovorax* sp BoFeN1. *Environ. Sci. Technol.* **2018**, *52*, (10), 5753-5763.
29. Scott, D. T.; McKnight, D. M.; Blunt-Harris, E. L.; Kolesar, S. E.; Lovley, D. R., Quinone moieties act as electron acceptors in the reduction of humic substances by humics-reducing microorganisms. *Environ. Sci. Technol.* **1998**, *32*, (19), 2984-2989.
30. Lovley, D. R.; Fraga, J. L.; Blunt-Harris, E. L.; Hayes, L. A.; Phillips, E. J. P.; Coates, J. D., Humic substances as a mediator for microbially catalyzed metal reduction. *Acta Hydroch. Hydrob.* **1998**, *26*, (3), 152-157.
31. Lv, J. T.; Han, R. X.; Huang, Z. Q.; Luo, L.; Cao, D.; Zhang, S. Z., Relationship between molecular components and reducing capacities of humic substances. *ACS Earth Space Chem.* **2018**, *2*, (4), 330-339.
32. Sachs, S., Geipel, G., & Bernhard, G. *Study of the redox stability of Uranium (VI) in presence of humic substances* FZKA--7070; Forschungszentrum Rossendorf e.V. (Germany). Inst. of Radiochemistry: 2005.
33. Granger H. C, S. E. S., Dean B. G., And Moore F. B. , Sandstone-type uranium deposits at Ambrosia Lake, New Mexico; an interim report. *Econ. Geol.* **1961**, *56*, (7), 1179-1210.
34. Nash, J. T., Uranium deposits in the Jackpile sandstone, New Mexico. *Econ. Geol.* **1968**, *63* (7), 737-750.

- 35.S. S. Adams, H. S. C., P. L. Hafen, H. Salek-Nejad, Interpretation of postdepositional processes related to the formation and destruction of the Jackpile-Paguate uranium deposit, Northwest New Mexico. *Econ. Geol.* **1978**, *73*, (8), 1635-1654.
- 36.El Hayek, E.; Torres, C.; Rodriguez-Freire, L.; Blake, J. M.; De Vore, C. L.; Brearley, A. J.; Spilde, M. N.; Cabaniss, S.; Ali, A.-M. S.; Cerrato, J. M., effect of calcium on the bioavailability of dissolved uranium(vi) in plant roots under circumneutral pH. *Environ. Sci. Technol.* **2018**, *52*, (22), 13089-13098.
- 37.Yang, Y.; Saiers, J. E.; Barnett, M. O., Impact of interactions between natural organic matter and metal oxides on the desorption kinetics of uranium from heterogeneous colloidal suspensions. *Environ. Sci. Technol.* **2013**, *47*, (6), 2661-2669.
- 38.Yang, Y.; Saiers, J. E.; Xu, N.; Minasian, S. G.; Tyliszczak, T.; Kozimor, S. A.; Shuh, D. K.; Barnett, M. O., Impact of natural organic matter on uranium transport through saturated geologic materials: from molecular to column scale. *Environ. Sci. Technol.* **2012**, *46*, (11), 5931-5938.
- 39.Bernier-Latmani, R.; Veeramani, H.; Vecchia, E. D.; Junier, P.; Lezama-Pacheco, J. S.; Suvorova, E. I.; Sharp, J. O.; Wigginton, N. S.; Bargar, J. R., Non-uraninite products of microbial U(VI) reduction. *Environ. Sci. Technol.* **2010**, *44*, (24), 9456-9462.
- 40.Lezama-Pacheco, J. S.; Cerrato, J. M.; Veeramani, H.; Alessi, D. S.; Suvorova, E.; Bernier-Latmani, R.; Giammar, D. E.; Long, P. E.; Williams, K. H.; Bargar, J. R., Long-Term in situ oxidation of biogenic uraninite in an alluvial aquifer: impact of dissolved oxygen and calcium. *Environ. Sci. Technol.* **2015**, *49*, (12), 7340-7347.
- 41.Massey, M. S.; Lezama-Pacheco, J. S.; Jones, M. E.; Ilton, E. S.; Cerrato, J. M.; Bargar, J. R.; Fendorf, S., Competing retention pathways of uranium upon reaction with Fe(II). *Geochim. Cosmochim. Ac.* **2014**, *142*, 166-185.

42. Ravel, B.; Newville, M., ATHENA, ARTEMIS, HEPHAESTUS: data analysis for X-ray absorption spectroscopy using IFEFFIT. *J. of Synchrotron Radiat.* **2005**, *12*, 537-541.
43. Kuwatsuka, S.; Watanabe, A.; Itoh, K.; Arai, S., Comparison of two methods of preparation of humic and fulvic acids, IHSS method and NAGOYA method. *Soil Sci. Plant Nutr.* **1992**, *38*, (1), 23-30.
44. Santín, C.; Yamashita, Y.; Otero, X. L.; Álvarez, M. Á.; Jaffé, R., Characterizing humic substances from estuarine soils and sediments by excitation-emission matrix spectroscopy and parallel factor analysis. *Biogeochemistry* **2009**, *96*, (1), 131-147.
45. Avasarala, S. Physical and chemical interactions affecting u and v transport from mine wastes. Dissertation, University of New Mexico, 2018.
46. Groudev, S.; Georgiev, P.; Spasova, I.; Nicolova, M., Bioremediation of acid mine drainage in a uranium deposit. *Hydrometallurgy* **2008**, (1-4), 93.
47. Blake, J. M.; Avasarala, S.; Artyushkova, K.; Ali, A.-M. S.; Brearley, A. J.; Shuey, C.; Robinson, W. P.; Nez, C.; Bill, S.; Lewis, J.; Hirani, C.; Pacheco, J. S. L.; Cerrato, J. M., Elevated concentrations of U and co-occurring metals in abandoned mine wastes in a Northeastern Arizona Native American Community. *Environ. Sci. Technol.* **2015**, *49*, (14), 8506-8514.
48. Ohno, T., Fluorescence inner-filtering correction for determining the humification index of dissolved organic matter. *Environ. Sci. Technol.* **2002**, *36*, (4), 742-746.
49. Leventhal, J. S., Organic geochemistry and uranium in grants mineral belt. *New Mexico Bureau of Mines & Mineral Resources* **1980**, *Memoir 38*, 10.
50. Omar F. Ruiz, B. M. T., José M. Cerrato In *Investigation of in situ leach (ISL) mining of uranium in New Mexico and post-mining reclamation*, New Mexico Geology, 2016; 2016; pp 77-89.

51. Cumberland, S. A.; Etschmann, B.; Brugger, J.; Douglas, G.; Evans, K.; Fisher, L.; Kappen, P.; Moreau, J. W., Characterization of uranium redox state in organic-rich Eocene sediments. *Chemosphere* **2018**, *194*, 602-613.
52. Shoesmith, D. W., Fuel corrosion processes under waste disposal conditions. *J. Nucl. Mater.* **2000**, *282*, (1), 1-31.
53. Fang, Q. L.; Chen, B. L.; Lin, Y. J.; Guan, Y. T., Aromatic and hydrophobic surfaces of wood-derived biochar enhance perchlorate adsorption via hydrogen bonding to oxygen-containing organic groups. *Environ. Sci. Technol.* **2014**, *48*, (1), 279-288.
54. von Gunten, K.; Alam, M. S.; Hubmann, M.; Ok, Y. S.; Konhauser, K. O.; Alessi, D. S., Modified sequential extraction for biochar and petroleum coke: Metal release potential and its environmental implications. *Bioresource Technol.* **2017**, *236*, 106-110.
55. Bogusz, A.; Oleszczuk, P.; Dobrowolski, R., Application of laboratory prepared and commercially available biochars to adsorption of cadmium, copper and zinc ions from water. *Bioresource Technol.* **2015**, *196*, 540-549.
56. Rahman, A.; El Hayek, E.; Blake, J. M.; Bixby, R. J.; Ali, A. M.; Spilde, M.; Otieno, A. A.; Miltenberger, K.; Ridgeway, C.; Artyushkoya, K.; Atudorei, V.; Cerrato, J. M., Metal reactivity in laboratory burned wood from a watershed affected by wildfires. *Environ. Sci. Technol.* **2018**, *52*, (15), 8115-8123.
57. Aiken, G., Fluorescence and Dissolved Organic Matter. In *Aquatic Organic Matter Fluorescence*, Baker, A.; Reynolds, D. M.; Lead, J.; Coble, P. G.; Spencer, R. G. M., Eds. Cambridge University Press: Cambridge, 2014; pp 35-74.
58. Zsolnay, A., Chapter 4 - Dissolved Humus in Soil Waters. In *Humic Substances in Terrestrial Ecosystems*, Piccolo, A., Ed. Elsevier Science B.V.: Amsterdam, 1996; pp 171-223.

59. Deshmukh, A. P.; Pacheco, C.; Hay, M. B.; Myneni, S. C. B., Structural environments of carboxyl groups in natural organic molecules from terrestrial systems. Part 2: 2D NMR spectroscopy. *Geochim. Cosmochim. Ac.* **2007**, *71*, (14), 3533-3544.
60. Hay, M. B.; Myneni, S. C. B., Structural environments of carboxyl groups in natural organic molecules from terrestrial systems. Part 1: Infrared spectroscopy. *Geochim. Cosmochim. Ac.* **2007**, *71*, (14), 3518-3532.
61. Murphy, R. J.; Lenhart, J. J.; Honeyman, B. D., The sorption of thorium (IV) and uranium (VI) to hematite in the presence of natural organic matter. *Colloid. Surface.* **1999**, *157*, (1), 47-62.
62. Li, D. E.; Kaplan, D. I.; Chang, H. S.; Seaman, J. C.; Jaffe, P. R.; van Groos, P. K.; Scheckel, K. G.; Segre, C. U.; Chen, N.; Jiang, D. T.; Newville, M.; Lanzirrotti, A., Spectroscopic Evidence of Uranium Immobilization in Acidic Wetlands by Natural Organic Matter and Plant Roots. *Environ. Sci. Technol.* **2015**, *49*, (5), 2823-2832.
63. Eby, D. M.; Artyushkova, K.; Paravastu, A. K.; Johnson, G. R., Probing the molecular structure of antimicrobial peptide-mediated silica condensation using X-ray photoelectron spectroscopy. *J. Mat. Chem.* **2012**, *22*, (19), 9875-9883.
64. Alessi, D. S.; Lezama-Pacheco, J. S.; Stubbs, J. E.; Janousch, M.; Bargar, J. R.; Persson, P.; Bernier-Latmani, R., The product of microbial uranium reduction includes multiple species with U(IV)-phosphate coordination. *Geochim. Cosmochim. Ac.* **2014**, *131*, (Supplement C), 115-127.
65. Cerrato, J. M.; Ashner, M. N.; Alessi, D. S.; Lezama-Pacheco, J. S.; Bernier-Latmani, R.; Bargar, J. R.; Giammar, D. E., Relative reactivity of biogenic and chemogenic uraninite and biogenic noncrystalline U(IV). *Environ. Sci. Technol.* **2013**, *47*, (17), 9756-9763.
66. Guo, X.; Szenknect, S.; Mesbah, A.; Labs, S.; Clavier, N.; Poinssot, C.; Ushakov, S. V.; Curtius, H.; Bosbach, D.; Ewing, R. C.; Burns, P. C.; Dacheux, N.; Navrotsky, A.,

Thermodynamics of formation of coffinite, USiO_4 . *Proc. Natl. Acad. Sci. U. S. A* **2015**, *112*, (21), 6551-6555.

67. Campbell, K.; Kukkadapu, R.; Qafoku, N.; D Peacock, A.; Leshner, E.; Williams, K. H.; Bargar, J.; Wilkins, M.; Figueroa, L.; Ranville, J.; Davis, J.; Long, P., Geochemical, mineralogical and microbiological characteristics of sediment from a naturally reduced zone in a uranium-contaminated aquifer. *Appl. Geochem.* **2012**, *27*, 1499-1511.

68. Qafoku, N. P.; Gartman, B. N.; Kukkadapu, R. K.; Arey, B. W.; Williams, K. H.; Mouser, P. J.; Heald, S. M.; Bargar, J. R.; Janot, N.; Yabusaki, S.; Long, P. E., Geochemical and mineralogical investigation of uranium in multi-element contaminated, organic-rich subsurface sediment. *Appl. Geochem.* **2014**, *42*, 77-85.

69. Wang, Y. H.; Fruttschi, M.; Suvorova, E.; Phrommavanh, V.; Descostes, M.; Osman, A. A. A.; Geipel, G.; Bernier-Latmani, R., Mobile uranium(IV)-bearing colloids in a mining-impacted wetland. *Nat. Comm.* **2013**, *4*, 9.

70. Mikutta, C.; Kretzschmar, R., Spectroscopic evidence for ternary complex formation between arsenate and ferric iron complexes of humic substances. *Environ. Sci. Technol.* **2011**, *45*, (22), 9550-9557.

71.....Stetten, L.; Blanchart, P.; Mangeret, A.; Lefebvre, P.; Le Pape, P.; Brest, J.; Merrot, P.; Julien, A.; Proux, O.; Webb, S. M.; Bargar, J. R.; Cazala, C.; Morin, G., Redox fluctuations and organic complexation govern uranium redistribution from U(IV)-phosphate minerals in a mining-polluted wetland soil, Brittany, France. *Environ. Sci. Technol.* **2018**.

Chapter 4. From Adsorption to Precipitation of U(VI) in the Presence of Natural Organic Matter

Carmen A. Velasco^{*1,2}, Adrian J. Brearley³, Jorge Gonzalez-Estrella⁴, Abdul-Mehdi S. Ali³,
María Isabel Meza¹, Stephen E. Cabaniss⁵, Bruce M. Thomson¹,
Tori Z. Forbes⁶, Juan S. Lezama Pacheco⁷, and José M. Cerrato¹

¹ Department of Civil, Construction & Environmental Engineering, MSC01 1070, University of New Mexico, Albuquerque, New Mexico 87131, USA

² Department of Chemical Engineering, Universidad Central del Ecuador, Ritter s/n & Bolivia, Quito 17-01-3972, Ecuador

³ Department of Earth and Planetary Sciences, MSC03 2040, University of New Mexico, Albuquerque, New Mexico 87131, USA

⁴ School of Civil and Environmental Engineering, Oklahoma State University, Stillwater Oklahoma 74078

⁵ Department of Chemistry and Chemical Biology, University of New Mexico, Albuquerque, New Mexico 87131, USA

⁶ Department of Chemistry, University of Iowa, Iowa City, Iowa 52242, USA

⁷ Department of Environmental Earth System Science, Stanford University, California 94305, USA

Abstract.

We investigated the interfacial reactions of U(VI) in the presence of natural organic matter (NOM) at pH 2, pH 4, and pH 7 in batch experiments with analyses done by chemical methods, electron microscopy, and advanced spectroscopy. Batch experiments reacted 200 mg L⁻¹ of Suwannee River NOM with 100 μM U(VI) in a 0.01M KCl solution. Soluble U concentrations at pH 2 and pH 4 after 0.5 h and 24h of reaction (p-value <0.05) decreased after reaction with NOM for 0.5 h, followed by an increase to near the initial concentration after 24 h. Soluble U at pH 7 at 0.5 h and 24 h remained close to the initial concentration of 100 μM, indicating that NOM facilitates the solubility of U at circum-neutral pH. Bulk analyses conducted by EXAFS indicate that U(VI) is mainly adsorbed to particulate organic matter (POM) at pH 4. Precipitates of U(VI)- and K-bearing crystalline solids at pH 4 characterized by transmission electron microscopy (TEM). This investigation demonstrates that adsorption and precipitation of U(VI) in the presence of NOM is relevant at pH 2 and pH 4, while the aqueous complexation of U by dissolved organic matter (DOM)¹ at pH 7 prevents its adsorption and precipitation. The reactions of U(VI) with NOM are relevant to mineralized deposits, radwaste repositories, wetlands, and other environmental systems.

4.1 Introduction

Uranium (U) ore deposits often have elevated concentrations of natural organic matter (NOM). Recent studies found the NOM abundance in U mineralized deposits ranging from 1% to 57%.^{2,3} The presence of NOM and pH fluctuations likely influence the seasonal variability of U concentration in surface waters and its accumulation in aquatic and riparian soils and plants.^{4,5} However, the mechanisms influencing the reactions of U in the presence of NOM are not well

understood. The toxic effects of U are well known.^{6,7} For reference the U.S. Safe Drinking Water Act regulations establish a maximum contaminant level (MCL) of $30 \mu\text{gL}^{-1}$ y.⁸

Natural organic matter is a complex combination of heterogeneous organic molecules, which often is characterized in part by its solubility. Dissolved organic matter (DOM) is operationally defined as the organic matter fraction that passes through a $0.45\text{-}\mu\text{m}$ filter; while particulate organic matter (POM) refers to the organic matter retained by a $0.45 \mu\text{m}$ filter.^{9 10} The solubility of NOM is determined in part by pH. At high pH values¹¹⁻¹³, the deprotonation of organic functional groups (e.g. phenolic and carboxylic groups) increases the hydrophilicity and, therefore, the solubility of NOM.^{14, 15} The solubility of NOM, in turn, influences the solubility of many metals, including U.¹⁶

The solubility of U is influenced by inorganic and organic reactions. For example, the solubility of uranyl minerals (e.g., uranyl-oxides, -silicates, -carbonates, -vanadates, or -phosphates) in oxidizing environments is influenced by pH, and complexation by inorganic and organic compounds, most notably carbonate ions.¹⁷⁻²⁰ Reactions with DOM and POM can affect the solubility of U as well. For instance, DOM may inhibit the precipitation of U minerals through the formation of U bidentate-mononuclear soluble complexes with carboxyl ligands.²¹⁻²⁸ Particulate organic matter may decrease the U solubility through adsorption, surface complexation, and possibly precipitation.²⁹⁻³² A previous study found that even at low pH conditions where U shows limited adsorption to sediment minerals, NOM immobilized U through its binding to carboxylic groups as a surface bidentate complex.³³ Another study that evaluated water discharged from a U mine site found that cationic forms of U are predominant (e.g $(\text{UO}_2)_3 (\text{OH})^{5+}$) at pH 6.0 to pH 6.6, and favored the adsorption of U onto the organic-rich sediments of a natural wetland.³⁴ Other studies have shown adsorption of UO_2^{2+} onto NOM in the pH range of 4 to 5.³⁵ It has also

been reported that the formation of U-humate complexes between pH 4 and 6 can influence the solubility of U in organic-rich environments.^{30, 31} Other studies suggest that low pH enhances U adsorption onto silica sand in the presence of FA²⁴ and onto hematite in the presence of HA.³⁶ Thus, the interactions of U with NOM are varied, depend on numerous chemical and surface characteristics, and not well understood.³⁷

The effect of pH on the precipitation of U in the presence of NOM needs to be further investigated. One approach has been modelling the reactivity of U according to a series of functional groups (e.g. carboxyl or phenolic) for fulvic acid (FA) and humic acid (HA).^{2, 10, 23} Few studies have been conducted to understand the influence of pH on the precipitation of U in the presence of natural organic matter² and humic acids.^{13, 27} Laboratory experiments conducted in a previous study showed that the complexation of uranyl with carboxyl groups from NOM may form uranyl-carboxyl complexes.⁴⁰

The objective of this study was to identify the effect of pH on the adsorption, precipitation, and solubilization of U(VI) in the presence of NOM by integrating laboratory-controlled batch experiments, spectroscopy, and electron microscopy. This investigation focused on U(VI) rather than both U(IV) and U(VI), because this is the oxidation state that is thermodynamically stable in most surface waters. The novelty of this investigation is the use of advanced microscopic and spectroscopic techniques to identify the adsorption and precipitation of U(VI) after reaction with NOM. The experimental conditions of our study are relevant for understanding the precipitation of U(VI) and NOM from mine drainage and source waters at circum-neutral pH. Our results provide insight into the interfacial reactions (i.e adsorption, complexation, precipitation) affecting the solubilization of U(VI) in organic-rich environments.

4.2 Materials and Methods

4.2.1 Chemicals. Suwannee River natural organic matter (NOM) was purchased from the International Humic Substance Society (IHSS). We used the Suwannee River NOM in our study because is a well characterized, commercially available, reference material, and has been used in numerous investigations of metal-NOM interactions.⁴¹⁻⁴⁴ Uranium in 4% HNO₃ for an analytical grade standard was acquired from SCP Science, Plasma Cal. Potassium Chloride (KCl) 99.999% trace metals basis was purchased from Sigma-Aldrich. We used 10 N NaOH solution from EMD, and 2% HNO₃ PlasmaPure grade from SCP Science to adjust pH.

4.2.2 Batch Experiments. In this paper we use U to denote U(VI) unless otherwise stated. We conducted 50-mL batch experiments at pH 2, pH 4, and pH 7 to assess the effect of pH on U and NOM precipitation. The variation on pH throughout the experiment was < 0.1. The U and NOM concentrations chosen for this study are based on conditions reported in a previous investigation using solid samples from the Jackpile Mine, New Mexico, USA.³ In this study, we used controlled experimental conditions to work in a more constrained system (i.e. the Suwannee River NOM and uranyl nitrate) to reduce the complexity of working with natural samples and enable specific reactions between U and NOM to be studied.³ We were interested in rapid reactions (< 24 h) between U and NOM which are relevant for certain natural and engineered systems. Thus, we chose reaction times of 0.5 h and 24 h for our experiments. Ionic strength can have a significant effect on cation binding to NOM at near neutral pH^{45, 46} and can influence cation adsorption to organic functional groups.⁴⁷ We therefore used 0.010 M KCl as a swamping electrolyte to minimize changes in ionic strength during the experiments. Two stock solutions of 400 mgL⁻¹ NOM and 200 μM-UO₂(NO₃)₂ in 0.02 M KCl were prepared. Equal volumes of stock solutions were added to 50-mL polypropylene centrifuge tubes to reach an initial concentration of 200 mgL⁻¹

¹ NOM and 100 $\mu\text{M-UO}_2(\text{NO}_3)_2$ in 0.01 M KCl as shown in Table S1. Control experiments containing only 100 $\mu\text{M-UO}_2(\text{NO}_3)_2$ in 0.01 M KCl (Control U), and only 200 mgL^{-1} NOM (Control NOM) were prepared as well. We conducted six replicates of each experiment. pH adjustments were conducted with HNO_3 or NaOH. Experiments were then capped and placed in a tumbler. One additional control experiment in the absence of KCl and NaOH was conducted to identify the effect of KCl and NaOH on interfacial reactions between U and NOM at the longest reaction time (24 h). We used NH_4OH to adjust pH. This sample was named Control 1; solids collected from this reaction were analyzed by TEM and XAS.

4.2.3 Aqueous Analyses. Chemical analyses were conducted on supernatant samples collected from all experiments after the reaction time (0.5 h and 24 h). Samples were centrifuged, and the supernatant was filtered through 0.20 μm syringe membranes (Pall Acrodisc, Westborough, MA, USA). Samples were acidified using ultrapure HNO_3 for subsequent measurement of the soluble U concentration by inductively coupled plasma mass spectroscopy (ICP-MS).

Dissolved Organic Carbon (DOC) measurements were conducted according to Standard Methods 5310c⁵² using the Persulfate-Ultraviolet method using a Teledyne-Tekmar Fusion TOC analyzer. All samples were filtered through a 0.20 μm syringe filter. An auto dilution of 10 to 1 for all samples was performed and analyzed by a Fusion TOC analyzer. The carbon content in the NOM used in this study was 50.7 wt. % according to the International Humic Substance Society catalog, so that a solution of 200 mg/L of NOM corresponds to 101.4 mgL^{-1} of DOC.

We measured the zeta potential of unfiltered samples from experiments U-KCl-NOM, control U, and control NOM after centrifugation and filtration using a Malvern Zetasizer Nano-ZS equipped with a He-Ne laser (633nm) and non-invasive backscatter optics (NIBS). The zeta potential in each sample was measured three times and the average was calculated.

Statistical analyses were conducted to analyze soluble U and DOC data using R statistical software.⁵³ The Shapiro-Wilks normality test was used to determine if the data were parametric or non-parametric. A three-way Anova was used for multivariate analyses as a function of pH (2, 4, and 7) considering concentrations of U and DOC in control experiment U, experiment U-NOM and time (0.5 h and 24 h). A t-test was also used to assess the significance of differences between U and U-NOM at each pH value tested in our experiments.

4.2.4 Solid Analyses. Solids were collected by centrifuging samples after the corresponding reaction time. Solids were combined from triplicate experiments, air dried and stored. Solid samples were analyzed by the following methods.

X-ray fluorescence. Bulk chemical analysis to determine the elemental composition of precipitates was done using an EDAX Orbis μ XRF spectrometer with a Rh anode X-ray tube. It was operated at 40 kV and 800 μ A with the 30 μ m polycapillary optic. The samples were evacuated to 0.3 torr and data were collected for 600 live seconds. We measured 5 analytical points on each sample, and we present the average of all measurements.

Electron Microprobe Microanalysis (EPMA) X-ray Mapping. We conducted EPMA on solid samples collected from experiments U-KCl-NOM after 0.5 h of reaction to confirm the presence of U on these samples. We chose these samples since soluble U concentration decreased after 0.5 h. A droplet of the disaggregated sample suspended in acetone was deposited on a silicon wafer and on 3 mm Cu mesh grids covered with a holey carbon support film for TEM analysis. Samples mounted on the silicon wafer for EPMA were coated with approximately 150 nm of gold, to enable quantitative determination of carbon. Qualitative X-ray mapping was performed on a JEOL 8200 Superprobe electron microprobe equipped with five wavelength dispersive spectrometers (WDS). Operating conditions were 15 kV accelerating voltage, 30 nA beam current, and a beam diameter

of 1 μm . Qualitative WDS mapping was also conducted on the TEM grids to locate U-rich particles prior to TEM analysis.

Transmission Electron Microscopy (TEM) and Electron Energy Loss Spectroscopy (EELS). TEM was conducted using Bright-Field TEM imaging (BFTEM), Selected Area Electron Diffraction (SAED), and Energy Dispersive X-ray Spectroscopy (EDS) using a JEOL 2010F Field Emission Gun scanning transmission electron microscope (FEG/STEM) instrument operating at 200 kV. Electron energy loss spectroscopy was carried out on the JEOL 2010F using GATAN GIF 2000 image filtering system and EDS X-ray analysis was performed using an Oxford AZTec EDS system with an ultrathin window XMax 80N 80 mm² SDD EDS detector. Both point EDS analysis in TEM mode and X-ray maps in STEM mode were obtained. Quantification of EDS data was carried out using the thin film approximation using theoretical K-factors. TEM analyses were conducted on solids collected from experiment U-KCl-NOM, Control U (U+KCl) and Control NOM (NOM). Table S1 summarizes these analyses.

Electron energy loss spectrometry (EELS) was carried out on a sample collected after 24 h from experiment U-KCl-NOM at pH 4 to investigate the composition of the crystalline solids. The EELS measurements on the solids were carried out using the GATAN GIF system at 197 kV in imaging mode on the carbon edge with an energy resolution of 1 eV. Calibration of each spectrum was carried out using the C K edge at 284 eV and the K L₂ edge at 296 eV.

X-ray Absorption Spectroscopy. XAS measurements were conducted on solids collected from experiments of U-KCl-NOM and U-NOM (Control 1) at pH 4 after 24h reaction time. We chose these samples because they showed the most prominent decrease in the soluble U concentration of the solution at pH 4 and to evaluate the effect of KCl on the reactions of U and NOM at pH 4. XAS measurements were conducted on beamline 7-3 at the Stanford Synchrotron Radiation

Lightsource (SSRL) at the U L_{III} edge in fluorescence mode. Data were collected at 10 K using a closed cycle cryostat. Samples were pulverized and pressed into the slots of aluminum holders and sealed with Kapton tape on both sides. Data processing and analyses for XAS were conducted using Athena and Artemis software.⁵⁴

4.3 Results and Discussion

4.3.1 Effect of NOM on U Solubility. Soluble U concentrations decreased after 0.5 h in experiments with NOM (U-KCl-NOM) at pH 2 and pH 4, compared to experiments without NOM (Control U) (Figure 1). However, soluble U concentrations subsequently increased after 24 h compared to results after 0.5 h (p-values <0.05). At pH 7, minimal changes in soluble U concentrations were observed in experiments with NOM after 0.5 h and 24 h. In experiments conducted at pH 7 without NOM we observed the precipitation of inorganic U-bearing solids at 0.5 h and 24 h. The pH did not change more than 0.1 pH units in these experiments. Results obtained for each experiment are presented in more detail below.

Experiments at pH 2. Soluble U concentration decreased in experiments U-KCl-NOM after 0.5 h from an initial concentration (100 μM), but then resolubilized after 24 h. The soluble U concentration was $78.5 \pm 10.8 \mu\text{M}$ after 0.5 h and increased to $99.2 \pm 3.7 \mu\text{M}$ after 24 h. In control experiments without NOM (Control U), soluble U concentration remained constant at $100.5 \pm 0.21 \mu\text{M}$ for the duration of the experiment. The DOC in all experiments at pH 2 ranged from 80 to 85 mgL^{-1} . In experiments U-KCl-NOM, DOC was $83.1 \pm 2.7 \text{mgL}^{-1}$ after 0.5 h, $82.6 \pm 2.2 \text{mgL}^{-1}$ after 24 h and in control experiments without U (Control NOM) it was $85.2 \pm 0.01 \text{mgL}^{-1}$ (Figure S1).

Our results showed that the soluble U concentration in the presence of NOM is affected by pH and reaction time. Several studies reported the effect of HA and FA on U mobility through

adsorption and complexation.^{21, 24, 27, 36} However, there are limited studies reporting adsorption and desorption of U onto NOM.³⁷ For example, in the presence of HA, the adsorption of U by hematite was enhanced at low pH.³⁶ The adsorption of U-humic complexes on quartz was enhanced between pH 3 to 6.²¹ The soluble U concentration likely decreased after 0.5 h by the adsorption of uranyl ions onto the POM. Consistent with our results, the adsorption of U onto other minerals and sediments have been observed to take place within 0.5 h.^{47, 55, 56} For instance, rapid adsorption of U onto ferrihydrite, independent of pH, has been observed within minutes of reaction.⁴⁷

The soluble U concentration likely increased after 24 h by U desorption reactions. Studies have shown that the desorption of U from minerals preloaded with U is completed within minutes to hours.⁵⁶⁻⁵⁹ A study using soils containing HA showed rapid desorption of U, while soils without HA did not show any U desorption.⁶⁰ A study found that the dissolution of Fe-oxides released adsorbed metals and may increase As and U mobility in ground water.⁶¹

Experiments at pH 4. The soluble U concentrations decreased more at pH 4 than at pH 2 after 0.5 h possibly due to rapid adsorption of uranyl ions onto POM. Soluble U concentration increased after 24 h relative to 0.5 h, as observed in experiments conducted at pH 2. Soluble U concentration was $62.6 \pm 19.7 \mu\text{M}$ after 0.5 h and increased to $95.3 \pm 3.1 \mu\text{M}$ after 24 h in experiments U-KCl-NOM, likely due to the desorption of the U. There was little change in the soluble U concentration in Control U experiments at 0.5 h and 24 h (Figure 1). The DOC in all experiments ranged from 84 to 88 mgL^{-1} . In experiments U-KCl-NOM, DOC was $86.6 \pm 1.3 \text{mgL}^{-1}$ after 0.5 h and $85.1 \pm 0.8 \text{mgL}^{-1}$ after 24 h. In experiments without U (Control NOM), DOC was $86.6 \pm 0.06 \text{mgL}^{-1}$. (Figure S1).

Our results showed that the association of U with POM increases from pH 2 to pH 4. Other investigations have found that the adsorption of U onto POM increases from pH 2 to pH ranging

from 4 – 6.^{13, 62, 47} Other studies suggested that HA and FA from NOM enhance the adsorption of U at low pH.^{24, 36} Uranyl ions can bind to HA significantly at pH 4.5 and 5.5.² The adsorption of U onto silica sand in the presence of FA at pH < 6.5 was lower compared to the adsorption onto silica sand without FA.²⁴ Rapid adsorption of U onto hematite at pH 4 occurred within 0.5 h,⁵⁵ and onto goethite at pH 6 was reported to be complete within minutes.⁵⁶ An important characteristic is that HA precipitates at acidic pH^{10-12, 23, 63-66}, thus we pursued solid characterization analyses to better investigate this precipitation reactions.

Experiments at pH 7. In experiments U-KCl-NOM at pH 7, soluble U concentrations remained close to the initial concentration (100 μM) over time. These results suggest that the aqueous complexation of U by DOM facilitates the solubility of U at pH 7. The soluble U concentration was $87.4 \pm 3.3 \mu\text{M}$ after 0.5 h and $99.6 \pm 3.7 \mu\text{M}$ after 24h (Figure 1). The aqueous complexation of U with organic ligands from DOM at circumneutral pH increases the mobility of U species.^{24, 25, 67} Consistent with our results, the aqueous complexation of dissolved humic substances with U at circumneutral pH can lead to less U adsorption onto POM.^{21, 27, 68, 69} Specifically, the formation of U-humate aqueous complexes at neutral pH decreases U adsorption onto POM.⁷⁰ Thus, our results confirm the effect of NOM on U solubility at pH 7.

The DOC concentrations measured in experiments U-KCl-NOM at pH 7 were slightly higher than those measured at pH 2 and pH 4. The DOC concentration in all experiments at pH 7 ranged from 87 to 89 mgL^{-1} . In experiments U-KCl-NOM at pH 7, the DOC concentration was $87.7 \pm 0.4 \text{ mgL}^{-1}$ after 0.5 h, and $88.6 \pm 0.1 \text{ mgL}^{-1}$ after 24 h. In experiments without U (Control NOM) at pH 7, the DOC concentration was $89.1 \pm 0.01 \text{ mgL}^{-1}$ (Figure S1). Our results suggest that as pH increases from pH 2 to pH 7, NOM becomes more soluble due to the deprotonation of carboxyl functional groups. The high DOC concentration detected at pH 7 is consistent with

literature studies reporting HA precipitate at low pH, while HA is soluble at high pH.^{10-12, 63, 66, 71,}
⁷² Our results are in agreement with literature showing that high DOC concentrations increase the solubility and mobility of U.^{21, 73, 74} Consistent with our findings, studies showed that higher pH promotes the dissolution of POM and increases the dissolved concentration of heavy metals through formation of metal-organic complexes.⁷⁵⁻⁷⁷

In the absence of NOM (U Control experiment), the soluble U concentration decreased over time due to inorganic precipitation reactions at pH 7. The soluble U concentration was 0.3 ± 0.3 μM after 0.5 h and 0.09 ± 0.1 μM after 24h compared to the initial concentration (100 μM). The inorganic precipitation of U (VI) from solution takes place at pH >4 and complete precipitation occurs at circumneutral pH.^{38, 39} The precipitation of uranyl oxide hydrate phases (e.g., metaschoepite ($\text{UO}_3(\text{H}_2\text{O})_2$), compreignacite ($\text{K}_2(\text{UO}_2)_6\text{O}_4(\text{OH})_6(\text{H}_2\text{O})_7$), sodium compreignacite ($\text{Na}_2(\text{UO}_2)_6\text{O}_4(\text{OH})_6(\text{H}_2\text{O})_7$), and clarkeite ($\text{Na}(\text{UO}_2)\text{O}(\text{OH})$) occurs at pH 5 to pH 7.^{19, 56, 78-82} The precipitation of these solids depends on the saturation caused by the concentration of cations and uranyl oxycations, and solution pH.^{19, 56, 78-82}

Statistical analyses indicate that our data are normally distributed (p-values>0.05). Thus, we conducted three-way parametric Anova tests. We found statistical differences in soluble U concentrations for pH 2 and pH 4 with respect to time (0.5 h and 24 h) and in U-KCl-NOM experiments (p-values <0.05). Statistical differences were detected for pH 2, pH 4, and pH 7 with respect to control U experiments (p<0.05). Statistical differences (p-value <0.05) were detected in the DOC concentration for pH 2, pH 4, and pH 7 with respect to NOM control and U-KCl-NOM experiments. There are no statistical differences in the DOC concentration between pH2, pH 4, and pH 7 with respect to time (p-value >0.05). See Tables S2 and S3.

We measured the ζ -potential of solids in unfiltered samples from experiments conducted at pH 2 and pH 4. We focused on samples at pH 2 and pH 4, because at these pH values we observed solids in these samples (Figure S2). ζ -potential measurements showed increasingly negative surface charge with increasing pH from pH 2 to pH 4. Even at pH 2 the dominant surface charge was negative, resulting in electrostatic attraction with positive uranyl cations. ζ -potential of samples from NOM control experiment is more negative compared to samples from the U-KCl-NOM experiment. ζ -potential in U control experiments is close to zero at pH 2 and pH 4. The ζ -potential indicates the dominant surface charge of a particle. The results suggest that adsorption of positive uranyl ions onto POM causes an increase in ζ -potential (to a more positive value) by neutralizing some of its negative functional groups. Other studies have reported that POM alone has a lower ζ -potential relative to experiments in which metals are present.^{83, 84}

4.3.2 Solid Analyses: From Adsorption to Precipitation. Solids collected from batch experiments were analyzed to study the effect of NOM on interfacial reactions with U, and to determine if the precipitation of U-bearing solid phases contributed to the changes in soluble U concentrations at different pH values. XAS measurements found that U is primarily adsorbed to POM on solids collected from U-KCl-NOM and U-NOM (Control 1) reactions at pH 4 after 24 h. Energy dispersive X-ray spectroscopy (EDS) using TEM detected adsorption of U onto POM at pH 2 and pH 4, and the precipitation of U-K-Na-bearing crystalline phases on samples from U-KCl-NOM experiments at pH 4 after 24 h. The Na in our experiments was introduced by NaOH solution used for pH adjustments. Higher concentrations of U were detected by μ XRF in solids collected from reactions of U-KCl-NOM at pH 4 than at pH 2 after 0.5h and 24h. Inorganic

precipitation was detected by integrating μ -XRF and TEM measurements on solids collected from U Control experiments at pH 7.

Micro X-ray fluorescence. Analysis by μ XRF detected higher U concentration on solids collected from experiments U-KCl-NOM at pH 4 (0.26 ± 0.05 atomic U % at 0.5 h and 0.20 ± 0.04 atomic U % at 24 h) compared to solids collected at pH 2 (0.09 ± 0.02 atomic U % at 0.5 h and 0.05 ± 0.01 U at 24 h, (Figure S2). No solids were recovered from experiments U-KCl-NOM at pH 7. The highest concentration of U detected in solids from this study was from the U control experiments (no NOM) at pH 7 (2.30 ± 0.09 atomic U % at 0.5 h and 3.97 ± 0.38 atomic U% at 24 h). No solids were detected in the control experiments at pH 2 and pH 4. These results are consistent with the observations from aqueous analyses on soluble U concentration discussed earlier. Experiments in which solutions showed a higher decrease in soluble U concentration, had a higher concentration of U on solids.

Analysis by μ XRF also detected higher concentration of K on solids collected from experiments U-KCl-NOM at pH 4 (6.90 ± 2.52 atomic K % at 0.5 h and 7.58 ± 2.28 atomic K % at 24 h) compared to solids collected at pH 2 (5.05 ± 2.92 atomic K % at 0.5 h and 2.99 ± 0.31 K at 24 h, Figure S1). The highest concentration of K detected was on solids collected from the Control experiment containing only U and KCl at pH 7 (27.22 ± 0.61 atomic K % at 0.5 h and 27.39 ± 7.86 atomic K% at 24 h). The μ -XRF measurements we report represent the mass fraction of U and K in the solid, but without accounting for the mass of C. This method does not measure the absolute concentration of U and K in the solid. Additional analyses were conducted to detect adsorbed and precipitated phases of U and K and NOM in these solids.

X-ray absorption spectroscopy. We observed the maximum decrease in the soluble U concentration in U-KCl-NOM experiments at pH 4. The maximum U concentration on the solids

analyzed by μ -XRF also corresponds to experiments U-KCl-NOM at pH 4. Thus, we chose the solid samples from reactions of U-KCl-NOM and U-NOM at pH 4 after 24 h to conduct XAS analyses. Note that XAS is a bulk, not a surface technique, thus these analyses correspond to the molecular-scale coordination of U associated with POM in the bulk. Results showed that U is mainly adsorbed to POM on both samples, U is likely bound to carboxylic functional groups adsorbed to POM (Figure 2). We identified distances of U-C pairs between $2.90 \pm 0.03 \text{ \AA}$ and $3.44 \pm 0.03 \text{ \AA}$ in samples from experiments U-KCl-NOM and U-NOM. We also identified a distance of $3.94 \pm 0.03 \text{ \AA}$ between U-U pairs possibly due to the presence of crystalline phases only in the sample from experiment U-KCl-NOM. As expected, XANES analyses found that U(VI) was the dominant form of U in both samples. The distances between U-O pairs were $2.27 \pm 0.04 \text{ \AA}$ and $2.43 \pm 0.03 \text{ \AA}$ for both reactors at pH 4. Our results agree with another study which identified distances of $2.36 \pm 0.05 \text{ \AA}$ for U-O bridging and $2.48 \pm 0.05 \text{ \AA}$ for bidentate ligand formation on the carboxylate groups of humics. Their results suggested a mix of these two surface complexes.⁸⁵ The U-C binding characteristics we present are within the range reported by another study which suggests that U-C distances can vary between 2.8 and 3.2 \AA depending on the organic compounds and pH value.⁸⁶ The signatures corresponding to U-C observed in our study are similar to those from monomeric U(IV) reported in previous studies.^{25, 87} These XAS signatures suggest the adsorption of U(IV) onto organic C.^{25, 87} Even though our system only contains U(VI), the signature U(IV)-C^{56, 72} previously identified should be highlighted as it suggests the adsorption of U onto organic C by surface complexation as we observed in our system. Electron microscopy analyzes were conducted to further analyze the solids obtained from experiments conducted in this study.

Electron Microscopy Analyses. The adsorption of U adsorbed onto amorphous POM was detected on solids collected from reactions of U-KCl-NOM at pH 2. Crystalline U-K phases associated with POM were detected at pH 4. U-K bearing solid phases were detected at pH 7 in the absence of NOM (Control U).

Experiment at pH 2. In samples collected from reactions of U-KCl-NOM, we found no evidence of distinct U-bearing particles on the POM, although U was detected on POM after 0.5 h and 24 h. EMPA showed the spatial association of U and organic carbon (C) from POM after 0.5 h likely due to the adsorption U onto POM. Energy dispersive X-ray spectroscopy (EDS) detected 0.30 U atomic % and 67.6 C atomic % (Figure S3). U-bearing crystalline solids were not detected by TEM on samples at 0.5 h and 24 h. The heterogeneity in U concentration within the POM observed at 0.5 h and 24 h and the absence of U-bearing particles suggests U is likely adsorbed onto POM at pH 2 (Figure 3 and Figure 4). Measurements by TEM-EDS found 0.6 atomic % U, 5.8 atomic % K, and 79.7 atomic % C on solids collected after 0.5 h (Figure S5 A-B) and 1 atomic % U, 1 atomic % K, and 74 atomic % C after 24 h (Figure 4B). TEM analysis did not detect crystalline U-bearing particles at pH 2. The DF-STEM images illustrate that higher Z nanoparticles are present associated with the POM at pH 2. However, STEM EDS mapping indicates that these particles are not U-rich particles (Figure S4).

Experiments pH 4. The heterogeneity of U concentration in solids collected from reaction of U-KCl-NOM at pH 4 indicated, in addition to the adsorption of U onto POM, the precipitation of U-Na-K-bearing crystalline phases. The identification of U associated with both amorphous and crystalline solids on these samples is a unique result compared to the observations at pH 2. EPMA X-ray mapping of solids at pH 4 collected after 0.5 h showed less spatial association of U and C from POM compared to the samples at pH 2, likely because there is a lower concentration of POM

as pH increases from 2 to 4. Dark-field scanning transmission electron microscopy (DF-STEM) conducted on the solids collected from U-KCl-NOM experiment after 0.5 h detected amorphous carbon-rich solids, which we infer is POM. TEM-EDS detected 0.4 atomic % U, 0.5 atomic % K and carbon (75 atomic %) after 0.5 h in these solids (Figure S5). DF-TEM detected amorphous solids and U -K and U-Na crystalline bearing particles (<0.5 μm) on the sample collected at 24 h. Heterogeneous composition was detected by TEM-EDS on amorphous and crystal solids. For instance, amorphous solids had lower U and K concentrations (0.4 atomic % U; 2.4 atomic % K) compared to the crystalline solids (3.31 atomic % U, 10.04 atomic % K).

Amorphous solids had a higher concentration of C (64 atomic % C) than the crystalline solids (9.72 atomic %) (Figure 3 E-H). These results suggest that U is adsorbed to the POM while inorganic precipitates are not associated with POM. SAED patterns show that the crystalline structures are consistent with grimselite [010] $[\text{K}_3\text{NaUO}_2(\text{CO}_3)_3 \cdot \text{H}_2\text{O}]$ (Figure X). Electron energy loss spectra obtained from several individual crystals confirm that the phase is a carbonate, as shown in Figure 4. Carbonates have a very distinct sharp peak at 290 eV; however, the K L_2 edge in EELS spectra occurs at 296 eV, resulting in significant peak overlap between the K edge and C edge for carbonate. Nevertheless, a distinct shoulder is apparent on the lower energy side of the K edge that occurs at ~ 289 eV, about 1 eV lower than the typical energy of the carbonate peak in most minerals that occurs at 290.2 eV.⁸⁸ One possibility is that the energy of the carbonate peak is shifted to slightly lower energy in grimselite, as occurs, for example, in cerussite (PbCO_3), where the carbonate peak energy is 289.9 eV, but the energy shift is significantly larger in the case of grimselite. A further possibility is that this 289 eV peak is due to the presence of carboxylate groups coordinated to U, instead of carbonate. Such structures have been reported where U(VI) could be coordinated with other tricarboxylates⁸⁹ but retain the hexagonal symmetry of grimselite.

However, such structures result in a much larger unit cell, which is inconsistent with our electron diffraction data. We therefore favor the interpretation that this peak is a carbonate peak, rather than the result of carboxylate. However, past studies have shown that grimselite forms under near-neutral to alkaline conditions and not at low pH,^{90, 91} suggesting that grimselite may have precipitated metastably in these experiments. Another investigation reports the formation of metaschoepite [$\text{UO}_3(\text{H}_2\text{O})_2$] at pH 4.2 - 4.3 and Na-compreignacite [$\text{Na}_2(\text{UO}_2)_6\text{O}_4(\text{OH})_6 \cdot 7\text{H}_2\text{O}$] at pH ~ 5 ⁹². However, the SAED patterns we found in our study do not coincide with metaschoepite or Na-compreignacite and the presence of K in the EDS and EELS data is inconsistent with either of these phases. Thus, the solid precipitated from experiment U-KCL-NOM at pH 4 likely corresponds to another U-phase. We are aware that the presence of CO_3 is unlikely at pH 4, so these data most likely suggests that U(VI) could be coordinated with other tricarboxylates in a similar manner than grimselite as other study suggests.⁸⁹ TEM-EDS analyses of samples collected from experiment of U-NOM in the absence of KCl at pH 4 after 24 h did not detect crystalline U-bearing solids. These results confirm that U is adsorbed to POM at pH 4 in the absence of KCl, in agreement with XAS results.

It has been shown that humic substances can influence the immobilization and removal of U ions from aqueous solutions through adsorption and surface complexation.⁹³ In the presence of HA, the adsorption of U is enhanced at lower pH and is decreased with increasing pH.²⁹ Previous studies suggest that the adsorption of U at low pH values is likely enhanced due to the formation of protonated solid HA.^{11, 13, 93} Other studies showed that HA enhances the adsorption of U on hematite particles at low pH.^{31, 35}

Experiments pH 7. No precipitates were recovered from the U-KCl-NOM experiments at pH 7 after 0.5 h or 24 h. However, we detected the inorganic precipitation of U- and K- crystalline

precipitates in the U control experiment by TEM (i.e. no NOM) at pH 7 (Figure S6). These solids are stable crystalline structures as they did not exhibit sensitivity to the electron beam. The composition and electron diffraction data are consistent with clarkeite $[\text{Na}(\text{UO}_2)\text{O}(\text{OH})(\text{H}_2\text{O})_{0-1}]$. Based on thermodynamic modeling, schoepite, $[(\text{UO}_2)_8\text{O}_2(\text{OH})_{12} \cdot 12(\text{H}_2\text{O})]$, would be stable under these conditions.⁹² Other studies conducted with goethite report U surface precipitation of crystalline uranyl precipitates (e.g., schoepite and metaschoepite) at pH 6⁵⁶ and at circumneutral pH.^{37, 94} However, the SAED data obtained for this sample in our study are not consistent either schoepite or metaschoepite.

4.4 Mechanistic Insights.

This study shows the effect of pH on U adsorption, precipitation, and solubility in the presence of NOM. EXAFS and TEM results found that U is primarily associated with POM at pH 2 and pH 4 due to adsorption. However, precipitation of crystalline U-bearing phases was also detected in solids from reactions with NOM in a KCl solution at pH 4. These observations indicate that POM serves as a substrate for the adsorption and precipitation of U at pH 4. The solid-aqueous interfacial reactions between U, KCl, and NOM at pH 7 show that complexation of U-KCl-DOM facilitates the solubility of U at circumneutral pH.

We found differences in the adsorption and precipitation of U at 0.5 h and 24 h in the presence of NOM at pH 4. The TEM data indicate heterogeneity in the distribution of amorphous and crystalline U-phases onto POM in samples collected after 0.5 h and 24 h, suggesting that crystal nucleation occurred as the reaction reaches 24 h. Precipitates formed in aqueous solutions containing U, KCl, and NOM. Within the first 0.5 h of reaction, U adsorbs onto small POM grains and then these possible aggregate into larger grains these aggregates rapidly adsorbed onto POM. Our findings suggest that at 0.5 h the adsorption of U onto POM is the primary mechanism of

reaction between NOM and U-KCl, while the precipitation of U-K crystalline bearing solids is evident after 24 h of reaction. The surface of the POM could act as sites for heterogeneous nucleation of U-K bearing crystals as the reaction time progresses from 0.5 h to 24 h. The initial adsorption of U onto POM might be a precursor step for the precipitation of crystalline U-K bearing solids. Our results are unique given that other studies reported exclusively the adsorption of U onto organic material.^{31,36} However, other investigations have shown that metal ions adsorbed to POM can lead to the growth of crystalline phases.^{95,96} Also, it has been reported the growth of new solid phases typically involves metastable amorphous nanoparticle or cluster compounds generated during the initial stages of heterogeneous precipitation reactions.^{97,98}

After an initial decrease, the U concentration increased after 24 h in experiment U-KCl-NOM at pH 2 and pH 4 due to: 1) U desorption reactions; or 2) the dissolution of U-bearing solids that may have precipitated during the reaction with NOM. Previous work investigating the adsorption of U onto natural sediments reports the temporary adsorption of U-NOM complexes.^{59,99,100} Further investigations are necessary to better understand the kinetics of adsorption and surface precipitation reactions of U with POM as a function of pH in environmentally relevant conditions.

Our observations show that at pH 7, U remains in solution in the presence of NOM. Aqueous complexation of U-DOM enhances the solubility of U at circumneutral pH. Other studies have shown the adsorption of U onto NOM increases with pH below pH 7.⁷⁴ Conversely, U adsorption decreases at pH 7.⁷⁴ Future research is needed to better understand changes in POM and DOM chemistry due to the reaction with U and other metals.

4.5 Environmental Implications

Results from this work reveal information about interfacial reactions of U and NOM in organic-rich environments using a well-characterized organic material, Suwanee River NOM. The influence of pH on U, POM, and DOM reactions can affect the solubility and accumulation of U in natural environments. Adsorption and precipitation were studied at a reaction time of 0.5 h and 24 h, which is applicable for short-term scenarios in natural and engineered systems. For example, the retention time in engineered systems for ion exchange and precipitation of U usually ranges from minutes to hours.¹⁰² However, these time scales are much shorter than those occurring in natural environments such as an aquifer or involving organic detritus in the bottom of a wetland.¹⁰³ These reactions may occur in remediation processes such as treatment of acid mine drainage solutions (pH ranging between 2 and 4) and in natural waters (circumneutral pH). This work highlights the importance of metal and NOM interactions as these affect surface complexation, precipitation, and solubilization reactions that should be considered in reactive transport models for risk assessment and remediation purposes. Future research is necessary to improve the understanding of the optimal conditions for adsorption and precipitation of U and NOM for metal immobilization. Such studies could improve our understanding about the role of kinetics on the adsorption and precipitation of U in organic-rich environments. This information could be useful for sites affected by anthropogenic activities such as mining legacy, nuclear repositories, and other energy related applications.

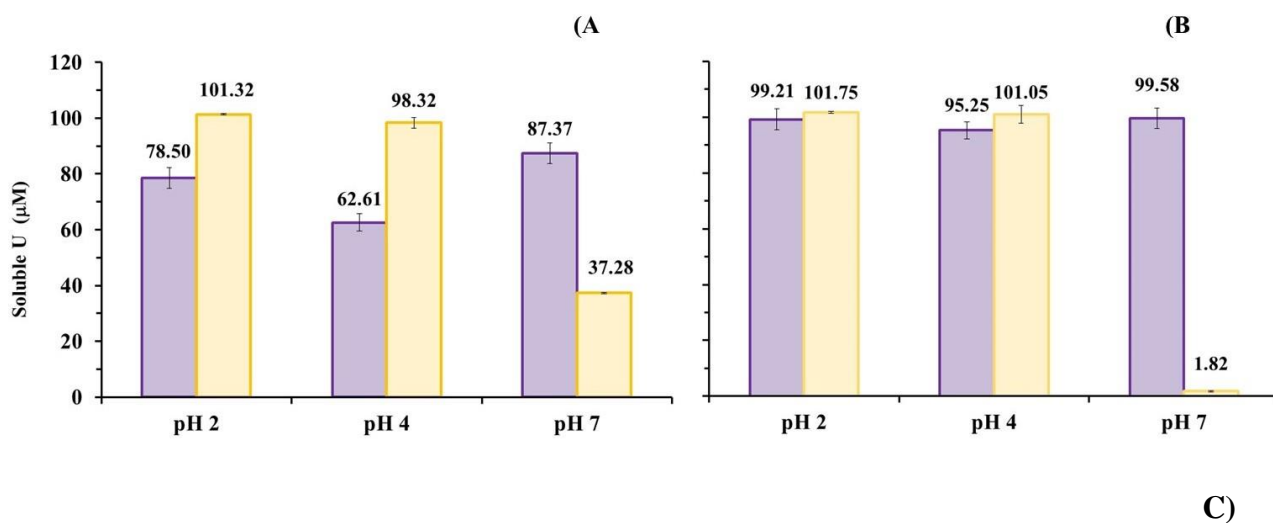
4.6 Acknowledgments

The authors would like to acknowledge the contributions of Dr. Mike Spilde (EPMA), Dr. Angelica Benavides (μ -XRF) and Dr. Achraf Nouredine (Zeta Potential) for their support and thoughtful comments, which contributed to significantly improve this study. Part of this research

was carried out at the Stanford Synchrotron Radiation Light source, a national user facility operated by Stanford University on behalf of the US DOE-OBER. Funding for this research was provided by the National Science Foundation (CAREER Award 1652619) and the National Institute of Environmental Health Sciences 472 Superfund Research Program (Award 1 P42 ES025589). Any opinions, findings, and conclusions or recommendations expressed in this publication are those of the author(s) and do not necessarily reflect the views of the National Science Foundation or the National Institutes of Health. Electron microscopy and electron microprobe analysis was carried out in the Electron Microbeam Facility, Department of Earth and Planetary Sciences and Institute of Meteoritics, University of New Mexico, a facility supported by the State of New Mexico and the National Science Foundation.

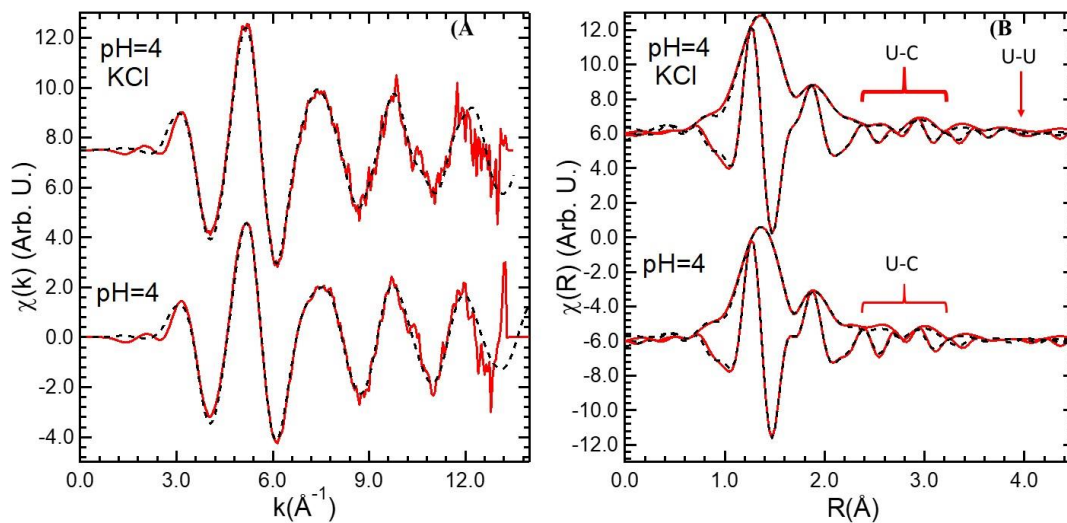
Supporting Information Available

Additional materials and methods, three tables (S1, S2, S3), and six figures (S1, S2, S3, S4, S5, S6 and S7) are available in SI. This material is available free of charge via the Internet at <http://pubs.acs.org>.



Soluble U (μM)	pH 2		pH 4		pH 7	
	U-KCl-NOM	U-KCl	U-KCl-NOM	U-KCl	U-KCl-NOM	U-KCl
After 0.5 hr.	78.5 \pm 10.8	101.3 \pm 5.3	62.6 \pm 19.3	98.3 \pm 0.5	87.4 \pm 3.3	37.3 \pm 13.1
After 24 hr.	99.2 \pm 3.7	101.7 \pm 1.8	95.3 \pm 3.1	101.1 \pm 1.8	99.6 \pm 3.7	1.8 \pm 0.7

Figure 5. Soluble U concentration in batch experiments containing NOM, U in 4% HNO₃ and KCl (purple) and U control experiment containing U in 4% HNO₃ (yellow) at (A) 0.5 h, (B) 24 h, and (C) Soluble U concentration summary results. Initial concentrations used are 200 mgL⁻¹ NOM and 100 μM -UO₂(NO₃)₂ in 0.01 M KCl



(C)

Correlations	U-NOM	U-KCl-NOM
N		2*
U-O1 R(Å)	1.78(1)	1.78(1)
$\sigma^2(\text{Å}^2)$	0.0028(1)	0.0025(2)
N	2.9(5)	3.3(2)
U-O2 R(Å)	2.27(4)	2.26(2)
$\sigma^2(\text{Å}^2)$	0.0098(24)	0.0057(1)
N	4.1(5)	3.7(2)
U-O21 R(Å)	2.43(3)	2.43(2)
$\sigma^2(\text{Å}^2)$	0.0098(24)	0.0057(1)
N	1.4(4)	0.9(4)
U-C1 R(Å)	2.90(2)	2.90(3)
$\sigma^2(\text{Å}^2)$	0.004*	
N	2.6(8)	3.0(8)
U-C2 R(Å)	3.43(4)	3.44(3)
$\sigma^2(\text{Å}^2)$	0.010*	
N		0.5(3)
U-U1 R(Å)		3.94(3)
$\sigma^2(\text{Å}^2)$		0.0053

*Denotes a fixed value derived from model compounds

Figure 2 X-ray absorption fine structure spectroscopy (XAFS) of solids collected from U-KCl-NOM and U-NOM batch experiments at pH 4 after 24 h reaction. (A) U L_{III}-edge EXAFS, (B) EXAFS Fourier transform and shell by shell fits indicate the presence of U likely bound to organic functional groups on POM through adsorption and U-U due presence of crystalline solid phases only in sample from U-KCl-NOM experiment. (C) Results table for shell by shell fits of the EXAFS signal.

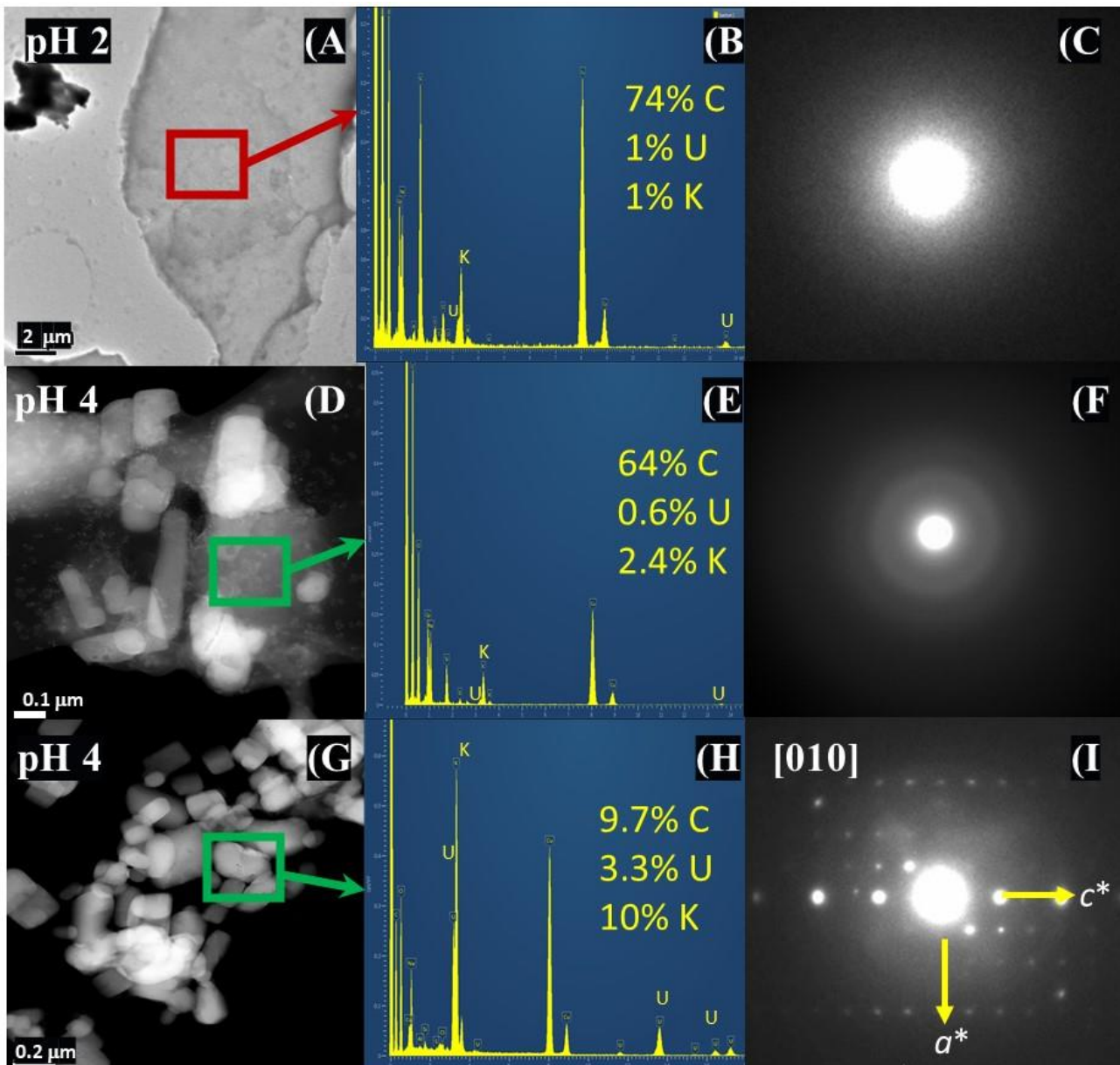


Figure 6 Bright-field TEM (TEM) and dark-field scanning transmission electron microscope (STEM) images, energy dispersive X-ray spectroscopy (EDS) spectra and selected area electron diffraction (SAED) patterns for solids collected from batch reactions of U-KCl-NOM after 24 at pH 2 (A, B, C) and pH 4 (D, E, F, G, H, I). TEM image and SAED pattern (A, C) show the adsorption of U onto amorphous POM at pH 2, indicated by the presence of a distinct U X-ray peaks in the EDS spectrum (B). EDS indicates low concentrations of U adsorbed onto POM (E), SAED shows diffuse diffraction rings characteristic of an amorphous phase (F) at pH 4 that contains lower concentrations of U than at pH 2. Crystallites of U-K-NA bearing solids with were identified at pH 4 (G, H) and slightly tilted SAED pattern that is consistent with the [010] zone axis of grimselite (I).

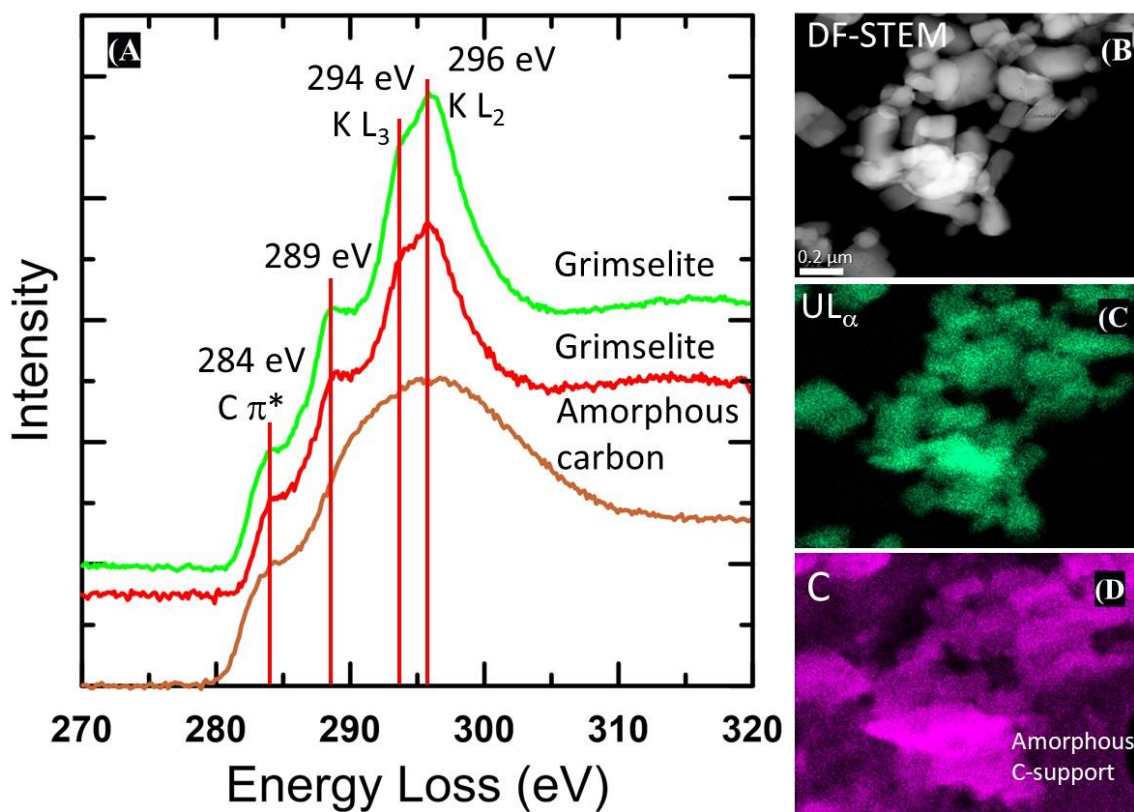


Figure 7 Electron energy loss spectra (EELS) (A), dark-field scanning transmission electron microscope (DF-STEM) image (B) and energy dispersive spectroscopy (STEM-EDS) X-ray (C, D). Two EEL spectra for grimselite are shown in red and green showing the presence of the K L_3 and $L_{2,3}$ edges at 294 and 296 eV, respectively. A distinct shoulder is present on the lower energy side of the K edge at 289 eV, which could be attributable to either carbonate or carboxylic groups. The lower spectrum (brown) is from the amorphous holey carbon film support with a distinct 284 eV edge that can be assigned to the C π^* peak. This feature is also apparent in the grimselite spectra because the crystallites occur directly on the holey carbon film support. The 289 eV feature is not present in the amorphous carbon substrate. Right hand images show a Dark-Field STEM image of the crystallites and X-ray maps of U and C, demonstrating that the crystallites contain C associated with U. An X-ray signal from the amorphous holey carbon film is clearly apparent in the lower right and upper left of the carbon X-ray map.

4.7 References.

1. Burdige, D. J.; Kline, S. W.; Chen, W., Fluorescent dissolved organic matter in marine sediment pore waters. *Marine Chemistry* **2004**, *89*, (1), 289-311.
2. Cumberland, S. A.; Etschmann, B.; Brugger, J.; Douglas, G.; Evans, K.; Fisher, L.; Kappen, P.; Moreau, J. W., Characterization of uranium redox state in organic-rich Eocene sediments. *Chemosphere* **2018**, *194*, 602-613.
3. Velasco, C. A.; Artyushkova, K.; Ali, A.-M. S.; Osburn, C. L.; Gonzalez-Estrella, J.; Lezama-Pacheco, J. S.; Cabaniss, S. E.; Cerrato, J. M., Organic functional group chemistry in mineralized deposits containing U(IV) and U(VI) from the Jackpile Mine in New Mexico. *Environmental Science & Technology* **2019**, *53*, (10), 5758-5767.
4. Blake, J. M.; De Vore, C. L.; Avasarala, S.; Ali, A.-M.; Roldan, C.; Bowers, F.; Spilde, M. N.; Artyushkova, K.; Kirk, M. F.; Peterson, E.; Rodriguez-Freire, L.; Cerrato, J. M., Uranium mobility and accumulation along the Rio Paguete, Jackpile Mine in Laguna Pueblo, NM. *Environ. Sci. Process. Impacts* **2017**, *19*, (4), 605-621.
5. El Hayek, E.; Torres, C.; Rodriguez-Freire, L.; Blake, J. M.; De Vore, C. L.; Brearley, A. J.; Spilde, M. N.; Cabaniss, S.; Ali, A.-M. S.; Cerrato, J. M., Effect of calcium on the bioavailability of dissolved uranium(VI) in plant roots under circumneutral pH. *Environ. Sci. Technol.* **2018**, *52*, (22), 13089-13098.
6. Zychowski, K. E.; Kodali, V.; Harmon, M.; Tyler, C. R.; Sanchez, B.; Ordonez Suarez, Y.; Herbert, G.; Wheeler, A.; Avasarala, S.; Cerrato, J. M.; Kunda, N. K.; Muttill, P.; Shuey, C.; Brearley, A.; Ali, A.-M.; Lin, Y.; Shoeb, M.; Erdely, A.; Campen, M. J., Respirable uranyl-vanadate-containing particulate matter derived from a legacy uranium mine site exhibits potentiated cardiopulmonary toxicity. *Toxicological Sciences* **2018**, *164*, (1), 101-114.

- 7.Hettiarachchi, E.; Paul, S.; Cadol, D.; Frey, B.; Rubasinghege, G., Mineralogy controlled dissolution of uranium from airborne dust in simulated lung fluids (SLFS) and possible health implications. *Environ. Sci. Technol. Let.* **2018**.
- 8.USEPA, Radionuclides Rule: A quick reference guide. Office of Water (4606). In EPA 816-F-01-003: 2001.
- 9.Potter, B. B. A. J. C. W. E. P. A., Washington, DC, 2005., Method 415.3 - Measurement of total organic carbon, dissolved organic carbon and specific UV absorbance at 254 nm in source water and drinking water. U.S. **2005**.
- 10.MacCarthy, I. H. S. a. P., *Aquatic Humic Substances: Influence on Fate and Treatment of Pollutants*. American Chemical Society: Washington, DC, 1988.
- 11.Kipton, H.; Powell, J.; Town, R. M., Solubility and fractionation of humic acid; effect of pH and ionic medium. *Analytica Chimica Acta* **1992**, 267, (1), 47-54.
- 12.Aiken, G. R.; McKnight, D. M.; Wershaw, R. L.; MacCarthy, P., Humic substances in soil, sediment, and water. 1985. *Soil Science* **1986**, 142, (5), 323.
- 13.Volkov, I. V.; Polyakov, E. V., Interaction of Humic Acids with Microelements/Radionuclides in Sorption Systems. *Radiochemistry* **2020**, 62, (2), 141-160.
- 14.Curtin, D.; Peterson, M. E.; Anderson, C. R., pH-dependence of organic matter solubility: Base type effects on dissolved organic C, N, P, and S in soils with contrasting mineralogy. *Geoderma* **2016**, 271, 161-172.
- 15.Nierop, K. G. J. J.; Jansen, B.; Verstraten, J. M., Dissolved organic matter, aluminium and iron interactions: precipitation induced by metal/carbon ratio, pH and competition. *Science of The Total Environment* **2002**, 300, (1), 201-211.

16. Weng, L.; Temminghoff, E. J. M.; Lofts, S.; Tipping, E.; Van Riemsdijk, W. H., Complexation with dissolved organic matter and solubility control of heavy metals in a sandy soil. *Environmental Science & Technology* **2002**, *36*, (22), 4804-4810.
17. Gorman-Lewis, D.; Burns, P. C.; Fein, J. B., Review of uranyl mineral solubility measurements. *The Journal of Chemical Thermodynamics* **2008**, *40*, (3), 335-352.
18. Finch, R.; Murakami, T., Systematics and paragenesis of uranium minerals. In 1999; Vol. 38, pp 91-180.
19. Kim, K.-W.; Kim, Y.-H.; Lee, S.-Y.; Lee, J.-W.; Joe, K.-S.; Lee, E.-H.; Kim, J.-S.; Song, K.; Song, K.-C., Precipitation characteristics of uranyl ions at different pHs depending on the presence of carbonate ions and hydrogen peroxide. *Environmental Science & Technology* **2009**, *43*, (7), 2355-2361.
20. Chang, P.; Yu, S.; Chen, T.; Ren, A.; Chen, C.; Wang, X., Effect of pH, ionic strength, fulvic acid and humic acid on sorption of Th(IV) on Na-rectorite. *Journal of Radioanalytical and Nuclear Chemistry* **2007**, *274*, (1), 153-160.
21. Du, L.; Li, S. C.; Li, X. L.; Wang, P.; Huang, Z. Y.; Tan, Z. Y.; Liu, C. L.; Liao, J. L.; Liu, N., Effect of humic acid on uranium(VI) retention and transport through quartz columns with varying pH and anion type. *J. Environ. Radioact.* **2017**, *177*, 142-150.
22. Luo, W.; Gu, B., Dissolution and mobilization of uranium in a reduced sediment by natural humic substances under anaerobic conditions. *Environ. Sci. Technol.* **2009**, *43*, (1), 152-156.
23. Sutton, R. S., G., Molecular structure in soil humic substances: the new view. *Environ. Sci. Technol.* **2005**, (39), 9009-9015.
24. Tinnacher, R. M.; Nico, P. S.; Davis, J. A.; Honeyman, B. D., Effects of fulvic acid on uranium(VI) sorption kinetics. *Environ. Sci. Technol.* **2013**, *47*, (12), 6214-6222.

25. Bone, S. E.; Dynes, J. J.; Cliff, J.; Bargar, J. R., Uranium(IV) adsorption by natural organic matter in anoxic sediments. *P. Natl. Acad. Sci. Usa* **2017**, (4), 711.
26. Bone, S. E.; Cahill, M. R.; Jones, M. E.; Fendorf, S.; Davis, J.; Williams, K. H.; Bargar, J. R., Oxidative uranium release from anoxic sediments under diffusion-limited conditions. *Environ. Sci. Technol.* **2017**, *51*, (19), 11039-11047.
27. Lenhart, J. J.; Cabaniss, S. E.; MacCarthy, P.; Honeyman, B. D., Uranium(VI) complexation with citric, humic and fulvic acids. *Radiochim. Acta* **2000**, *88*, (6), 345-353.
28. von der Heyden, B. P.; Roychoudhury, A. N.; Mtshali, T. N.; Tyliczszak, T.; Myneni, S. C. B., Chemically and geographically distinct solid-phase iron pools in the southern Ocean. *Science* **2012**, *338*, (6111), 1199-1201.
29. Tan, L.; Wang, X.; Tan, X.; Mei, H.; Chen, C.; Hayat, T.; Alsaedi, A.; Wen, T.; Lu, S.; Wang, X., Bonding properties of humic acid with attapulgite and its influence on U(VI) sorption. *Chem. Geol.* **2017**, *464*, 91-100.
30. Bordelet, G.; Beaucaire, C.; Phrommavanh, V.; Descostes, M., Chemical reactivity of natural peat towards U and Ra. *Chemosphere* **2018**, *202*, 651-660.
31. Omar, H. A.; Aziz, M.; Shakir, K., Adsorption of U(VI) from dilute aqueous solutions onto peat moss. *Radiochim. Acta* **2007**, *95*, (1), 17-24.
32. Mikutta, C.; Langner, P.; Bargar, J. R.; Kretzschmar, R., Tetra- and hexavalent uranium forms bidentate-mononuclear complexes with particulate organic matter in a naturally uranium-enriched peatland. *Environ. Sci. Technol.* **2016**, *50*, (19), 10465-10475.
33. Li, D. E.; Kaplan, D. I.; Chang, H. S.; Seaman, J. C.; Jaffe, P. R.; van Groos, P. K.; Scheckel, K. G.; Segre, C. U.; Chen, N.; Jiang, D. T.; Newville, M.; Lanzirrotti, A., Spectroscopic evidence

of uranium immobilization in acidic wetlands by natural organic matter and plant roots. *Environ. Sci. Technol.* **2015**, *49*, (5), 2823-2832.

34.Noller, B. N.; Watters, R. A.; Woods, P. H., The role of biogeochemical processes in minimising uranium dispersion from a mine site. *Journal of Geochemical Exploration* **1997**, *58*, (1), 37-50.

35.Ho, C. H.; Miller, N. H., Effect of humic acid on uranium uptake by hematite particles. *Journal of Colloid and Interface Science* **1985**, *106*, (2), 281-288.

36.Lenhart, J. J.; Honeyman, B. D., Uranium(VI) sorption to hematite in the presence of humic acid. *Geochimica et Cosmochimica Acta* **1999**, *63*, (19), 2891-2901.

37.Cumberland, S. A.; Douglas, G.; Grice, K.; Moreau, J. W., Uranium mobility in organic matter-rich sediments: A review of geological and geochemical processes. *Earth Sci. Rev.* **2016**, *159*, 160-185.

38.Tomažič, B.; Branica, M., Precipitation and hydrolysis of uranium(VI) in aqueous solutions—VII: Boundary conditions for precipitation from solutions of $\text{UO}_2(\text{NO}_3)_2\text{-KOH-K}$, Ba, La and Eu nitrate. *Journal of Inorganic and Nuclear Chemistry* **1972**, *34*, (4), 1319-1332.

39.Tomažič, B.; Samaržija, M.; Branica, M., Precipitation and hydrolysis of uranium (VI) in aqueous solutions-VI. *Journal of Inorganic and Nuclear Chemistry* **1969**, *31*, 1771.

40.Rallakis, D.; Michels, R.; Brouand, M.; Parize, O.; Cathelineau, M., The Role of Organic Matter on Uranium Precipitation in Zoovch Ovoo, Mongolia. *Minerals* **2019**, *9*, 310.

41.Kuhn, K.; Neubauer, E.; Hofmann, T.; von der Kammer, F.; Aiken, G.; Maurice, P., Concentrations and Distributions of Metals Associated with Dissolved Organic Matter from the Suwannee River (GA, USA). *Environ. Eng. Sci.* **2015**, *32*, 54-65.

- 42.Green, N.; McInnis, D.; Hertkorn, N.; Maurice, P.; Perdue, E., Suwannee River Natural Organic Matter: Isolation of the 2R101N Reference Sample by Reverse Osmosis. *Environ. Eng. Sci.* **2015**, *32*, 38-44.
- 43.Averett, R. C.; Leenheer, J.; McKnight, D.; Thorn, K. In *Humic substances in the Suwannee River, Georgia; interactions, properties, and proposed structures*, 1994; 1994.
- 44.Chen, H.; Johnston, R. C.; Mann, B. F.; Chu, R. K.; Tolic, N.; Parks, J. M.; Gu, B., Identification of Mercury and Dissolved Organic Matter Complexes Using Ultrahigh Resolution Mass Spectrometry. *Environmental Science & Technology Letters* **2017**, *4*, (2), 59-65.
- 45.Bartschat, B. M.; Cabaniss, S. E.; Morel, F. M. M., Oligoelectrolyte model for cation binding by humic substances. *Environmental Science & Technology* **1992**, *26*, (2), 284-294.
- 46.Cabaniss, S. E., Ph.D. Thesis, University of North Carolina, Chapel Hill. **1986**.
- 47.Waite, T. D.; Davis, J. A.; Payne, T. E.; Waychunas, G. A.; Xu, N., Uranium(VI) adsorption to ferrihydrite: Application of a surface complexation model. *Geochimica et Cosmochimica Acta* **1994**, *58*, (24), 5465-5478.
- 48.Blake, J. M.; Avasarala, S.; Artyushkova, K.; Ali, A.-M. S.; Brearley, A. J.; Shuey, C.; Robinson, W. P.; Nez, C.; Bill, S.; Lewis, J.; Hirani, C.; Pacheco, J. S. L.; Cerrato, J. M., Elevated Concentrations of U and Co-occurring Metals in Abandoned Mine Wastes in a Northeastern Arizona Native American Community. *Environ. Sci. Technol.* **2015**, *49*, (14), 8506-8514.
- 49.Blake, J. M.; De Vore, C. L.; Avasarala, S.; Ali, A.-M.; Roldan, C.; Bowers, F.; Spilde, M. N.; Artyushkova, K.; Kirk, M. F.; Peterson, E.; Rodriguez-Freire, L.; Cerrato, J. M., Uranium mobility and accumulation along the Rio Paguete, Jackpile Mine in Laguna Pueblo, NM. *Environ. Sci-Proc. Imp.* **2017**, *19*, (4), 605-621.

50. Avasarala, S. Physical and Chemical Interactions Affecting U and V Transport from Mine Wastes. Dissertation, University of New Mexico, 2018.
51. Avasarala, S.; Lichtner, P. C.; Ali, A.-M. S.; González-Pinzón, R.; Blake, J. M.; Cerrato, J. M., Reactive Transport of U and V from Abandoned Uranium Mine Wastes. *Environmental Science & Technology* **2017**, *51*, (21), 12385-12393.
52. Rice, E., Baird, R., Eaton, A. ., & Clesceri, L. . 5310 Total Organic Carbon (TOC). Standard Methods for the Examination of Water and Wastewater. In *Standard Methods For the Examination of Water and Wastewater*, American Public Health Association: 2005; pp 1–16.
53. R foundation for statistical computing: Vienna, A., *R Core Team R: A language and environment for statistical computing* **2015**.
54. Ravel, B.; Newville, M., Athena, Artemis, Hephaestus: data analysis for X-ray absorption spectroscopy using IFEFFIT. *J. of Synchrotron Radiat.* **2005**, *12*, 537-541.
55. Bargar, J. R.; Reitmeyer, R.; Lenhart, J. J.; Davis, J. A., Characterization of U(VI)-carbonato ternary complexes on hematite: EXAFS and electrophoretic mobility measurements. *Geochimica et Cosmochimica Acta* **2000**, *64*, (16), 2737-2749.
56. Giammar, D. E.; Hering, J. G., Time Scales for Sorption–Desorption and Surface Precipitation of Uranyl on Goethite. *Environmental Science & Technology* **2001**, *35*, (16), 3332-3337.
57. Liu, C.; Zachara, J.; Qafoku, N.; Wang, Z., Scale-dependent desorption of uranium from contaminated subsurface sediments. *Water Resources Research* **2008**, *44*.
58. Liu, C.; Shi, Z.; Zachara, J. M., Kinetics of Uranium(VI) Desorption from Contaminated Sediments: Effect of Geochemical Conditions and Model Evaluation. *Environmental Science & Technology* **2009**, *43*, (17), 6560-6566.

59. Manaka, M.; Seki, Y.; Okuzawa, K.; Watanabe, Y., Uranium sorption onto natural sediments within a small stream in central Japan. *Limnology* **2008**, *9*, (3), 173-183.
60. Bednar, A. J.; Medina, V. F.; Ulmer-Scholle, D. S.; Frey, B. A.; Johnson, B. L.; Brostoff, W. N.; Larson, S. L., Effects of organic matter on the distribution of uranium in soil and plant matrices. *Chemosphere* **2007**, *70*, (2), 237-247.
61. Swift Bird, K.; Navarre-Sitchler, A.; Singha, K., Hydrogeological controls of arsenic and uranium dissolution into groundwater of the Pine Ridge Reservation, South Dakota. *Applied Geochemistry* **2020**, *114*, 104522.
62. Baik, M. H.; Cho, W. J.; Hahn, P. S., Sorption of U(VI) onto granite surfaces: A kinetic approach. *Journal of Radioanalytical and Nuclear Chemistry* **2004**, *260*, (3), 495-502.
63. de Melo, B. A. G.; Motta, F. L.; Santana, M. H. A., Humic acids: Structural properties and multiple functionalities for novel technological developments. *Materials Science and Engineering: C* **2016**, *62*, 967-974.
64. Santín, C.; Yamashita, Y.; Otero, X. L.; Álvarez, M. Á.; Jaffé, R., Characterizing humic substances from estuarine soils and sediments by excitation-emission matrix spectroscopy and parallel factor analysis. *Biogeochemistry* **2009**, *96*, (1), 131-147.
65. Yamashita, Y.; Scinto, L. J.; Maie, N.; Jaffe, R., Dissolved Organic Matter Characteristics Across a Subtropical Wetland's Landscape: Application of Optical Properties in the Assessment of Environmental Dynamics. *Ecosystems* **2010**, *13*, (7), 1006-1019.
66. Zsolnay, A., Chapter 4 - Dissolved Humus in Soil Waters. In *Humic Substances in Terrestrial Ecosystems*, Piccolo, A., Ed. Elsevier Science B.V.: Amsterdam, 1996; pp 171-223.
67. Daugherty, E. E.; Gilbert, B.; Nico, P. S.; Borch, T., Complexation and Redox Buffering of Iron(II) by Dissolved Organic Matter. *Environ. Sci. Technol.* **2017**, *51*, (19), 11096-11104.

68. Czerwinski, K. R.; Buckau, G.; Scherbaum, F.; Kim, J. I., Complexation of the uranyl-ion with aquatic humic-acid. *Radiochimica Acta* **1994**, *65*, (2), 111-119.
69. Yang, Y.; Saiers, J. E.; Xu, N.; Minasian, S. G.; Tyliczszak, T.; Kozimor, S. A.; Shuh, D. K.; Barnett, M. O., Impact of Natural Organic Matter on Uranium Transport through Saturated Geologic Materials: From Molecular to Column Scale. *Environ. Sci. Technol.* **2012**, *46*, (11), 5931-5938.
70. Krepelova, A.; Sachs, S.; Bernhard, G., Uranium(VI) sorption onto kaolinite in the presence and absence of humic acid. *Radiochimica Acta* **2006**, *94*, (12), 825-833.
71. Gouré-Doubi, H.; Martias, C.; Smith, A.; Villandier, N.; Sol, V.; Gloaguen, V.; Feuillade, G., Adsorption of fulvic and humic like acids on surfaces of clays: Relation with SUVA index and acidity. *Appl. Clay Sci.* **2018**, *154*, 83-90.
72. Moulin, V.; Tits, J.; Ouzounian, G., Actinide speciation in the presence of humic substances in natural water conditions. *Radiochimica Acta* **1992**, *58-59*, (pt1), 179-190.
73. Cumberland, S. A.; Douglas, G.; Grice, K.; Moreau, J. W., Uranium mobility in organic matter-rich sediments: A review of geological and geochemical processes. *Earth-Sci. Rev.* **2016**, *159*, 160-185.
74. Payne, T.; Davis, J.; Waite, T., Uranium Adsorption on Ferrihydrite - Effects of Phosphate and Humic Acid. *Radiochimica Acta* **1996**, *74*, 239-243.
75. McBride, M. B., Reactions controlling heavy metal solubility in soils. In *Advances in Soil Science: Volume 10*, Stewart, B. A., Ed. Springer New York: New York, NY, 1989; pp 1-56.
76. Sauv e, S.; McBride, M.; Hendershot, W., Soil solution speciation of lead(II): Effects of organic matter and pH. *Soil Science Society of America Journal* **1998**, *62*, (3), 618-621.

- 77.Zsolnay, A.; Baigar, E.; Jimenez, M.; Steinweg, B.; Saccomandi, F., Differentiating with fluorescence spectroscopy the sources of dissolved organic matter in soils subjected to drying. *Chemosphere* **1999**, *38*, (1), 45-50.
- 78.Sowder, A. G.; Clark, S. B.; Fjeld, R. A., The effect of silica and phosphate on the transformation of schoepite to becquerelite and other uranyl phases. *Radiochimica Acta* **1996**, *74*, 45-49.
- 79.Kanematsu, M.; Perdrial, N.; Um, W.; Chorover, J.; O'Day, P. A., Influence of phosphate and silica on u(vi) precipitation from acidic and neutralized wastewaters. *Environmental Science & Technology* **2014**, *48*, (11), 6097-6106.
- 80.Zheng, Z.; Wan, J.; Song, X.; Tokunaga, T. K., Sodium meta-autunite colloids: Synthesis, characterization, and stability. *Colloids and Surfaces A: Physicochemical and Engineering Aspects* **2006**, *274*, (1), 48-55.
- 81.Kang, M. J.; Han, B. E.; Hahn, P. S., Precipitation and adsorption of uranium(VI) under various aqueous conditions. *Environmental Engineering Research* **2002**, *7*, (3), 149-157.
- 82.Giammar, D. E.; Hering, J. G., Influence of Dissolved sodium and cesium on uranyl oxide hydrate solubility. *Environmental Science & Technology* **2004**, *38*, (1), 171-179.
- 83.Ahmad, A.; Rutten, S.; Eikelboom, M.; de Waal, L.; Bruning, H.; Bhattacharya, P.; van der Wal, A., Impact of phosphate, silicate and natural organic matter on the size of Fe(III) precipitates and arsenate co-precipitation efficiency in calcium containing water. *Separation and Purification Technology* **2020**, *235*, 116117.
- 84.Russell, C. G.; Lawler, D. F.; Speitel, G. E.; Katz, L. E., Effect of Softening precipitate composition and surface characteristics on natural organic matter adsorption. *Environmental Science & Technology* **2009**, *43*, (20), 7837-7842.

85. Denecke, M. A.; Pompe, S.; Reich, T.; Moll, H.; Bubner, M., Measurements of the structural parameters for the interaction of uranium(VI) with natural and synthetic humic acids using EXAFS. *Radiochimica Acta* **1997**, *79*, (3), 151-159.
86. Regenspurg, S.; Margot-Roquier, C.; Harfouche, M.; Froidevaux, P.; Steinmann, P.; Junier, P.; Bernier-Latmani, R., Speciation of naturally-accumulated uranium in an organic-rich soil of an alpine region (Switzerland). *Geochimica et Cosmochimica Acta* **2010**, *74*, (7), 2082-2098.
87. Ulrich, K.-U.; Ilton, E. S.; Veeramani, H.; Sharp, J. O.; Bernier-Latmani, R.; Schofield, E. J.; Bargar, J. R.; Giammar, D. E., Comparative dissolution kinetics of biogenic and chemogenic uraninite under oxidizing conditions in the presence of carbonate. *Geochimica et Cosmochimica Acta* **2009**, *73*, (20), 6065-6083.
88. Brandes, J. A.; Wirick, S.; Jacobsen, C., Carbon K-edge spectra of carbonate minerals. *Journal of Synchrotron Radiation* **2010**, *17*, (5), 676-682.
89. Charushnikova, I. A.; Grigor'ev, M. S.; Krot, N. N., Synthesis and crystal structure of new U(VI) and Np(VI) benzoates, $K_{11}(AnO_2)_{23}(O_2C_6H_5)_{57}(H_2O)_{18+x}$. *Radiochemistry* **2010**, *52*, (2), 138-144.
90. Kubatko, K. A.; Helean, K. B.; Navrotsky, A.; Burns, P. C., Thermodynamics of uranyl minerals: Enthalpies of formation of rutherfordine, UO_2CO_3 , andersonite, $Na_2CaUO_2(CO_3)_3(H_2O)_5$, and grimselite, $K_3NaUO_2(CO_3)_3H_2O$. *American Mineralogist* **2005**, *90*, (8-9), 1284-1290.
91. O'Brien, T. J.; Williams, P. A., The aqueous chemistry of uranium minerals .4. Schrockingerite, grimselite, and related alkali uranyl carbonates. *Mineralogical Magazine* **1983**, *47*, (342), 69-73.
92. Gorman-Lewis, D.; Fein, J. B.; Burns, P. C.; Szymanowski, J. E. S.; Converse, J., Solubility measurements of the uranyl oxide hydrate phases metaschoepite, compreignacite, Na-

compreignacite, becquerelite, and clarkeite. *The Journal of Chemical Thermodynamics* **2008**, *40*, (6), 980-990.

93. Manahan, S. E., Interactions of Hazardous-Waste Chemicals with Humic Substances. In *Aquatic Humic Substances*, American Chemical Society: 1988; Vol. 219, pp 83-92.

94. Grenthe, I.; Wanner, H.; Forest, I.; Agency, O. N. E., *Chemical thermodynamics of uranium*. North-Holland ; Distributors for the U.S. and Canada, Elsevier Science Pub. Co.: Amsterdam; New York; New York, N.Y., U.S.A., 1992.

95. Maurice, A. P., Environmental Surfaces and Interfaces from the Nanoscale to the Global Scale. *Journal of Environmental Quality* - **2010**, *39*.

96. Gavrilescu, M.; Pavel, L. V.; Cretescu, I., Characterization and remediation of soils contaminated with uranium. *Journal of Hazardous Materials* **2009**, *163*, (2), 475-510.

97. Benning, L. G. W., G. A. In ; Brantley, S. L., Kubicki, J. D., White, A. F., Eds., Chapter 7. Nucleation, growth, and aggregation of mineral phases: mechanisms and kinetic controls. In *Kinetics of Water-Rock Interactions*, Springer: New York, 2008; pp 259-333.

98. Aiken, G. R.; Hsu-Kim, H.; Ryan, J. N., Influence of dissolved organic matter on the environmental fate of metals, Nanoparticles, and Colloids. *Environmental Science & Technology* **2011**, *45*, (8), 3196-3201.

99. Manaka, M.; Seki, Y.; Okuzawa, K.; Kamioka, H.; Watanabe, Y., Natural attenuation of dissolved uranium within a small stream of central Japan. *Limnology* **2007**, *8*, (2), 143-153.

100. Izquierdo, M.; Young, S. D.; Bailey, E. H.; Crout, N. M. J.; Lofts, S.; Chenery, S. R.; Shaw, G., Kinetics of uranium(VI) lability and solubility in aerobic soils. *Chemosphere* **2020**, *258*, 127246.

101. Gonzalez-Estrella, J.; Meza, I.; Burns, A. J.; Ali, A. S.; Lezama-Pacheco, J. S.; Lichtner, P.; Shaikh, N.; Fendorf, S.; Cerrato, J. M., Effect of bicarbonate, calcium, and pH on the reactivity of As(V) and U(VI) mixtures. *Environ Sci Technol* **2020**, *54*, (7), 3979-3987.
102. Toet, S.; Van Logtestijn, R. S. P.; Kampf, R.; Schreijer, M.; Verhoeven, J. T. A., The effect of hydraulic retention time on the removal of pollutants from sewage treatment plant effluent in a surface-flow wetland system. *Wetlands* **2005**, *25*, (2), 375-391.
103. Deditius, A. P., Utsunomiya, S., Ewing, R.C., The chemical stability of coffinite, $USiO_4 \cdot nH_2O$; $0 < n < 2$, associated with organic matter: a case study from Grants uranium region, New Mexico, USA. *Chem. Geol.* **2008**, *1-4*, (251), 33-49.

Chapter 5. Changes in dissolved natural organic matter chemistry resulting from reaction with U(VI)

Carmen A. Velasco^{1,2}, Jaqueline Jarvis³, Malak Tfaily⁴, Adrian J. Brearley⁵, Omar Holguin³,
Carson Odell¹, Angelica D. Benavidez⁶, Abdul-Mehdi S. Ali⁵, Juan S. Lezama Pacheco⁷,
Stephen E. Cabaniss⁸, Kateryna Artyushkova⁹, and José M. Cerrato¹

¹ Department of Civil, Construction & Environmental Engineering, MSC01 1070, University of New Mexico, Albuquerque, New Mexico 87131, USA

² Department of Chemical Engineering, Universidad Central del Ecuador, Ritter s/n & Bolivia, Quito 17-01-3972, Ecuador

³ Plant and Environmental Sciences College of Agricultural, Consumer, and Environmental Sciences New Mexico State University, Las Cruces, NM 88003, USA

⁴ Department of Soil, Water and Environmental Science, University of Arizona, Tucson, Arizona 85719, USA

⁵ Department of Earth and Planetary Sciences, MSC03 2040, University of New Mexico, Albuquerque, New Mexico 87131, USA

⁶ Department of Chemical and Biological Engineering, MSC01 1120, University of New Mexico, Albuquerque, New Mexico 87131, USA

⁷ Department of Environmental Earth System Science, Stanford University, California 94305, USA

⁸ Department of Chemistry and Chemical Biology, University of New Mexico, Albuquerque, New Mexico 87131, USA

Abstract.

We investigated the changes in dissolved organic matter (DOM) chemical composition resulting from the reaction of U(VI) with natural organic matter (NOM) at acidic and neutral pH in batch experiments. We used 200 mg L⁻¹ of Suwannee River NOM with 100 μM U(VI) for 24 h in batch reactors. Chemical and structural differences were detected in experiments at pH 2, pH 4 and pH 7, caused by the decrease in dissolved organic carbon (DOC) after reaction of U with NOM. The relative percent content of phenols and carboxylic functional groups in the supernatant decrease in U-NOM experiments compared to Control NOM at pH 2, pH 4, and pH 7 (p-value <0.05) as indicated by XPS analyses. At low pH, the abundance of compounds with higher O/C ratio in Control NOM experiments found acid-catalyzed hydrolysis products, but the abundance of these products is lower in U-NOM experiments, as indicated by ESI FTI-CR MS. These results, integrated with TEM and XAS analyses, suggest that the aqueous complexation of U with phenols and carboxylic groups from DOM, and, the adsorption of U onto POM affect the molecular composition of NOM. This study provides insights into the possible molecular changes in the organic functional chemistry due to reactions between U and NOM in organic-rich environments.

5.1 Introduction.

Uranium (U) naturally accumulates in organic-rich soils and geologic formations such as sandstone deposits, and roll-front formations.¹⁻³ Understanding the mechanisms affecting the reactivity of U and natural organic matter (NOM) is relevant to predicting the solubility of these constituents caused by natural and anthropogenic processes for risk assessment and remediation strategies. However, the reactions influencing the solubility U and NOM in environmentally relevant conditions remain poorly understood.

Interactions between U and NOM can affect the solubility of U in soils. Natural organic matter is most abundant in litter layers and upper mineral horizons, and is transported to subsoils in water as dissolved molecules and fine suspended colloids (collectively, “dissolved organic matter” or “DOM”)^{6, 7} Changes in pH and reactions with metals affect the molecular composition of NOM. Acid-catalyzed hydration reactions cause a shift towards highly oxygenated, high-molecular weight compounds by oxidation of carbon–carbon double bonds. These reactions increase O/C ratios without affecting the total number of carbons or H/C ratios in a molecule.⁸ High aromaticity is indicated by a low H/C ratio, while low O/C represents low hydrophilicity and polarity. Complexation of U by DOM is a relevant mechanism affecting U solubility in natural waters. DOM facilitates the solubility and mobility of U^{1, 9-11} through the complexation of U with humic acid (HA) between pH 4.5 and 7.¹² Alternatively, particulate organic matter (POM) decreases U solubility through adsorption, and precipitation reactions.¹³⁻¹⁵ At pH<3, carboxylic groups in NOM can increase the adsorption of U to mineral surfaces likely due to the low solubility of HA at low pH.^{10, 16 17} Previous studies conducted by our group and others found that the solubility of U from an organic-rich deposit is greatly influenced by pH, due to the reactions of NOM and U^{1, 2, 9, 10, 18} Despite these observations, the changes in DOM functional group chemistry due to the reaction with U will benefit from further investigation.

While there are several studies of the interactions between DOM and U, there is limited information about the reactions of U-DOM that control the complexation chemistry and its effect on U solubility in the environment.^{9, 19-21} Dissolved organic matter contains metal-binding functional groups (such as carboxylates, phenols, amines, thiols) with binding affinities and ligand densities spanning many orders of magnitude.²² Binding of U by DOM remains poorly defined at the molecular scale under environmentally relevant conditions.²² Understanding the reaction

mechanisms between U and DOM continues to be challenging at the molecular scale by the intrinsic complexity of DOM and U chemistry. Information is especially lacking on the binding constants, as well as significant analytical challenges.²² Improving the current understanding of the influence of pH on U-DOM complexes will help understand how the solubility of U changes in natural waters.^{19, 20, 23, 24} Although there is evidence that the hydrophobicity of DOM influences U mobility²⁵, the influence of pH and U on the organic functional chemistry of DOM is still not well understood.

The objective of this study is to identify changes in DOM chemistry due to the reaction of NOM and U at acidic and neutral pH. The novelty of this investigation is the identification of the molecular changes in DOM after the reaction with U by coupling batch reactions with advanced mass spectrometry, microscopy and spectroscopy. The experimental approach provides insights on the mechanisms affecting the solubility of U due to the reaction with NOM at environmentally relevant pH.

5.2 Materials and Methods

5.2.1 Chemicals.

Suwannee River natural organic matter (NOM) was purchased from the International Humic Substance Society. We used the Suwannee River NOM in our study because it is a widely used and well characterized reference material available from the International Humic Substances Society (IHSS), and has been used in numerous other investigations of metal-NOM interactions.²⁶⁻²⁸ Analytical grade uranium in 4% HNO₃ was acquired from SCP Science PlasmaCal. We used 28% NH₄OH purified by double distillation from Sigma-Aldrich and 2% HNO₃ PlasmaPure grade from SCP Science to adjust pH. Water LC-MS and methanol LC-MS, purchased from Fluka

Chromasolv, were used to conduct solid phase extraction on the DOC samples prior to conducting Fourier-transform ion cyclotron resonance mass spectrometry (FTICR-MS).

5.2.2 Batch Experiments.

We use U in this paper to denote U(VI) unless otherwise stated. 50-mL batch experiments at pH 2, pH 4, and pH 7 were used to assess the effect of pH on DOM chemistry and U solubility. The U and NOM concentrations were selected to represent relevant conditions found in mine wastes.^{2, 18, 29} We used well characterized Suwannee River NOM (SRNOM) to limit the complexity that would be encountered with working with natural samples from a mineralized deposit.² Two individual stock solutions of 200 μM - $\text{UO}_2(\text{NO}_3)_2$ and 0.4 g/L SRNOM were prepared to provide a source of U(VI) and NOM. Stock solutions were added to 50-mL polypropylene centrifuge tubes to reach an initial concentration of 100 μM of U and 0.2 g/L SRNOM according to Table S1. We also prepared control experiments using the same concentrations described earlier to determine the effect of U (Control NOM) and NO_3^- on DOM structure, and a control reactor to monitor the effect of NOM on U solubility (Control U). Six replicates of batch reactors were prepared, reactors were then capped and placed in a tumbler to allow reaction for 24h.

Statistical analyses were conducted to analyzed soluble U and DOC concentration data using R statistical software.³⁰ The Shapiro-Wilks normality test was used to assess if data were parametric or non-parametric. A three-way Anova was used for multivariate analyses as a function of pH (2, 4, and 7) considering concentrations of U and DOC in control reactor U and reactor U-NOM. A t-test was also used to compare statistical significance between U and U-NOM at each pH value tested in our experiments.

5.2.3 Microscopy and spectroscopy analyses.

After 24 h, reactors were centrifuged and filtered through a 0.2 μm syringe filter. Supernatant was analyzed by X-ray photoelectron spectroscopy (XPS) and solids collected were analyzed by transmission electron microscopy (TEM) and X-ray absorption spectroscopy (XAS). *X-ray photoelectron spectroscopy.* Drops of the decanted and filtered supernatant at pH 2, pH 4, and pH 7 were drop-cast on a freshly cleaved mica surface and allowed to dry. Dried supernatant and reacted solids from batch extraction experiments were then analyzed by XPS to obtain high-resolution spectra for C 1s, O 1s, and U 4f. High-resolution C 1s and O1s spectrum from freshly cleaved mica was obtained to account for the adventitious carbon present on the mica surface. Out of the total carbon detected, less than 10% was due to adventitious carbon on the surface of freshly cleaved mica (Figure S1). The rest of the carbon corresponded to the NOM in the supernatant. Details about sample preparation for XPS analyses were provided previously.²

Transmission electron microscopy (TEM). TEM was conducted using Bright-Field TEM imaging (BFTEM), Selected Area Electron Diffraction (SAED) and Energy Dispersive X-ray Spectroscopy (EDS) using a JEOL 2010F Field Emission Gun scanning transmission electron microscope (STEM) (FEG/STEM) instrument operating at 200 kV. This instrument is equipped with a GATAN GIF 2000 image filter system and an Oxford AZTec EDS system with an ultrathin window XMax 80N 80 mm² SDD EDS detector.

X-ray absorption spectroscopy. XAS measurements were conducted on beamline 7-3 at the Stanford Synchrotron Radiation Lightsource (SSRL) at the U L_{III} edge in fluorescence mode. Data were collected at 10 K using a close cycle cryostat. Samples were pulverized and pressed into the slots of aluminum holders and sealed with Kapton tape on both sides. Data processing and analyses for XAS were conducted using Athena and Artemis software.³¹

5.2.4 DOM analyses.

Supernatant was centrifuged and filtered through a 0.2 μm syringe filter prior to FTICR-MS and DOC analyses.

Electrospray ionization Fourier-transform ion cyclotron resonance mass spectrometry (ESI FT-ICR MS). Samples were desalted using solid phase extraction (SPE) using a styrene-divinylbenzene copolymer (PPL, Varian Bond Elut).³²⁻³⁴ Details of SPE extraction and recoveries are available in the Supplementary Information section. Samples recovered from SPE were diluted with methanol and analyzed at the National High Magnetic Field Laboratory at Florida State University on a 9.4 T FT-ICR MS. Electrospray ionization (ESI) was used in negative mode to generate largely unfragmented molecular ions. A detailed description of the instrument is given elsewhere.³⁵ The ESI negative mode favors the detection of molecules with acidic functional groups^{36,37} and has been used to study DOM from the Suwannee River.³³ Experimental conditions were: needle voltage, +4.4 kV; Q1 set to 50 m/z; and the heated, resistively-coated glass capillary operated at 180 °C. Ninety-six individual scans were averaged for each sample and internally calibrated using an organic matter homologous series separated by 14 Da ($-\text{CH}_2$ groups). Mass spectra were externally calibrated with a polyethylene glycol standard and then internally calibrated using a set of m/z values within the samples. Several criteria were met for picking out the calibration list: (1) peaks have a signal-to-noise (S/N) ratio ≥ 5 , (2) peaks that have intermediate intensities to minimize instrumental artifacts that yield peaks with too high or too low intensities, and (3) peaks have an error. All m/z lists, with an S/N ≥ 4 , were first searched for ^{13}C peaks and confirmed they were mostly singly-charged. The ^{13}C peaks were not included in the formulae calculations. The mass measurement accuracy was less than 1 ppm for singly-charged ions across a broad m/z range (100–900 m/z). The mass resolution was 350 K at 339 m/z. Data analysis

software (PetroOrg version X) was used to convert raw spectra to a list of m/z values (“features”), applying FTMS peak picker with a signal-to-noise ratio (S/N) threshold set to 7 and absolute intensity threshold to the default value of 100. Chemical formulae were assigned using in-house software following the Compound Identification Algorithm (CIA), described by Kujawinski and Behn (2006) and modified by Minor et al. (2012). Chemical formulae were assigned based on the criteria listed above and taking into consideration the presence of C, H, O, N, S, and P and excluding other elements.

We evaluated the chemical character of all of the data points for each sample spectrum using Van Krevelen diagrams on the basis of their molar H:C ratios (y-axis) and molar O:C ratios (x-axis)³⁸ We used Van Krevelen diagrams to visualize and compare NOM chemistry between samples from U-NOM and control reactors at different pH values, and enable approximate grouping of compounds into major biochemical classes (i.e., lipids, proteins, lignin, carbohydrates, and condensed aromatics)³⁹ We report, compound classes as relative abundance values based on counts of C, H, and O for the following H:C and O:C ranges: lipids ($0 < \text{O:C} \leq 0.3$, $1.5 \leq \text{H:C} \leq 2.5$), unsaturated hydrocarbons ($0 \leq \text{O:C} \leq 0.125$, $0.8 \leq \text{H:C} < 2.5$), proteins ($0.3 < \text{O:C} \leq 0.55$, $1.5 \leq \text{H:C} \leq 2.3$), amino sugars ($0.55 < \text{O:C} \leq 0.7$, $1.5 \leq \text{H:C} \leq 2.2$), carbohydrates ($0.7 < \text{O:C} \leq 1.5$, $1.5 \leq \text{H:C} \leq 2.5$), lignin ($0.125 < \text{O:C} \leq 0.65$, $0.8 \leq \text{H:C} < 1.5$), tannins ($0.65 < \text{O:C} \leq 1.1$, $0.8 \leq \text{H:C} < 1.5$), and condensed hydrocarbons ($0 \leq \text{O:C} \leq 0.95$, $0.2 \leq \text{H:C} < 0.8$)^{40, 41}

Dissolved Organic Carbon (DOC). Prior to conducting DOC analyses, MeOH was evaporated to dryness with nitrogen gas at 60 °C for 24 hours. Samples were then rehydrated with 10 mL Milli-Q water and sonicated for 15 minutes before DOC analysis. DOC analyses were done according to Standard Methods 5310c⁴² using the Persulfate-Ultraviolet method and a Teledyne-Tekmar Fusion TOC analyzer. All samples were filtered through a 0.20 µm syringe filter to remove

colloidal particles. A 10 to 1 auto dilution was done for all samples by the Fusion TOC analyzer. The carbon content in the NOM used in this study was 50.7% according to the International Humic Substance Society catalog, so that a solution of 200 mg/L of NOM corresponds to 101.4 mgL⁻¹ of DOC.

5.2.5 Aqueous Inorganic Analyses.

After the reaction time (24 h), reactors were centrifuged, and supernatant was filtered through 0.2 µm syringe membranes. Samples were acidified using ultrapure HNO₃ to quantify the soluble U in the supernatant from each batch extraction reactor by inductively coupled plasma optical emission spectroscopy (ICP-OES) and trace metal concentrations by inductively coupled plasma mass spectroscopy (ICP-MS).

5.3. Results and Discussion

5.3.1 Uranium and NOM Chemistry on Unreacted and Reacted Solids.

We analyzed the unreacted NOM and the solids collected from experiments U-NOM and control NOM experiments conducted at pH 2, pH 4, and pH 7.

Organic Functional Chemistry in Unreacted NOM. Fitting of high-resolution XPS C 1s data showed the characteristic peaks for phenolic (286.5 eV), carbonyl (288 eV), and carboxylic (289 eV) functional groups in the unreacted solid samples. Surface of unreacted solid NOM samples (as received) has phenolic (9.92±2.5 rel%), carbonyl (6.06±0.7 rel%), and carboxylic (80.1±0.2 rel%) functional groups. The identification of these functional groups by XPS is consistent with that presented in a previous publication from our research group about solids from mineralized deposits.²

Association of U and POM on Reacted Solids. We conducted XAS and TEM to understand the association and coordination of U in solids collected from U-NOM experiments at pH 2 and pH 4.

XAS measurements detected that U is primarily adsorbed to POM on solids collected from reactions of U and NOM at pH 2 and pH 4. Electron microscopy analyses detected the adsorption of U onto POM at pH 2 and pH 4. Inorganic precipitation was detected by integrating μ -XRF and microscopy in reactors without NOM (U control) at pH 7. Analyses conducted by TEM on the solid samples collected from reactors U-NOM at pH 2 and pH 4 by TEM detected amorphous solids, which we infer is POM. In the absence of NOM (Control U) at pH 7, we detected inorganic precipitation of U-K bearing solid phases, likely corresponding to clarkeite. Batch reactions of U and NOM experiments at pH 2, 4, and 7 were conducted to investigate changes in functional chemistry of DOM as a function of solution pH and the reaction with U.

XAS results show that U is mainly adsorbed to POM on both samples, U is likely bound to carboxylic functional groups adsorbed to POM (Figure 1). We identified distances between U-C pairs between $2.90 \pm 0.03 \text{ \AA}$ and $3.44 \pm 0.03 \text{ \AA}$ in samples from reactors at pH 2 and pH 4. The distances we found for the U-O pairs are $2.27 \pm 0.04 \text{ \AA}$ and $2.43 \pm 0.03 \text{ \AA}$ for both experiments. A shoulder identified at pH 2 at 3.95 \AA is likely caused by the self-absorption of functional groups in POM. In both samples U was assumed to be present as U(VI) only, and XANES analyses confirmed that U(VI) is the predominant U oxidation state. These results are consistent with those presented in Ch 4 in which the bulk of U is adsorbed to POM. Our results are also in agreement with another study of the reactions of U and organic acids which identified U-O for bridging ($2.36 \pm 0.05 \text{ \AA}$) and bidentate ($2.48 \pm 0.05 \text{ \AA}$) ligand formation on the carboxylate groups of HA suggesting a mix of these two surface complexes.⁴³ The U-C binding characteristics we report are within the range reported by another study which suggest that U-C distances can vary between 2.8 and 3.2 \AA depending on the organic compounds and pH value.³ The signatures corresponding to U-C observed in our study are similar to those from monomeric U(IV) reported in previous

studies.^{44, 45} Even though our system contains only U(VI), the similarities found between U(IV)-C by XAS should be highlighted as they show the adsorption of U onto POM. Microscopy analyzes were conducted to further analyze the solids obtained from reactions conducted in this study.

5.3.2 Effect of U and pH on DOM Chemistry.

The DOC concentration increased with pH and it ranged from 80 to 85 mg/L. The DOC concentration in U-NOM experiments is lower than in the Control NOM experiments, indicating the reaction with U affects the DOC concentration. In reactors containing U and NOM, DOC decreased by $1.8 \pm 0.27 \text{ mgL}^{-1}$ at pH 2, by $1.6 \pm 0.26 \text{ mgL}^{-1}$ at pH 4, and by $0.4 \pm 0.79 \text{ mgL}^{-1}$ at pH 7 compared to control reactors without U (Figure 2A). Statistical analyses indicate that our data are parametric (p -values > 0.05). Thus, we conducted three-way parametric Anova tests. Statistical differences (p -value < 0.05) were detected in the DOC concentration for pH 2, pH 4, and pH 7 with respect to control NOM and U-NOM experiments (p -value < 0.05).

At pH 2 and pH 4, soluble U concentration decreased in U-NOM experiments compared to Control NOM experiments (Figure 2B). At pH 7, soluble U concentration remained close to the initial concentration ($\sim 100 \text{ }\mu\text{M}$) in U-NOM experiments, indicating that U complexation with NOM facilitates U solubility. In contrast, in the absence of NOM (U Control) the soluble U concentration remaining after 24 h is negligible, likely due to the inorganic precipitation of U at pH 7 (Fig 3B). These findings are consistent with the results presented in Chapter 4. Differences in soluble U concentration were detected for pH 2, pH 4, and pH 7 with respect to control U experiments ($p < 0.05$). We did not find statistical differences in soluble U concentrations for pH 2, pH 4, and pH 4 in U-NOM experiments (p -values < 0.05). See Tables S2 and S3 in the SI.

Effect of U and pH on DOM Organic Functional Group Chemistry. Fitting of high resolution XPS C 1s spectra obtained from supernatant samples show a decrease in peak intensity of phenol, and

carboxylic functional groups following reaction with U at different pH values with respect to control experiments without U (Control NOM). Statistical analysis shows that phenol and carboxylic groups in experiments U-NOM are statistically different ($p < 0.05$) at pH 2, pH 4, and pH 7 while in Control NOM experiments, they are not different ($p > 0.05$). This suggests that the changes observed in the functional chemistry of DOM are likely due to the reaction with U at the pH values tested in this study. There was no difference in the carbonyl functional groups. High resolution spectra for C 1s from reactor U-NOM at pH 4 show the most noticeable decrease across our experimental design with respect to Control NOM. The number of phenolic functional groups decreased from 20.6 rel% to 12.4 rel% and carboxylic functional groups decreased from 12.6 rel% to 7.6 rel% when comparing reactor U-NOM to NOM control reactor. However, high resolution spectra for C 1s show less changes on the functional groups relative percent when comparing reactor U-NOM to control NOM at pH 7 (Figure 3).

.....Previous studies suggest that U in peat systems was coordinated to C atoms with carboxyl groups from particulate NOM through bidentate-mononuclear U(IV/VI) complexes.⁴⁶ Other studies found that U-phenolic bonds are prevalent at pH 6 while UO₂-carboxyl bonding is predominant at pH 3.5.⁴⁷ We previously found that phenols are the most abundant functional groups in NOM from a U mineralized deposit and were the most sensitive to pH changes.² Further analyses were conducted by ESI FT-ICR MS to identify changes on the molecular composition of DOM due to the reaction with U.

ESI FT-ICR MS Analysis on DOC Chemistry. We used ESI FT-ICR MS to compare the molecular composition of DOM due to the reaction with U at environmentally relevant pH. We analyzed samples from U-NOM and Control NOM, and Control HNO₃ experiments at pH 2, pH 4, and pH 7. We quantified the recovery of DOC and soluble U during the SPE process to have a basis of

how representative the purified DOC and U is in relation to the initial concentrations before the SPE process. The DOC recovery from the SPE in this work is within the range reported by another study using PPL cartridges (20%-65%).⁴⁸ Our results show that pH affects the DOC and U recovery. The DOC recovery decreases as pH increases from pH 2 to pH 7, while the recovery of soluble U increases with pH. We summarize our results by pH in Figure 4. The limited recovery might be due to incomplete elution of a fraction of apparent high molecular weight from the solid phase. A study comparing the original samples and SPE extracts using PPL cartridges found no significant differences in their molecular weight distribution.⁴⁸ Other studies have shown that PPL cartridge material offered the highest DOM recoveries and extracted a more representative proportion of DOM.⁴⁹ Thus, the DOM recovery by SPE is less critical for subsequent FT-ICR MS analysis, because those fractions that are not sufficiently recovered have comparatively small effects on the mass spectra.³³

Out of the total compounds detected in U-NOM experiment at pH 4, 70% are also seen in U-NOM at pH 2. This shows that experiments conducted at pH 2 and pH 4 share great similarities in the molecular structure of DOM. Additionally, from a chemical standpoint conditions at pH 2 and pH 4 can be classified as acidic. Also, ESI-FTICR-MS is not a quantitative technique due to variations in ionization efficiency among analytes and the SPE recovery variations among the experiments we conducted. Thus, we decided to only focus on comparing pH 2 and pH 7 experiments for the rest of the analyses shown.

Van Krevelen diagrams of experiments conducted at pH 2 show higher O/C ratios in unique compounds detected in Control NOM experiments indicating the presence of acid catalyzed (hydrolysis) products (Figure 5). The identification of high O/C elemental ratio at pH 2 observed in our study is consistent with observations from another study that attributed this to the presence

of acid-base catalyzed hydrolysis products.⁸ However, unique compounds detected in U-NOM experiments are shifted to a lower O/C elemental ratio compared to NOM control experiments at pH 2. These results suggest that the products of the reaction of U with NOM are different to those from the NOM Control experiment. The low O/C ratio (0.2-0.5) and low H/C ratio (0.5-1.0) of unique compounds detected in the U-NOM experiments suggest the presence of less saturated compounds with low degrees of oxidation, such as lignin-like and condensed hydrocarbon compounds. In contrast, unique compounds detected in Control NOM experiment have higher abundance of compounds with higher elemental O/C ratios (0.4-0.8) and higher elemental H/C ratios (0.7-1.5) compared to U-NOM experiment. This suggests the presence of tannin-like and lignin-like compounds.⁵⁰

At neutral pH, we did not detect a shift in the O/C and H/C ratios on the NOM Control experiments compared to the U-NOM experiments. In contrast to experiments conducted at acidic pH, we found that at pH 7, unique compounds detected in U-NOM experiments show a slight higher relative abundance of compounds with an O/C ratio (0.4-0.6) and H/C ratio (0.8-1.5), which corresponds to the lignin-like and tannin-like compounds. Control NOM do not show trends in the relative abundance of compounds with elemental ratios of O/C and H/C (0.8-1.5). The molecular composition of the SRNOM we report is consistent with that found in terrestrial and aquatic DOM, with C, H, and O formulae among the most abundant and atomic O:C (0-1.2) and H:C (0.3-2.5) ratios.⁵¹⁻⁵³

The shift observed in the van Krevelen diagrams for O/C elemental ratio at pH 2 is consistent with the shift observed in m/z spectra for NOM compared to U-NOM. All compounds were distributed over the mass range of m/z 200–800 (Figure SX). At pH 2, the mass spectrum in

U-NOM experiment is skewed to the lower m/z region compared to Control NOM. Experiments conducted at pH 7 did not show significant changes on the m/z distributions as observed at pH 2.

We did not identify any U-C soluble compounds in this work. This observation could be attributed to the following: (1) U likely formed complexes with DOM molecules with low abundances, such that these complexes were not detected by FTICR-MS as the presence of metals (Na) is an obstacle for ionization of the analytes of interest,^{54, 55} or complicate molecular formulae identification as metal-humic complexes do not stand out from the bulk and can only be identified through time-consuming molecular formula calculations on each individual measured mass.⁵⁶ (2) U-DOM complexes may have dissociated during ESI (e.g., those weakly or singly coordinated with S- or N-containing functional groups) and (3) U-DOM complexes were removed during the SPE (low U concentration measured after the SPE).⁵⁶⁻⁵⁸

5.4 Considerations about U-NOM Reactions.

This work shows the effect of the reaction between U and NOM on the DOM organic functional group chemistry at environmentally relevant pH. We found differences on the organic functional chemistry of DOM between experiments conducted with and without U. Our results show that the reaction with U primarily affects the relative concentration of phenol and carboxylic groups due to the complexation of U-DOM and the adsorption of U onto POM as indicated by EXAFS and TEM. We used ESI FT-ICR MS to complement XPS results on the supernatant to elucidate changes in the composition of organic matter due to the reaction with U at acidic and neutral pH. Our results show differences in the molecular composition of DOM after the reaction with U at pH 2 and pH 7, suggesting that pH and U play a role on the chemistry of DOM. The compositional similarity in the DOM of Control NOM experiments upon changing the pH suggests that likely the changes observed in DOM are due to the reaction with U. At acidic pH, more compounds

were ionized in U-NOM experiments suggesting that the reaction with U causes DOM to be more ionizable. Increases of the O/C and H/C ratios in DOM control experiments at pH 2 suggest that acid-catalyzed reactions (hydrolysis)⁸ is the main mechanism causing the changes in the DOM. However, in experiments with U at the same pH, we observed that unique compounds have lower O/C and H/C molecular ratios. Other studies have reported the presence of U-humate complexes at acidic pH.⁵⁶⁻⁵⁸ Overall, this work highlights the importance of phenol groups in the reactivity of U, aside from carboxylic groups. It is likely that U binds to phenolic and carboxylic functional groups in DOM through complexations reactions. Further work should be pursued to identify the U-DOM complexes are likely being formed in reactors at pH 2, pH 4, and pH 7.

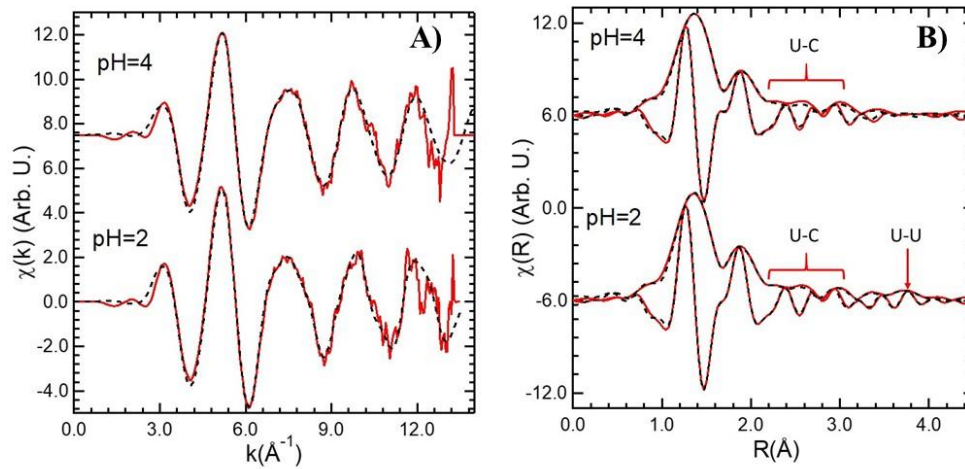
5.5. Environmental Implications.

Results from this work reveal information about interfacial reactions of U and NOM under pH conditions relevant to organic-rich environments. The influence of pH on U and DOM reactions can affect the solubility and accumulation of U in natural environments. Our work suggests that complexation reactions between U and phenolic and carboxylic functional groups in DOM could play an important role on the U chemistry in organic-rich environments.² The ability of dissolved organic matter (DOM) to complex with metals through phenol and carboxylic functional groups has profound implications for metal transport, solubility, bioavailability, and toxicity.^{56, 59-61} Understanding the molecular mechanisms of U-DOM can help to improve the understanding on U reactivity in organic-rich environments and lead to a better assessment of its solubilization and associated risks to the environment. Trace metal complexation by DOM has been studied for decades, but even today, determination of binding constants is hampered by the intrinsic complexity of DOM, the lack of stoichiometric information, and analytical limitations.¹⁸ Metal binding by DOM remains poorly defined at the molecular scale under environmentally relevant

conditions, such as low concentrations of metals relative to DOM.²² Future studies are warranted to further optimize and validate the methodology and to explore detailed molecular compositions and structures of U–DOM complexes that affect biological uptake and speciation of U in the environment.

5.6. Acknowledgments.

The authors would like to acknowledge the partnership with the New Mexico State University and the National High Magnetic Field Laboratory at Florida State. Part of this research was carried out at the Stanford Synchrotron Radiation Light source, a national user facility operated by Stanford University on behalf of the US DOE-OBER. Funding for this research was provided by the National Science Foundation (CAREER Award 1652619) and the National Institute of Environmental Health Sciences 472 Superfund Research Program (Award 1 P42 ES025589). Any opinions, findings, and conclusions or recommendations expressed in this publication are those of the author(s) and do not necessarily reflect the views of the National Science Foundation or the National Institutes of Health.



C)

Correlations		pH 2	pH 4
N			2*
U-O1	R(Å)	1.78(1)	1.78(1)
	$\sigma^2(\text{Å}^2)$	0.0025(2)	0.0028(1)
N		3.4(5)	2.9(5)
U-O2	R(Å)	2.29(2)	2.27(4)
	$\sigma^2(\text{Å}^2)$	0.0069(10)	0.0098(24)
N		3.6(5)	4.1(5)
U-O21	R(Å)	2.44(3)	2.43(3)
	$\sigma^2(\text{Å}^2)$	0.0069(10)	0.0098(24)
N		1.6(4)	1.4(4)
U-C1	R(Å)	2.90(2)	2.90(2)
	$\sigma^2(\text{Å}^2)$		0.004*
N		2.9(8)	2.6(8)
U-C2	R(Å)	3.42(4)	3.43(4)
	$\sigma^2(\text{Å}^2)$		0.010*
N		0.7(6)	
U-U1	R(Å)	3.90(3)	
	$\sigma^2(\text{Å}^2)$	0.0053(44)	

*Denotes a fixed value derived from model compounds

Figure 8 X-ray absorption fine structure spectroscopy (XAFS) of solids collected from U- NOM experiments conducted for 24 h reaction. U L_{III}-edge EXAFS of sample at **A)** pH 2 and **B)** pH 4. **C)** Results table for shell by shell fits of the EXAFS signal.

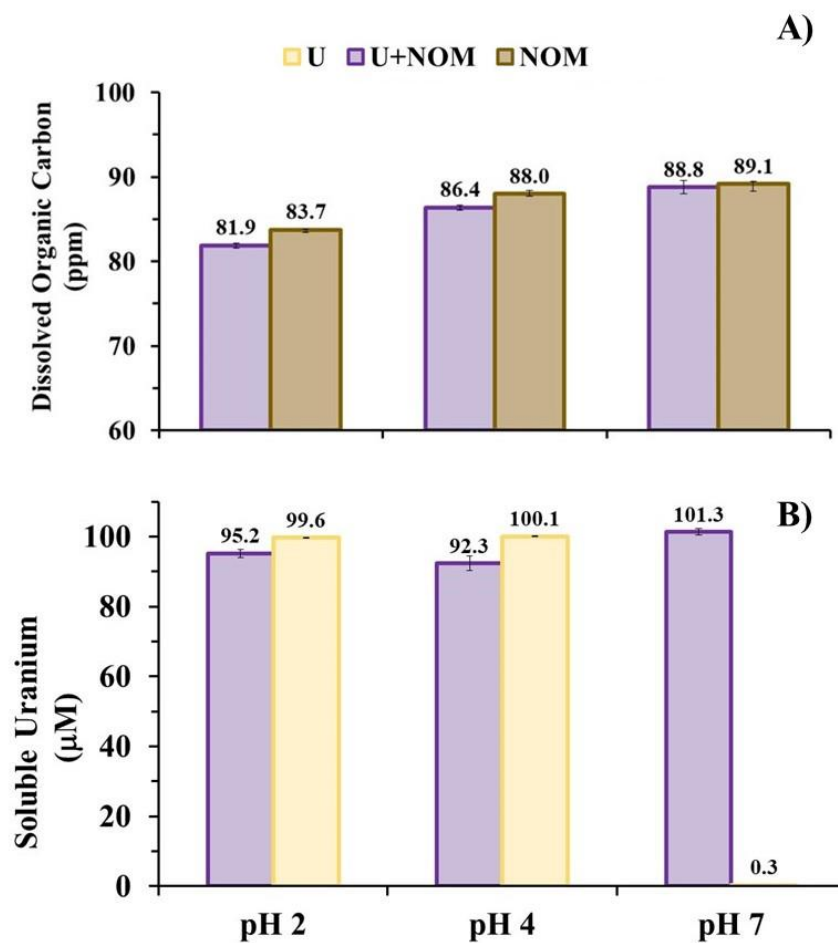
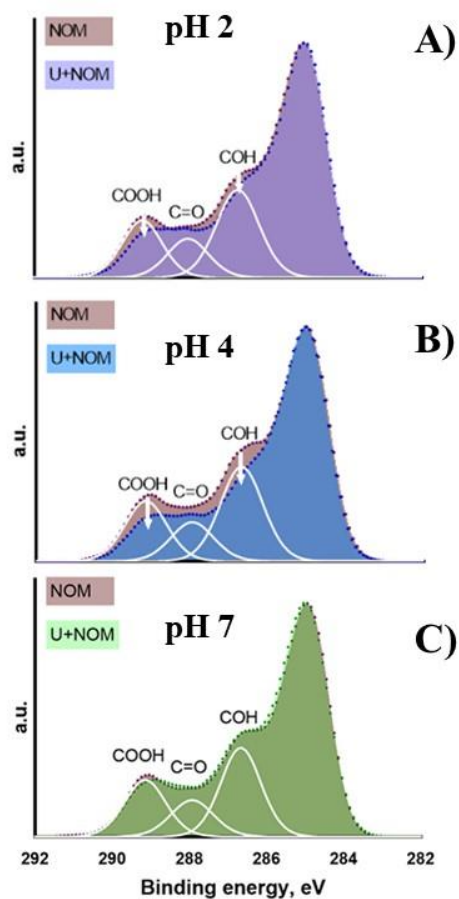


Figure 9. A) Dissolved organic matter (DOM) and B) soluble U concentration after 24 h reaction of NOM and U in 4% NO₃ (purple), control experiments containing only NOM (brown) and only U in 4% NO₃ (yellow).

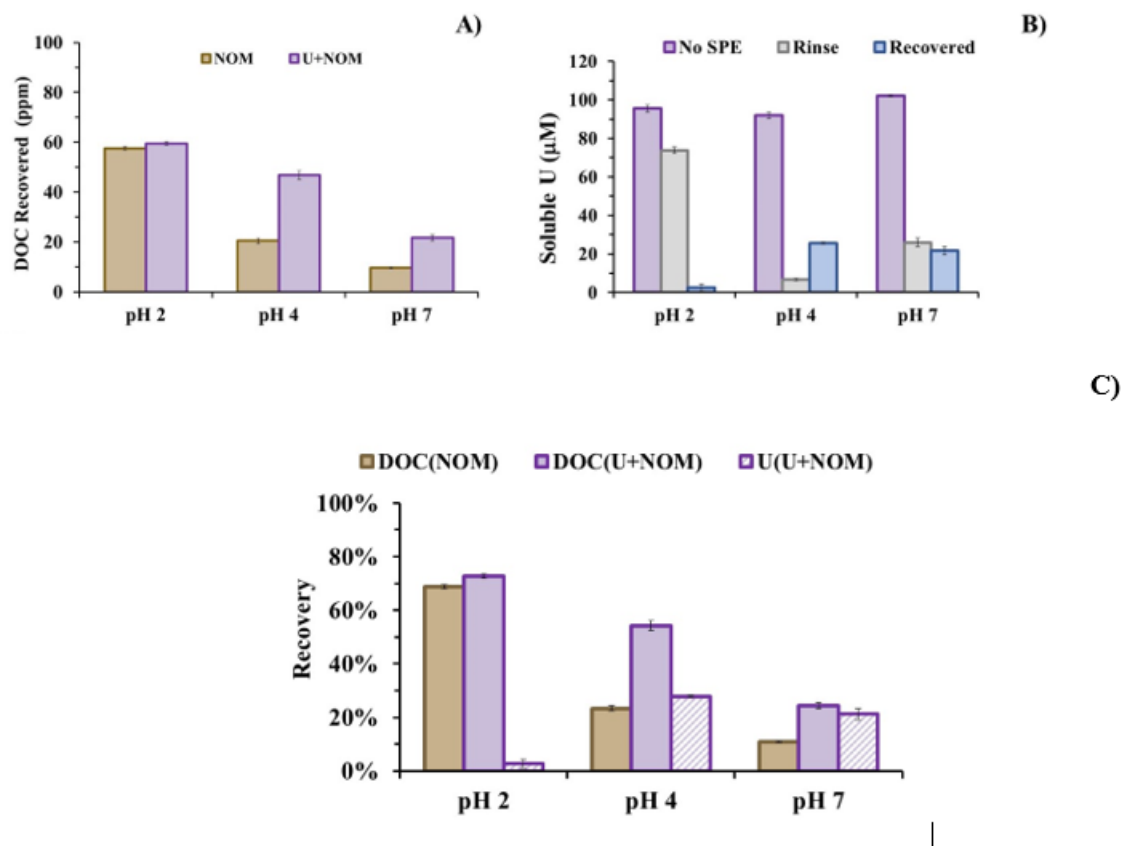
Supernatant: NOM vs U+NOM



D)

		Percent Concentration		
Reaction		Phenol (COH)	Carboxylic (COOH)	Carbonyl (C=O)
pH 2	U+NOM	18.9±0.6	11.4±0.9	8.1±0.5
	NOM	20.3±0.7	13.1±0.3	8.1±0.5
pH 4	U+NOM	18.7±0.5	10.2±0.4	7.4±0.5
	NOM	26.4±2.5	15.9±1.2	9.9±0.8
pH 7	U+NOM	20.4±0.4	11.4±0.3	8.9±0.2
	NOM	21.2±1.3	13.6±0.3	8.9±0.8

Figure 10. Fitting of high resolution XPS Carbon (C1s) of NOM control reactors and U+NOM as a function of pH of supernatant samples after 24 h reaction A) pH 2, B) pH 4, C) pH 7 and D) percent composition of C 1s.



Percent Recovery (%)	pH 2		pH 4		pH 7	
	U-NOM	NOM	U-NOM	NOM	U-NOM	NOM
DOC	72.7±0.8	68.8±0.8	54.2±1.8	23.4±1.1	24.4±1.2	10.8±0.3
U	2.7±1.7	-	27.9±0.5	-	21.2±2.2	-

Figure 11. Recovery from solid phase extraction (SPE) using a styrene-divinylbenzene copolymer (PPL, Varian Bond Elut) of batch experiments containing NOM and U in 4% NO₃ (purple) and Control NOM (brown) conducted at pH 2, pH 4, and pH 7: A) Dissolved organic carbon (DOC) and B) soluble uranium (U) concentration, and C) Summary of percent DOC and U recovery from SPE. Initial concentration of DOC 87 mgL⁻¹ and 100 µM U.

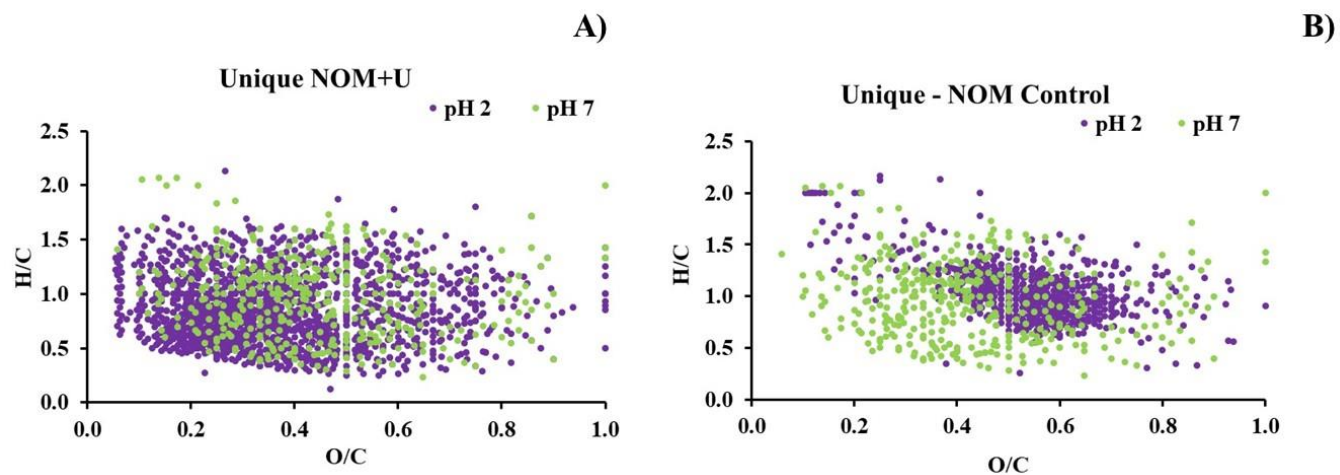


Figure 5. Van Krevelen diagrams of the masses uniquely calculated from the ultrahigh-resolution mass spectrum of U-NOM and NOM Control experiments conducted at pH 2 (purple) and pH 7 (green). Elemental ratios O/C and H/C for unique compounds in **A)** U-NOM experiments and **B)** NOM Control experiments.

5.7. References

1. Cumberland, S. A.; Douglas, G.; Grice, K.; Moreau, J. W., Uranium mobility in organic matter-rich sediments: A review of geological and geochemical processes. *Earth-Sci. Rev.* **2016**, *159*, 160-185.
2. Velasco, C. A.; Artyushkova, K.; Ali, A.-M. S.; Osburn, C. L.; Gonzalez-Estrella, J.; Lezama-Pacheco, J. S.; Cabaniss, S. E.; Cerrato, J. M., Organic Functional Group Chemistry in Mineralized Deposits Containing U(IV) and U(VI) from the Jackpile Mine in New Mexico. *Environmental Science & Technology* **2019**, *53*, (10), 5758-5767.
3. Regenspurg, S.; Margot-Roquier, C.; Harfouche, M.; Froidevaux, P.; Steinmann, P.; Junier, P.; Bernier-Latmani, R., Speciation of naturally-accumulated uranium in an organic-rich soil of an alpine region (Switzerland). *Geochimica et Cosmochimica Acta* **2010**, *74*, (7), 2082-2098.
4. Hoover, J. H.; Coker, E.; Barney, Y.; Shuey, C.; Lewis, J., Spatial clustering of metal and metalloid mixtures in unregulated water sources on the Navajo Nation – Arizona, New Mexico, and Utah, USA. *Science of The Total Environment* **2018**, *633*, 1667-1678.
5. Domingo, J. L., Reproductive and developmental toxicity of natural and depleted uranium: a review. *Reprod Toxicol* **2001**, *15*, (6), 603-9.
6. Kaiser, K.; Kalbitz, K., Cycling downwards – dissolved organic matter in soils. *Soil Biology and Biochemistry* **2012**, *52*, 29-32.
7. Nebbioso, A.; Piccolo, A., Molecular characterization of dissolved organic matter (DOM): a critical review. *Anal Bioanal Chem* **2013**, *405*, (1), 109-24.

8. Tfaily, M. M.; Podgorski, D. C.; Corbett, J. E.; Chanton, J. P.; Cooper, W. T., Influence of acidification on the optical properties and molecular composition of dissolved organic matter. *Analytica Chimica Acta* **2011**, *706*, (2), 261-267.
9. Du, L.; Li, S. C.; Li, X. L.; Wang, P.; Huang, Z. Y.; Tan, Z. Y.; Liu, C. L.; Liao, J. L.; Liu, N., Effect of humic acid on uranium(VI) retention and transport through quartz columns with varying pH and anion type. *J. Environ. Radioact.* **2017**, *177*, 142-150.
10. Payne, T.; Davis, J.; Waite, T., Uranium Adsorption on Ferrihydrite - Effects of Phosphate and Humic Acid. *Radiochimica Acta* **1996**, *74*, 239-243.
11. Burgos, W. D.; Senko, J. M.; Dempsey, B. A.; Roden, E. E.; Stone, J. J.; Kenmer, K. M.; Kelly, S. D., Soil humic acid decreases biological uranium(VI) reduction by *Shewanella putrefaciens* CN32. *Environ. Eng. Sci.* **2007**, *24*, (6), 755-761.
12. Lenhart, J. J.; Honeyman, B. D., Uranium(VI) sorption to hematite in the presence of humic acid. *Geochimica et Cosmochimica Acta* **1999**, *63*, (19), 2891-2901.
13. Tan, L.; Wang, X.; Tan, X.; Mei, H.; Chen, C.; Hayat, T.; Alsaedi, A.; Wen, T.; Lu, S.; Wang, X., Bonding properties of humic acid with attapulgite and its influence on U(VI) sorption. *Chem. Geol.* **2017**, *464*, 91-100.
14. Bordelet, G.; Beaucaire, C.; Phrommavanh, V.; Descostes, M., Chemical reactivity of natural peat towards U and Ra. *Chemosphere* **2018**, *202*, 651-660.
15. Omar, H. A.; Aziz, M.; Shakir, K., Adsorption of U(VI) from dilute aqueous solutions onto peat moss. *Radiochim. Acta* **2007**, *95*, (1), 17-24.
16. Krepelova, A.; Sachs, S.; Bernhard, G., Uranium(VI) sorption onto kaolinite in the presence and absence of humic acid. *Radiochimica Acta* **2006**, *94*, (12), 825-833.

- 17.Li, D. E.; Kaplan, D. I.; Chang, H. S.; Seaman, J. C.; Jaffe, P. R.; van Groos, P. K.; Scheckel, K. G.; Segre, C. U.; Chen, N.; Jiang, D. T.; Newville, M.; Lanzirotti, A., Spectroscopic Evidence of Uranium Immobilization in Acidic Wetlands by Natural Organic Matter and Plant Roots. *Environ. Sci. Technol.* **2015**, *49*, (5), 2823-2832.
- 18.Avasarala, S.; Torres, C.; Ali, A.-M. S.; Thomson, B. M.; Spilde, M. N.; Peterson, E. J.; Artyushkova, K.; Dobrica, E.; Lezama-Pacheco, J. S.; Cerrato, J. M., Effect of bicarbonate and oxidizing conditions on U(IV) and U(VI) reactivity in mineralized deposits of New Mexico. *Chemical Geology* **2019**, *524*, 345-355.
- 19.Luo, W.; Gu, B., Dissolution and Mobilization of Uranium in a Reduced Sediment by Natural Humic Substances under Anaerobic Conditions. *Environ. Sci. Technol.* **2009**, *43*, (1), 152-156.
- 20.Tinnacher, R. M.; Nico, P. S.; Davis, J. A.; Honeyman, B. D., Effects of Fulvic Acid on Uranium(VI) Sorption Kinetics. *Environ. Sci. Technol.* **2013**, *47*, (12), 6214-6222.
- 21.Lenhart, J. J.; Cabaniss, S. E.; MacCarthy, P.; Honeyman, B. D., Uranium(VI) complexation with citric, humic and fulvic acids. *Radiochim. Acta* **2000**, *88*, (6), 345-353.
- 22.Aiken, G. R.; Hsu-Kim, H.; Ryan, J. N., Influence of Dissolved Organic Matter on the Environmental Fate of Metals, Nanoparticles, and Colloids. *Environmental Science & Technology* **2011**, *45*, (8), 3196-3201.
- 23.Manaka, M.; Seki, Y.; Okuzawa, K.; Kamioka, H.; Watanabe, Y., Natural attenuation of dissolved uranium within a small stream of central Japan. *Limnology* **2007**, *8*, (2), 143-153.
- 24.Manaka, M.; Seki, Y.; Okuzawa, K.; Watanabe, Y., Uranium sorption onto natural sediments within a small stream in central Japan. *Limnology* **2008**, *9*, (3), 173-183.
- 25.Novotnik, B.; Chen, W.; Evans, R. D., Uranium bearing dissolved organic matter in the porewaters of uranium contaminated lake sediments. *Applied Geochemistry* **2018**, *91*, 36-44.

- 26.Kuhn, K.; Neubauer, E.; Hofmann, T.; von der Kammer, F.; Aiken, G.; Maurice, P., Concentrations and Distributions of Metals Associated with Dissolved Organic Matter from the Suwannee River (GA, USA). *Environ. Eng. Sci.* **2015**, *32*, 54-65.
- 27.Green, N.; McInnis, D.; Hertkorn, N.; Maurice, P.; Perdue, E., Suwannee River Natural Organic Matter: Isolation of the 2R101N Reference Sample by Reverse Osmosis. *Environ. Eng. Sci.* **2015**, *32*, 38-44.
- 28.Averett, R. C.; Leenheer, J.; McKnight, D.; Thorn, K. In *Humic substances in the Suwannee River, Georgia; interactions, properties, and proposed structures*, 1994; 1994.
- 29.Blake, J. M.; De Vore, C. L.; Avasarala, S.; Ali, A.-M.; Roldan, C.; Bowers, F.; Spilde, M. N.; Artyushkova, K.; Kirk, M. F.; Peterson, E.; Rodriguez-Freire, L.; Cerrato, J. M., Uranium mobility and accumulation along the Rio Paguete, Jackpile Mine in Laguna Pueblo, NM. *Environ. Sci-Proc. Imp.* **2017**, *19*, (4), 605-621.
- 30.R foundation for statistical computing: Vienna, A., *R Core Team R: A language and environment for statistical computing* **2015**.
- 31.Ravel, B.; Newville, M., ATHENA, ARTEMIS, HEPHAESTUS: data analysis for X-ray absorption spectroscopy using IFEFFIT. *J. of Synchrotron Radiat.* **2005**, *12*, 537-541.
- 32.Li, Y.; Harir, M.; Uhl, J.; Kanawati, B.; Lucio, M.; Smirnov, K. S.; Koch, B. P.; Schmitt-Kopplin, P.; Hertkorn, N., How representative are dissolved organic matter (DOM) extracts? A comprehensive study of sorbent selectivity for DOM isolation. *Water Research* **2017**, *116*, 316-323.
- 33.Li, Y.; Harir, M.; Lucio, M.; Kanawati, B.; Smirnov, K.; Flerus, R.; Koch, B. P.; Schmitt-Kopplin, P.; Hertkorn, N., Proposed Guidelines for Solid Phase Extraction of Suwannee River Dissolved Organic Matter. *Analytical Chemistry* **2016**, *88*, (13), 6680-6688.

34. Hertkorn, N.; Harir, M.; Cawley, K. M.; Schmitt-Kopplin, P.; Jaffé, R., Molecular characterization of dissolved organic matter from subtropical wetlands: a comparative study through the analysis of optical properties, NMR and FTICR/MS. *Biogeosciences* **2016**, *13*, (8), 2257-2277.
35. Senko, M. W.; Hendrickson, C. L.; Paša-Tolić, L.; Marto, J. A.; White, F. M.; Guan, S.; Marshall, A. G., Electrospray Ionization Fourier Transform Ion Cyclotron Resonance at 9.4 T. *Rapid Communications in Mass Spectrometry* **1996**, *10*, (14), 1824-1828.
36. Sleighter, R. L.; Hatcher, P. G., The application of electrospray ionization coupled to ultrahigh resolution mass spectrometry for the molecular characterization of natural organic matter. *J Mass Spectrom* **2007**, *42*, (5), 559-74.
37. Lin, P.; Rincon, A. G.; Kalberer, M.; Yu, J. Z., Elemental Composition of HULIS in the Pearl River Delta Region, China: Results Inferred from Positive and Negative Electrospray High Resolution Mass Spectrometric Data. *Environmental Science & Technology* **2012**, *46*, (14), 7454-7462.
38. Fenn, J.; Mann, M.; Meng, C.; Wong, S.; Whitehouse, C., Electrospray ionization for mass spectrometry of large biomolecules. *Science* **1989**, *246*, (4926), 64-71.
39. Kim, S.; Kramer, R. W.; Hatcher, P. G., Graphical Method for Analysis of Ultrahigh-Resolution Broadband Mass Spectra of Natural Organic Matter, the Van Krevelen Diagram. *Analytical Chemistry* **2003**, *75*, (20), 5336-5344.
40. Tfaily, M. M.; Chu, R. K.; Tolić, N.; Roscioli, K. M.; Anderton, C. R.; Paša-Tolić, L.; Robinson, E. W.; Hess, N. J., Advanced Solvent Based Methods for Molecular Characterization of Soil Organic Matter by High-Resolution Mass Spectrometry. *Analytical Chemistry* **2015**, *87*, (10), 5206-5215.

41. Fox, P. M.; Nico, P. S.; Tfaily, M. M.; Heckman, K.; Davis, J. A., Characterization of natural organic matter in low-carbon sediments: Extraction and analytical approaches. *Organic Geochemistry* **2017**, *114*, 12-22.
42. Rice, E., Baird, R., Eaton, A. ., & Clesceri, L. . 5310 Total Organic Carbon (TOC). Standard Methods for the Examination of Water and Wastewater. In *Standard Methods For the Examination of Water and Wastewater*, American Public Health Association: 2005; pp 1–16.
43. Denecke, M. A.; Pompe, S.; Reich, T.; Moll, H.; Bubner, M., Measurements of the structural parameters for the interaction of uranium(VI) with natural and synthetic humic acids using EXAFS. *RADIOCHIMICA ACTA* **1997**, *79*, (3), 151-159.
44. Ulrich, K.-U.; Ilton, E. S.; Veeramani, H.; Sharp, J. O.; Bernier-Latmani, R.; Schofield, E. J.; Bargar, J. R.; Giammar, D. E., Comparative dissolution kinetics of biogenic and chemogenic uraninite under oxidizing conditions in the presence of carbonate. *Geochimica et Cosmochimica Acta* **2009**, *73*, (20), 6065-6083.
45. Bone, S. E.; Dynes, J. J.; Cliff, J.; Bargar, J. R., Uranium(IV) adsorption by natural organic matter in anoxic sediments. *P. Natl. Acad. Sci. Usa* **2017**, (4), 711.
46. Mikutta, C.; Langner, P.; Bargar, J. R.; Kretzschmar, R., Tetra- and Hexavalent Uranium Forms Bidentate-Mononuclear Complexes with Particulate Organic Matter in a Naturally Uranium-Enriched Peatland. *Environ. Sci. Technol.* **2016**, *50*, (19), 10465-10475.
47. Murphy, R. J.; Lenhart, J. J.; Honeyman, B. D., The sorption of thorium (IV) and uranium (VI) to hematite in the presence of natural organic matter. *Colloid. Surface.* **1999**, *157*, (1), 47-62.
48. Raeke, J.; Lechtenfeld, O. J.; Wagner, M.; Herzsprung, P.; Reemtsma, T., Selectivity of solid phase extraction of freshwater dissolved organic matter and its effect on ultrahigh resolution mass spectra. *Environ. Sci.-Process Impacts* **2016**, *18*, (7), 918-927.

49. Dittmar, T.; Koch, B.; Hertkorn, N.; Kattner, G., A simple and efficient method for the solid-phase extraction of dissolved organic matter (SPE-DOM) from seawater: SPE-DOM from seawater. *Limnology and Oceanography: Methods* **2008**, *6*, 230-235.
50. Xu, C.; Lin, P.; Sun, L.; Chen, H.; Xing, W.; Kamalanathan, M.; Hatcher, P. G.; Conte, M. H.; Quigg, A.; Santschi, P. H., Molecular Nature of Marine Particulate Organic Iron-Carrying Moieties Revealed by Electrospray Ionization Fourier-Transform Ion Cyclotron Resonance Mass Spectrometry (ESI-FTICRMS). *Frontiers in Earth Science* **2020**, *8*, (266).
51. D'Andrilli, J.; Chanton, J. P.; Glaser, P. H.; Cooper, W. T., Characterization of dissolved organic matter in northern peatland soil porewaters by ultra high resolution mass spectrometry. *Organic Geochemistry* **2010**, *41*, (8), 791-799.
52. Bhatia, M. P.; Das, S. B.; Longnecker, K.; Charette, M. A.; Kujawinski, E. B., Molecular characterization of dissolved organic matter associated with the Greenland ice sheet. *Geochimica et Cosmochimica Acta* **2010**, *74*, (13), 3768-3784.
53. Chen, H.; Johnston, R. C.; Mann, B. F.; Chu, R. K.; Tolic, N.; Parks, J. M.; Gu, B., Identification of Mercury and Dissolved Organic Matter Complexes Using Ultrahigh Resolution Mass Spectrometry. *Environmental Science & Technology Letters* **2017**, *4*, (2), 59-65.
54. Stenson, A. C.; Landing, W. M.; Marshall, A. G.; Cooper, W. T., Ionization and Fragmentation of Humic Substances in Electrospray Ionization Fourier Transform-Ion Cyclotron Resonance Mass Spectrometry. *Analytical Chemistry* **2002**, *74*, (17), 4397-4409.
55. Brown, T. L.; Rice, J. A., Effect of experimental parameters on the ESI FT-ICR mass spectrum of fulvic acid. *Anal Chem* **2000**, *72*, (2), 384-90.
56. Stenson, A. C., Fourier transform ion cyclotron resonance mass spectral characterization of metal-humic binding. *Rapid Communications in Mass Spectrometry* **2009**, *23*, (4), 465-476.

57. Burford, N.; Eelman, M. D.; LeBlanc, W. G., Identification of complexes involving toxic heavy metals with amino acid ligands by electrospray ionization mass spectrometry. *Canadian Journal of Chemistry-Revue Canadienne De Chimie* **2004**, *82*, (8), 1254-1259.
58. Waska, H.; Koschinsky, A.; Dittmar, T., Fe- and Cu-Complex Formation with Artificial Ligands Investigated by Ultra-High Resolution Fourier-Transform ion Cyclotron Resonance Mass Spectrometry (FT-ICR-MS): Implications for Natural Metal-Organic Complex Studies. *Frontiers in Marine Science* **2016**, *3*, (119).
59. Ross, A. R. S.; Ikononou, M. G.; Orians, K. J., Characterization of copper-complexing ligands in seawater using immobilized copper(II)-ion affinity chromatography and electrospray ionization mass spectrometry. *Marine Chemistry* **2003**, *83*, (1), 47-58.
60. Collins, R. N., Separation of low-molecular mass organic acid-metal complexes by high-performance liquid chromatography. *Journal of Chromatography A* **2004**, *1059*, (1), 1-12.
61. Figueroa, J. A. L.; Wrobel, K.; Afton, S.; Caruso, J. A.; Felix Gutierrez Corona, J.; Wrobel, K., Effect of some heavy metals and soil humic substances on the phytochelatin production in wild plants from silver mine areas of Guanajuato, Mexico. *Chemosphere* **2008**, *70*, (11), 2084-2091.

Chapter 6. Conclusions and Implications

6.1 Overall Conclusions.

The results from the experimental work conducted in this research contribute to a better understanding of the role of NOM on U(IV) and U(VI) solubility, adsorption, and precipitation reactions. This work also highlights the effects of U on the organic functional chemistry of POM, and DOM at environmentally relevant pH. The experimental work involved the use of natural samples and laboratory control experiments. Samples were analyzed with analytical techniques including X-ray spectroscopy (XPS, XAS), microscopy (TEM, SEM, EDS, EELS) ultrahigh-resolution mass spectrometry (ESI FT-IRC MS) and aqueous measurements (IPC-MS, TOC). Chapter 3 of this dissertation investigated the functional group chemistry of natural organic matter (NOM) associated with U(IV) and U(VI) in solids from mineralized deposits from the Jackpile Mine, Laguna Pueblo, NM. Chapter 3 represents a novel effort toward better understanding the role of organic matter on U speciation under environmentally relevant pH conditions. The main contribution of Chapter 3 is to emphasize that phenolic and carbonyl functional groups are more abundant in the organic matter fraction in these mineralized deposits in which both reduced U(IV) and oxidized U(VI) were present. Carboxyl groups were less abundant in the organic matter fraction of the samples obtained from the study site, which is contrary to what has been observed in other studies. Chapter 3 is a contribution to the limited literature related to organic matter-uranium interactions and therefore it is relevant to other organic-rich sandstone formations where U and other heavy metals co-occur.

Chapter 4 investigated the effect of pH on the adsorption, precipitation, and solubilization reactions of U(VI) in the presence of NOM. The main contribution of this chapter is to highlight that adsorption of U onto POM leads to the precipitation of U-bearing crystalline solids at pH 4

after 24 h. Results also showed that adsorption reactions are relevant as in the bulk, U(VI) was mostly adsorbed to POM at pH 2 and pH 4. These results confirm that complexation of U and DOM favors the solubility of U at pH 7. Chapter 4 contributes to the scarce body of knowledge related to the effect of NOM and pH on the precipitation of U in organic-rich environments

Chapter 5 studied changes on chemistry of dissolved organic matter (DOM) resulting from the reaction with U(VI) at acidic and neutral pH. The relative percent content of phenols and carboxylic acids decreased after the reaction with U for 24 h compared to control experiments without U. Compounds from DOM had a lower atomic O/C ratio at acidic pH because of the reaction with U. This finding suggests that the aqueous complexation of U and DOM compounds, and the adsorption of U onto POM (Chapter 4) at acidic pH can influence the molecular composition of DOM. The compositional similarity in the DOM detected in control experiments (without U) upon changing the pH suggests that the changes observed in DOM are likely due to the reaction with U. Overall, this work highlights the importance of phenol groups in the reactivity of U, aside from carboxylic groups. Further work should be pursued to identify the U-DOM complexes are likely being formed in reactors at pH 2, pH 4, and pH 7.

6.2 Environmental Implications and Future Research.

The elevated concentrations of U in surface waters neighboring U mineral deposits is a concern for the nearby communities. This study investigated the combined roles of NOM and pH on the interfacial chemical reactions affecting the solubility, adsorption, and precipitation of U in organic-rich environments.

This work is significant given that the reactions studied in this Ph.D. research may occur in remediation processes such as treatment of acid mine drainage solutions (pH ranging between 2 and 4) and at natural waters (circumneutral pH). Understanding changes in organic functional

chemistry at pH 7 and pH 2 is environmentally relevant due to their influence on chemical reactions that could impact U mobility and transport from the U mineralized deposits to surface waters and plants. This work highlights the importance of metal and NOM interactions as these affect surface complexation, precipitation, and solubilization reactions that should be considered in reactive transport models for risk assessment and remediation purposes.

The results from this investigation suggest that complexation reactions between U and phenolic and carboxylic functional groups in DOM play an important role on the U chemistry in organic-rich environments. The ability of DOM through phenol and carboxylic functional groups to complex with metals has implications for metal transport, solubility, bioavailability, and toxicity. Understanding the molecular mechanisms of U-DOM interactions can help to improve the understanding of U reactivity in the organic-rich environments and lead to a better assessment of its solubilization and associated risks to the environment.

The findings reported in this Ph.D. dissertation also identify the need for further investigations related to the influence of organic functional groups on heavy metal transport and reactivity. Future studies are necessary to investigate the role of kinetics on the adsorption, precipitation, and re-solubilization of U in the presence of NOM. The design of column experiments using similar conditions to the ones studied in this research also remain subject to future investigations. Further studies are necessary to investigate the role of NOM and pH in engineered devices to remove U (constructed wetlands, NOM- filters, etc).

Appendix A

Supplementary Information from Chapter 3: Organic Functional Group Chemistry in Mineralized Deposits Containing U(IV) and U(VI) from the Jackpile Mine in New Mexico

Additional Materials and Methods.

X-ray Fluorescence. Bulk chemistry analysis was performed on the unreacted samples using X-ray Fluorescence (XRF) with a Rigaku ZSX Primus II with Rhodium X-ray tube that quantitatively determines major and minor atomic elements, from B to U. The software is ZSX Primus II that performs both qualitative and quantitative analysis.

Thermal analyses for solids. The OM content in the mineralized surface deposits from the Jackpile Mine solid samples was estimated by loss-on-ignition (LOI) and thermogravimetry (TGA). Samples were dried at 105°C for 12 h in ceramic crucibles to remove the moisture and then heated in a muffle furnace at 550°C for 5 h. The weight difference between 105 and 550°C is attributed to the OM content.¹⁻³ A thermogravimetric analyzer (TGA Q50-TA Instruments, USA) was used to corroborate the results obtained by LOI and to assess additional mass loss in the samples after 550°C. For the TGA, we used ≈ 5 mg of samples in alumina crucibles and raised the temperature from ambient ($\sim 25^\circ\text{C}$) to 1000°C at $15^\circ\text{C min}^{-1}$ under air atmosphere flowing at 100 mL min^{-1} . Thermal analyses were tested on triplicates for each sample.

Elemental Analysis. Carbon, hydrogen, oxygen and nitrogen content as weight percent was determined by Elemental Analyzer Continuous Flow Isotope Ratio Mass Spectrometry using a Costech ECS 4010 Elemental Analyzer coupled to a ThermoFisher Scientific Delta V Advantage mass spectrometer via a CONFLO IV interface.

X-ray Photoelectron Spectroscopy. A Kratos Ultra DLD X-ray Photoelectron Spectrometer (XPS) was used to acquire the near surface (<10 nm) elemental composition and oxidation states. Monochromatic Al source was used at 150 W power to obtain C 1s and U 4f high-resolution spectra from top ~4-10 nm of the surface. Charge neutralization was used during acquisition. 99.9% pure Au reference powder was used to calibrate the spectra. Three areas per samples were analyzed. Average and standard deviations are reported. Shirley background was used to process the spectra. Quantification utilized sensitivity factors that were provided by the manufacturer. A 70% Gaussian / 30% Lorentzian (GL (30)) line shape was used for the curve fittings. Constraints used in curve fitting of U 4f spectra were established in our previous study.⁴ Five peaks have been used to curve high-resolution C 1s spectra – aliphatic C-C at 285 eV, secondary carbon (C*-C-OH/C*-C=O) at 285.8 eV, phenol carbon at 286.5 eV, carbonyl carbon at 288.0 eV and carboxylic C at 289.2 eV. High-resolution O 1s were fitted using 2 peaks, one due to single bonded O-C (532.5 eV) and one due to double bonded O=C (531.5 eV). These values are based on the reference database.⁵ Qualitative X-ray mapping of epoxy-mounted polished ore samples was performed on a JEOL 8200 electron microprobe.

.....XPS on supernatant from batch reactors. The C 1s spectrum from freshly cleaved mica and drop-cast supernatant samples were acquired simultaneously. High-resolution C 1s spectrum from fresh cleaved mica was obtained to account for the adventitious carbon present on the mica surface. In fresh mica, carbon peaks were constrained in intensity and position with respect to the intensity and position of K 2p_{3/2} peak (Figure S1 A). For supernatant samples drop-cast on the mica surface, the C peaks constrained to the intensity of K 2p were included in the curve fit first, and then the additional peaks due to deposited supernatant were added. Figure S1 shows the contribution of C from the mica into the overall C 1s spectrum.

X-ray Absorption Spectroscopy. X-ray Absorption Spectroscopy measurements were performed at Beamline 7-3 at the Stanford Synchrotron Radiation Laboratory. Measurements were conducted at the U L_{III} Edge in fluorescence mode using a 30 element Ge detector and a double crystal Si(220) Monochromator, calibrated at the first inflection point of a Y metal foil absorption at 17038.4 eV. Data was collected at room temperature in a He purged environmental chamber. No change was observed through consecutive scans, nor changes in the absorption when first and last scans of the series, ruling out beam damage during the measurement. Data were normalized and background subtracted using the IFEFFIT software package. Samples sets were reduced and analyzed using Athena and Artemis⁶ with standard methods and benchmarks.

Aqueous Chemical Extraction. To assess the acid extractable elements from the mineralized surface deposits from the Jackpile Mine samples, acid digestions were conducted on triplicates by adding 2 mL HNO₃ and 6 mL HCl and 3 mL concentrated HF into 50 mL Teflon digestion tubes containing 2.000 ± 0.002 g of homogenized sample. All reagents used were ultra high purity. The digestion tubes were then heated in a Digi prep MS SCP Science block digester at 95° C for 2 hours. Following heating, acid extracts were diluted to 50 mL with mega ohm waster and filtered through a 0.45 µm filter to remove suspended solids. Metal concentrations in solution were measured by ICP-OES and ICP-MS.

Inductively Coupled Plasma (ICP). Elemental concentrations in supernatant from the filtered acid digestion of the mineralized surface deposits from the Jackpile Mine samples and the batch experiments were measured using a PerkinElmer Optima 5300DV Inductively Coupled Plasma-

Optical Emission Spectrometer (ICP-OES). Trace elemental concentrations were measured using a PerkinElmer NexION 300D (Dynamic Reaction Cell) Inductively Coupled Plasma-Mass Spectrometer (ICP-MS). Both ICPs are calibrated with a 5-point calibration standards and QC samples were analyzed periodically to ensure quality results.

Modified approach of the Nagoya Method. Glassware, plasticware, and vials were precleaned by soaking in 1 N NaOH for 3 h followed by thorough rinse with 18.2 M Ω water followed by soak in 1 N HCl for 3 h followed by thorough rinse with 18.2 M Ω water and dried before use. Homogenized mineralized surface deposits from the Jackpile Mine samples (500 mg) were placed in 15 ml polypropylene falcon tubes then 10 ml of 0.1 N NaOH were added. The tubes were capped and mixed with a vortex for 1 min to disaggregate particles and suspend in base solution. Reactions were carried for 24 h at 4°C with periodic hand shaking. After 24 h, samples were centrifuged at 3000 revolutions per minute (rpm) for 15 min. The supernatant was decanted and filter using 0.2 μ m filter into VOE vials purchased from AWR.

Table S1. Linear combination fitting of the U-L_{III} EXAFS spectra.

Solids Analyzed	U(IV) Coffinite	U(IV) Monomeric	U(IV) Uraninite	U(VI) Adsorbed
After LOI	0.153	0	0	0.608
Unreacted 1	0.179	0.338	0	0.484
Unreacted 2	0.199	0.251	0	0.512
pH 7	0.104	0.281	0.08	0.556
pH 2	0.223	0.211	0.071	0.521

Table S2. Non-normalized elemental composition (% weight) measured by XRF from unreacted samples from mineralized surface deposits from the Jackpile Mine.

Element	JP ₁	JP ₂
Si	25.7%	23.6%
U	1.02%	8.22%
Fe	10.3%	4.6%
K	1.4%	1.2%
Ca	5.22%	0.60%
V	0.07%	0.02%

Table S3. Acid extractable elemental composition (% weight) from unreacted samples from mineralized surface deposits from the Jackpile Mine.

Sample	JP ₁		JP ₂	
Element	average	stdev	average	stdev
Si	19.2%	0.54%	17.32%	1.06%
U	0.44%	0.02%	2.61%	0.09%
Fe	4.21%	0.23%	1.19%	0.06%
K	0.45%	0.02%	0.19%	0.02%
Ca	2.10%	0.07%	0.03%	0.02%
Al	3.29%	0.06%	0.52%	0.01%
V	0.01%	0.00%	-0.01%	0.00%
Mg	0.75%	0.06%	0.04%	0.01%
Cu	0.01%	0.00%	0.00%	0.00%

Table S4. Standard deviation for fitting of high resolution XPS spectra obtained for carbon (C 1s) and uranium (U 4f). Note that high resolution spectra were collected from 3 locations per sample (n=3).

Sample	pH	Carbonyl (C=O)	Phenol (COH)	Carboxylic (COOH)	C-O-M	U (IV)	U (VI)
Unreacted Mine Wastes	as is	0.7%	2.5%	0.2%	0.0%	0.8%	0.8%
	13	2.1%	0.8%	0.1%	0.2%	12.3%	12.3%
Supernatant	7	2.7%	2.0%	0.9%	0.0%	5.5%	5.5%
	2	1.1%	2.1%	0.6%	0.0%	4.8%	4.8%
Reacted Solids	13	0.6%	1.1%	0.2%	0.0%	2.8%	2.8%
	7	0.9%	2.5%	0.6%	0.0%	1.9%	1.9%
	2	0.7%	1.8%	0.1%	0.0%	2.1%	2.1%

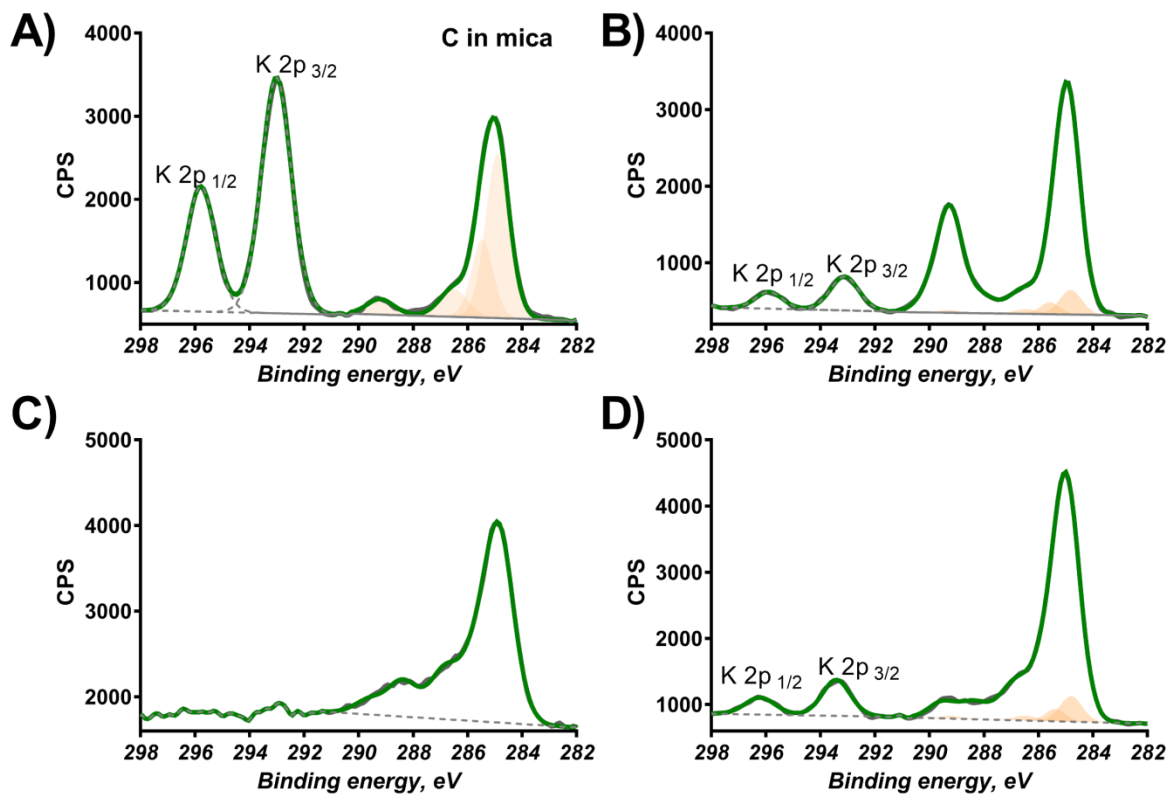


Figure S1. Fitting of high resolution C 1s XPS spectra constraining peaks due to carbon on the surface of mica to the intensity of peaks of K 2p peaks: A) freshly cleaved mica; B) Supernatant from reactor at pH 13; C) Supernatant from reactor at pH 7; and D) Supernatant from reactor at pH 2. Highlighted peaks are due to carbon present on the surface of mica.

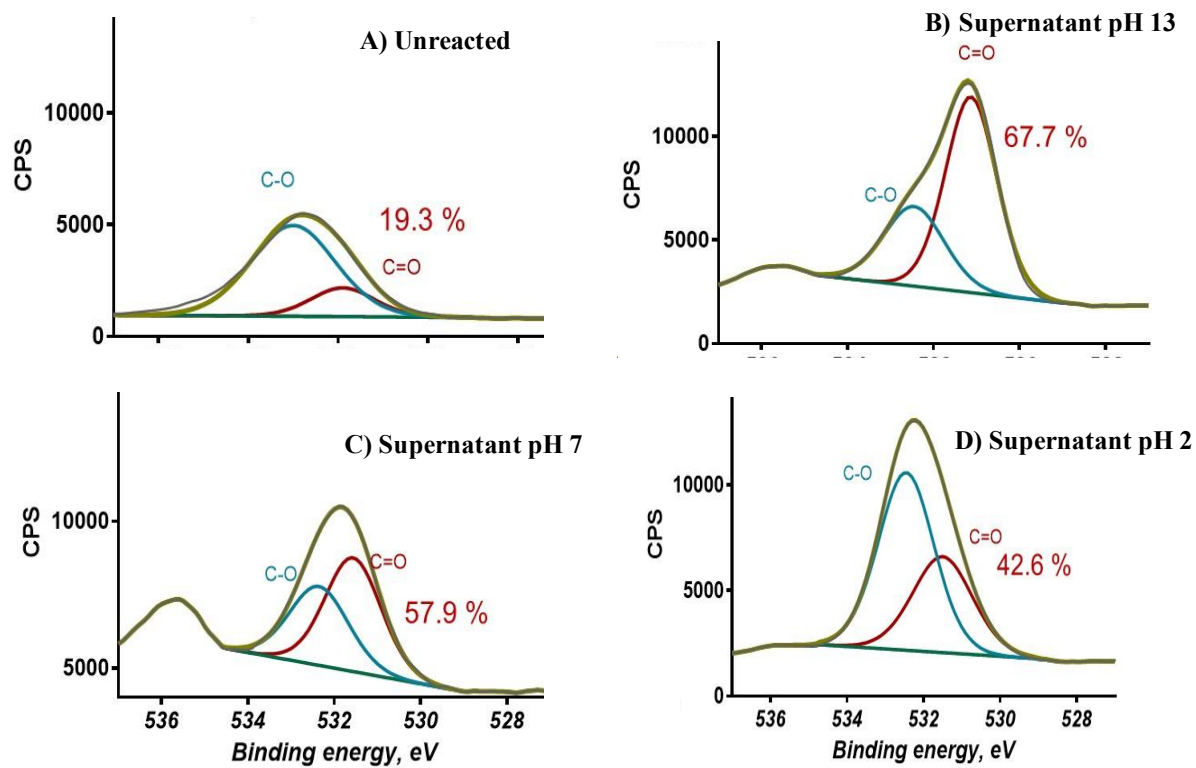
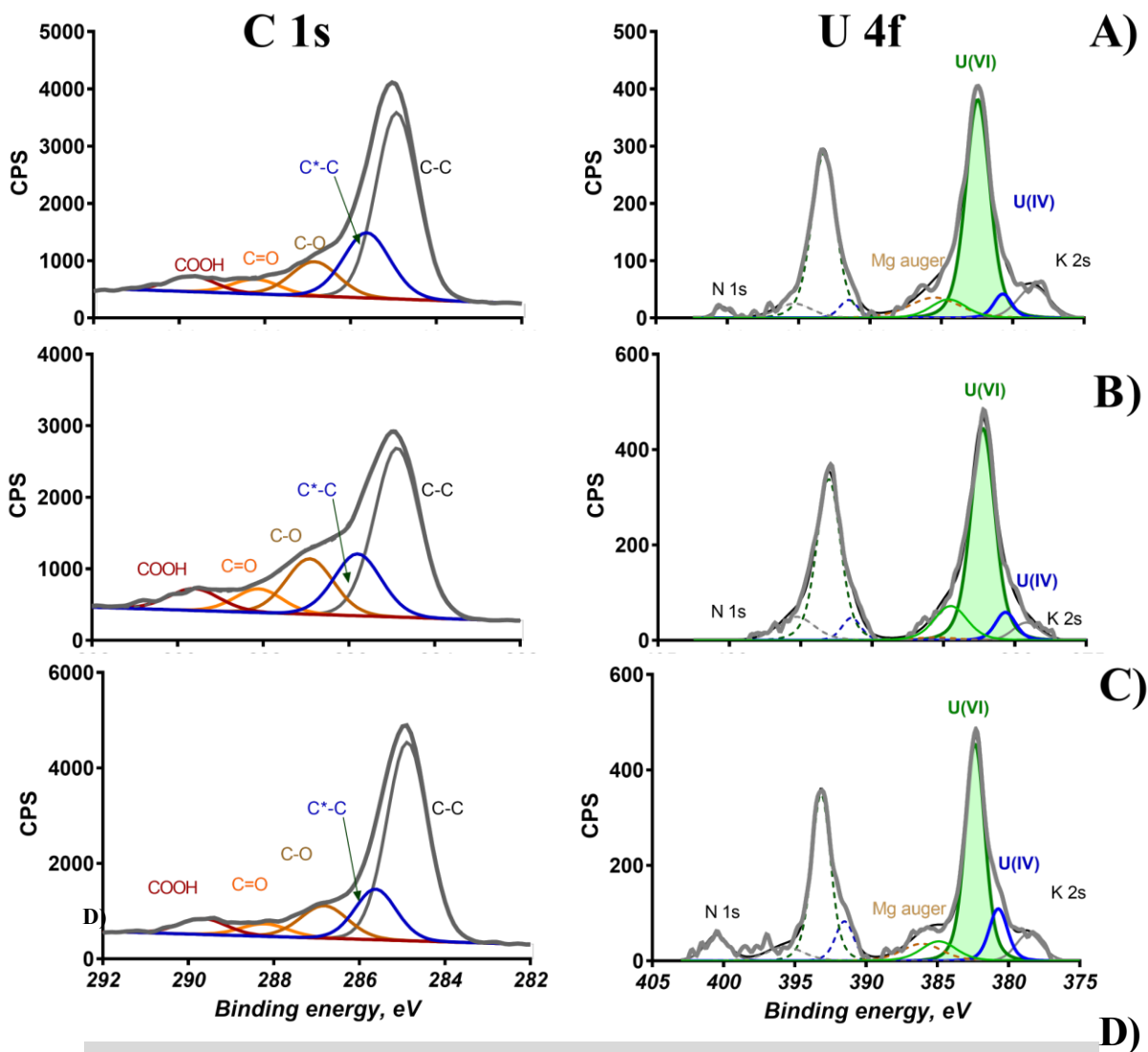


Figure S2. Fitting of high resolution O 1s XPS spectra of mineralized deposits from the Jackpile Mine. Relative percent of C=O is shown in red.: A) unreacted samples; B) Supernatant from reactor at pH 13; C) Supernatant from reactor at pH 7; and D) Supernatant from reactor at pH 2.



Sample	pH	Carbonyl (C=O)	Phenol (COH)	Carboxylic (COOH)	U (IV)	U (VI)
Reacted Solids	13	10.3%	14.6%	5.3%	5.4%	94.6%
	7	5.7%	12.7%	3.6%	15.0%	85.0%
	2	2.2%	5.9%	5.2%	4.8%	95.2%

Figure S3. Fitting of high resolution XPS carbon (left hand side: C 1s) and uranium (right hand side: U 4f) spectra of reacted solids from sample JP₂: A) pH 13; B) pH 7; C) pH 2 and D) Percent composition of C 1s and U 4f spectra.

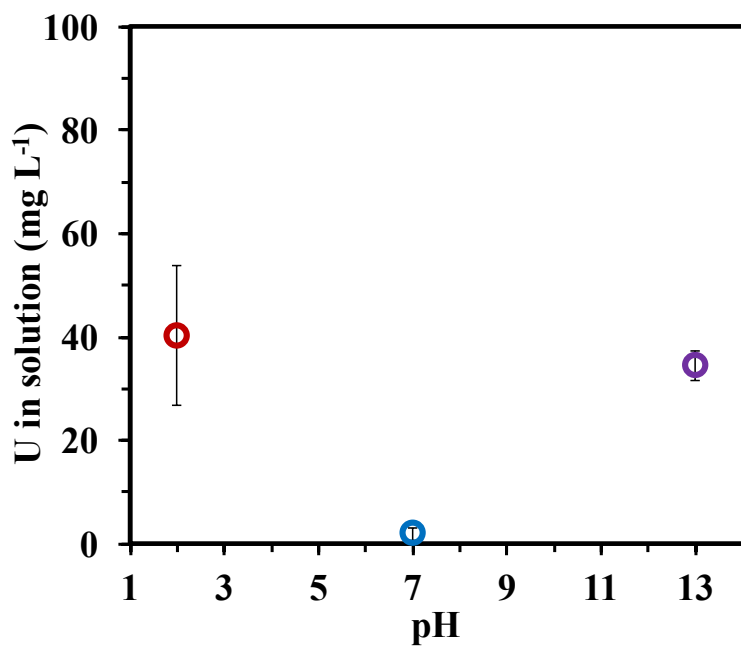


Figure S4. Uranium concentration in supernatant from batch extraction reactors at pH 2, 7 and 13 after a 24h reaction.

References.

- 1.....Cawley, K. M.; Hohner, A. K.; Podgorski, D. C.; Cooper, W. T.; Korak, J. A.; Rosario-Ortiz, F. L., Molecular and spectroscopic characterization of water extractable organic matter from thermally altered soils reveal insight into disinfection byproduct precursors. *Environ. Sci. Technol.* **2017**, *51*, (2), 771-779.
- 2.....Dean, W. E. J., Determination of carbonate and organic matter in calcareous sediments and sedimentary rocks by loss on ignition: Comparison with other methods. *J. Sediment. Petrol.* **1974**, *44*, 242–248.
- 3.....Santisteban, J. I.; Mediavilla, R.; Lopez-Pamo, E.; Dabrio, C. J.; Zapata, M. B. R.; Garcia, M. J. G.; Castano, S.; Martinez-Alfaro, P. E., Loss on ignition: a qualitative or quantitative method for organic matter and carbonate mineral content in sediments? *J. Paleolimn.* **2004**, *32*, (3), 287-299.
- 4.....Blake, J. M.; Avasarala, S.; Artyushkova, K.; Ali, A.-M. S.; Brearley, A. J.; Shuey, C.; Robinson, W. P.; Nez, C.; Bill, S.; Lewis, J.; Hirani, C.; Pacheco, J. S. L.; Cerrato, J. M., Elevated concentrations of u and co-occurring metals in abandoned mine wastes in a Northeastern Arizona native american community. *Environ. Sci. Technol.* **2015**, *49*, (14), 8506-8514.
- 5.....Beamson, G.; Briggs, D., High resolution XPS of organic polymers: The Scienta ESCA300 Database *J. Chem. Educ.* **1993**, *70*, (1), A25.
- 6.....Ravel, B.; Newville, M., ATHENA, ARTEMIS, HEPHAESTUS: data analysis for X-ray absorption spectroscopy using IFEFFIT. *J. of Synchrotron Radiat.* **2005**, *12*, 537-541.

Appendix B

**Supplementary Information from Chapter 4: From Adsorption to Precipitation of U(VI) in
the Presence of Natural Organic Matter**

Additional Materials and Methods.

Micro X-ray Fluorescence. Bulk chemistry analysis was performed on the unreacted samples using X-ray Fluorescence (XRF) with a Rigaku ZSX Primus II with Rhodium X-ray tube that quantitatively determines major and minor atomic elements, from B to U. The software is ZSX Primus II that performs both qualitative and quantitative analysis.

X-ray Absorption Spectroscopy. X-ray Absorption Spectroscopy measurements were performed at Beamline 7-3 at the Stanford Synchrotron Radiation Laboratory. Measurements were done at the U LIII Edge in fluorescence mode using a 30 element Ge detector and a double crystal Si(220) Monochromator, calibrated at the first inflection point of a Y metal foil absorption at 17038.4 eV. Measurements were performed at room temperature in a He filled acrylic box. No change was observed through consecutive scans, nor changes in the absorption when first and last scans of the series, ruling out beam damage during the measurement. Samples sets were reduced and analyzed using Athena and Artemis 1 with standard methods and benchmarks.

Inductively Coupled Plasma (ICP). Elemental concentrations in supernatant from the filtered acid digestion of the mineralized surface deposits from the Jackpile Mine samples and the batch experiments were measured using a PerkinElmer Optima 5300DV Inductively Coupled Plasma-Optical Emission Spectrometer (ICP-OES). Trace elemental concentrations were measured using a PerkinElmer NexION 300D (Dynamic Reaction Cell) Inductively Coupled Plasma-Mass Spectrometer (ICP-MS). Both ICPs are calibrated with a 5-point calibration standards and QC samples were analyzed periodically to ensure quality results.

Table S1. Batch reactors setup

ID	Reaction	U (μM)	KCl (M)	NOM (mgL^{-1})	pH adjust	Reaction time (h)	U_{aq} and DOC	TEM	μXRF	XAS	Purpose
U- KCl-NOM	U+ KCl +NOM	100	0.01	0.2	NaOH	0.5, 24	Yes	Yes	Yes	Yes	Reaction to evaluate the precipitation of U in the presence of NOM at ionic strength conditions observed in the field ²⁻⁴ (environmentally relevant).
Control U	U + KCl	100	0.01	0	NaOH	0.5, 24	Yes	Yes	Yes	No	Control to evaluate the precipitation of U and KCl in the absence of NOM.
Control NOM	NOM	100	0.01	0.2	NaOH	24	Yes	Yes	Yes	No	Control to evaluate the precipitation of POM in the absence of U and KCl.
Control 1	U + NOM	100	0	0.2	NH_4OH	24	No	Yes	No	Yes	Control to evaluate the precipitation of U in the presence of NOM and absence of KCl and NaOH.

Table S2. p-values (Shapiro-Wilken Test for Normality)

Reactor	Results Normality Test for Soluble U						Results Normality Test for DOC					
	pH 2	pH 4	pH 7	pH 2	pH 4	pH 7	pH 2	pH 4	pH 7	pH 2	pH 4	pH 7
NOM+U	0.46	0.50	0.13	0.47	0.43	0.14	0.36	0.36	0.92	0.31	0.57	0.35
U	0.31	0.46	0.18	0.25	0.38	0.29	0.11	0.69	0.37	0.84	0.36	0.17

Table S2. ANOVA Tests

**Anova: All pH values - time - U - UNOM
(Soluble U μM)**

Response: pH 2, pH 4 and pH 7

	Df	Sum Sq	Mean Sq	F value	Pr(>F)
U	1	120.34	120.34	128.86	9.34E-13
U_NOM	1	1.43	1.43	1.53	0.22
time	1	0.35	0.35	0.37	0.55
Residuals	32	29.88	0.93		

**Anova: pH 2 pH 4 - time - U - UNOM
(Soluble U μM)**

Response: pH 2 and H 4

	Df	Sum Sq	Mean Sq	F value	Pr(>F)
U	1	0.09	0.09	0.14	0.72
U_NOM	1	3.26	3.26	4.92	0.04
time	1	7.41	7.41	11.19	3.22E-03
Residuals	20	13.24	0.66		

**Anova: All pH values - time - NOM - UNOM
(DOC ppm)**

Response: pH 2, pH 4 and pH 7

	Df	Sum Sq	Mean Sq	F value	Pr(>F)
NOM	1	83.76	83.76	461.21	3.18E-13
U_NOM	1	2.13	2.13	11.75	3.45E-03
time	1	4E-03	4E-03	0.02	0.89
Residuals	16	2.91	0.18		

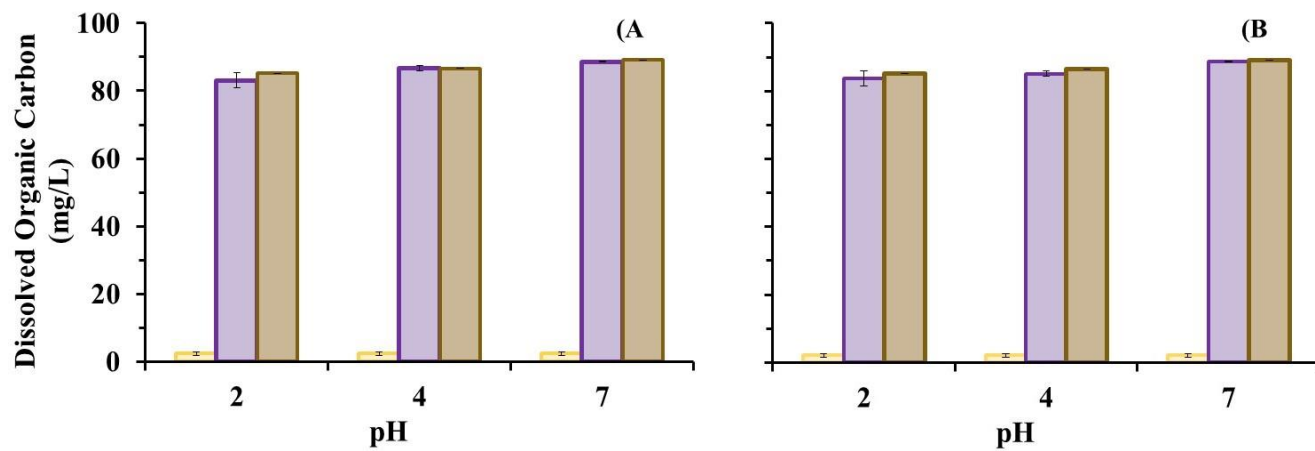


Figure S1. Dissolved organic matter (DOM) concentration in solution in batch reactors containing U-KCl-NOM (purple), U control reactor containing (yellow) and NOM control reactor (brown) after a reaction of A) 0.5 h, B) 24h.

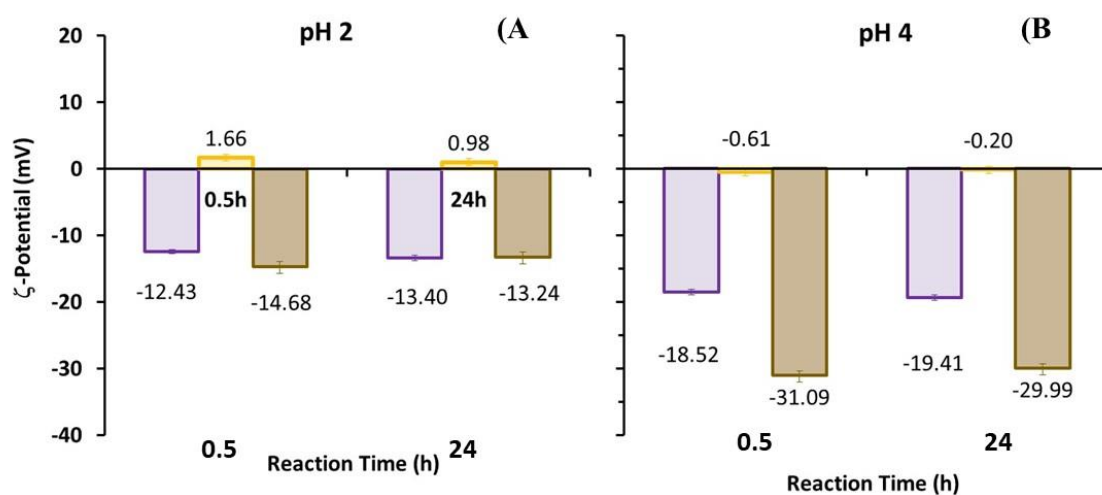


Figure S2. ζ -Potential of supernatant samples from batch reactors U-KCl-NOM (purple), U control reactor containing (yellow) and NOM control reactor (brown) after a reaction time of 0.5 h. and 24 h. at A) pH 2, B) pH 4.

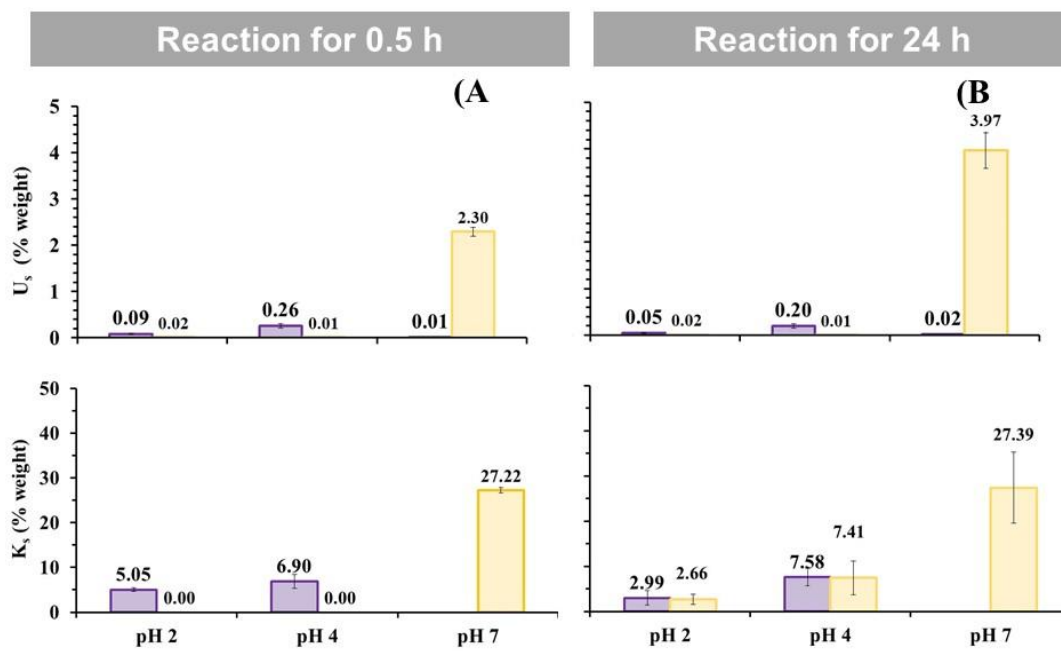


Figure S2. Solid Analysis by μ -XRF on samples collected from batch experiments U-NOM-KCl (purple) and U control reactor without NOM (yellow) after a reaction of **A)** 0.5 h and **B)** 24 h. Data presents U concentration as weight percent.

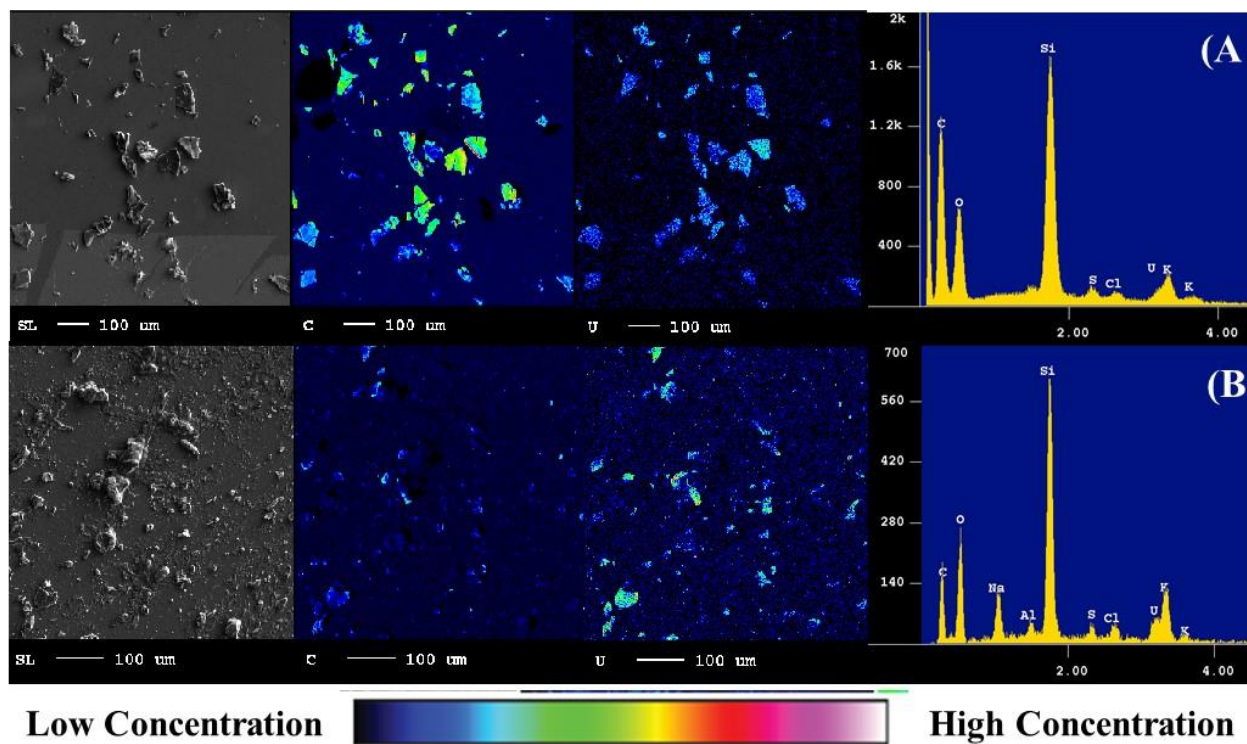


Figure S3. Electron microprobe images, WDX maps and qualitative energy dispersive spectra (EDS) on solids collected after 0.5 h batch reactions of SRNMO, uranium in 4% NO₃ and KCl at A) pH 2, and B) pH 4.

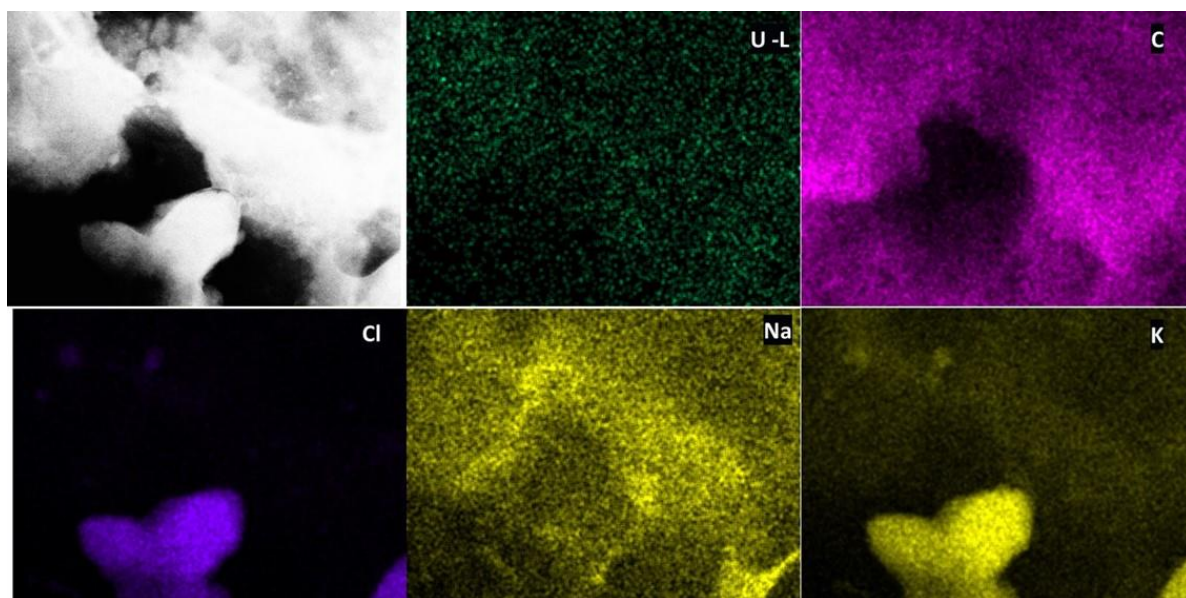


Figure S4. Scanning transmission electron microscope - energy dispersive spectroscopy (STEM-EDS) maps for solids for solids collected from batch reactions of U-KCl-NOM after 24 at pH 2 indicating the association of U, C, Cl, Na and K in these solids. K-rich particles, likely KCl, are not associated with POM. U-rich particles are not detected in this sample.

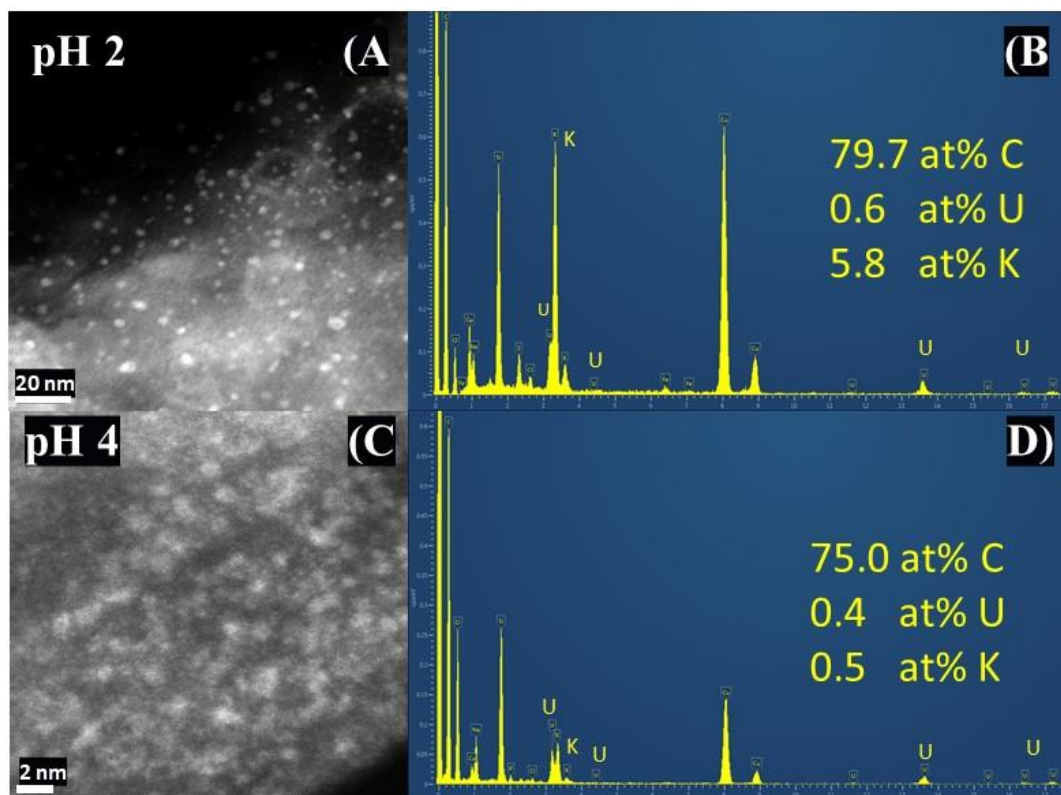


Figure S5. Dark-field scanning transmission electron microscope (DF-STEM) images and energy dispersive X-ray spectroscopy (EDS) spectra for solids collected from batch reactors U-KCl-NOM after 0.5 h at pH 2 and pH 4 indicating the adsorption of U onto POM at pH 2 (A, B) and pH 4 (C, D) shown by the presence of distinct U peaks in the EDS spectra.

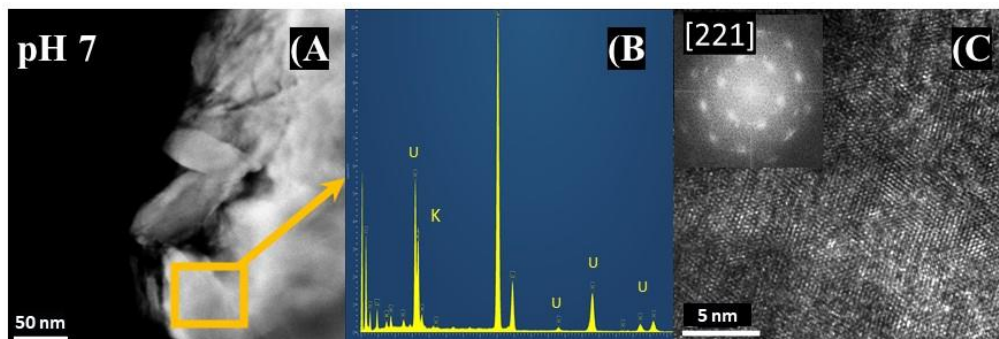


Figure S6. Dark-field scanning transmission electron microscope (DF-STEM) images, energy dispersive spectroscopy (EDS) spectra, high resolution transmission electron microscopy (HRTEM) and (inset) Fast Fourier Transform extracted from HRTEM image. for solids collected from U control reactor containing (U-KCl) at pH 7 after 0.5 h indicating (A, B, C) the precipitation of U- and K- bearing nanocrystalline bearing solids. The compositional and electron diffraction data are most consistent with clarkeite nanocrystals, but possibly with another U-bearing phase that remains unidentified.

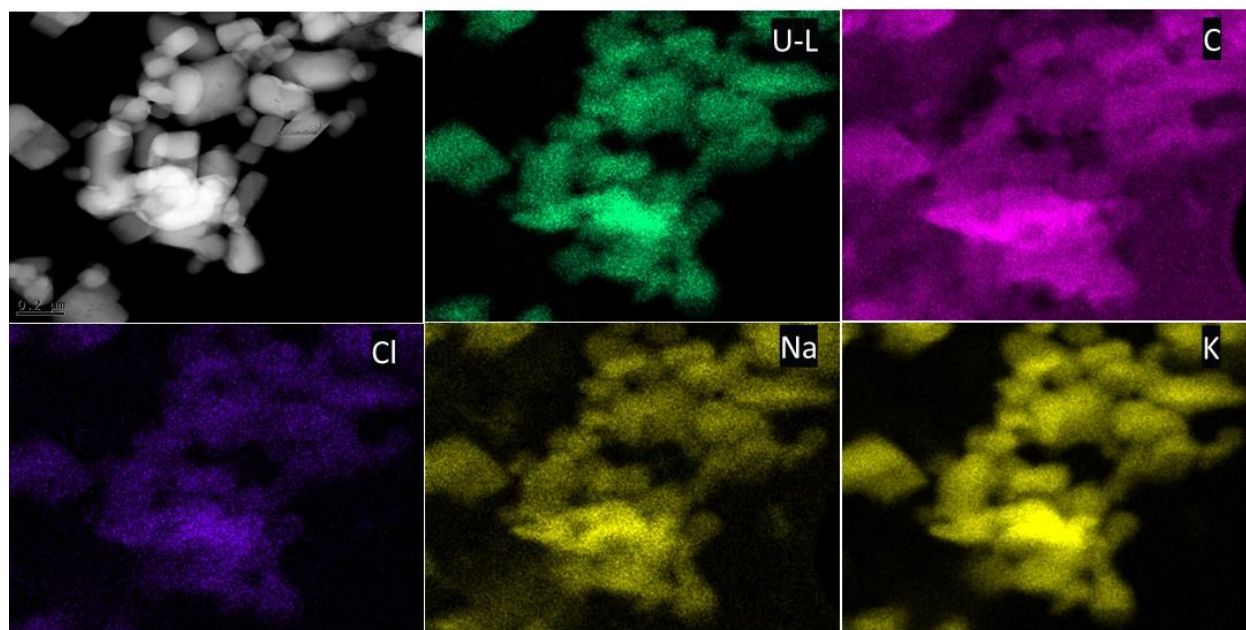


Figure S7. Scanning transmission electron microscope - energy dispersive spectroscopy (STEM-EDS) maps for solids for solids collected from batch reactions of U-KCl-NOM after 24 at pH 4 indicating the association of U, C, Cl, Na and K in these solids. U and K-rich particles are detected in this sample. The intensity of the color is correlated with the concentration of the element in the sample.

References.

- 1.....Ravel, B.; Newville, M., ATHENA, ARTEMIS, HEPHAESTUS: data analysis for X-ray absorption spectroscopy using IFEFFIT. *J. of Synchrotron Radiat.* **2005**, *12*, 537-541.
- 2.....Avasarala, S.; Lichtner, P. C.; Ali, A.-M. S.; González-Pinzón, R.; Blake, J. M.; Cerrato, J. M., Reactive Transport of U and V from Abandoned Uranium Mine Wastes. *Environmental Science & Technology* **2017**, *51*, (21), 12385-12393.
- 3.....Avasarala, S.; Torres, C.; Ali, A.-M. S.; Thomson, B. M.; Spilde, M. N.; Peterson, E. J.; Artyushkova, K.; Dobrica, E.; Lezama-Pacheco, J. S.; Cerrato, J. M., Effect of bicarbonate and oxidizing conditions on U(IV) and U(VI) reactivity in mineralized deposits of New Mexico. *Chemical Geology* **2019**, *524*, 345-355.
- 4.....Blake, J. M.; De Vore, C. L.; Avasarala, S.; Ali, A.-M.; Roldan, C.; Bowers, F.; Spilde, M. N.; Artyushkova, K.; Kirk, M. F.; Peterson, E.; Rodriguez-Freire, L.; Cerrato, J. M., Uranium mobility and accumulation along the Rio Paguete, Jackpile Mine in Laguna Pueblo, NM. *Environ. Sci-Proc. Imp.* **2017**, *19*, (4), 605-621.

Appendix C

**Supplementary Information from Chapter 5: Changes on dissolved natural organic matter
resulting from the reaction with U(VI) at acidic and neutral pH**

Additional Materials and Methods.

X-ray Absorption Spectroscopy. X-ray Absorption Spectroscopy measurements were performed at Beamline 7-3 at the Stanford Synchrotron Radiation Laboratory. Measurements were done at the U LIII Edge in fluorescence mode using a 30 element Ge detector and a double crystal Si(220) Monochromator, calibrated at the first inflection point of a Y metal foil absorption at 17038.4 eV. Measurements were performed at room temperature in a He filled acrylic box. No change was observed through consecutive scans, nor changes in the absorption when first and last scans of the series, ruling out beam damage during the measurement. Samples sets were reduced and analyzed using Athena and Artemis¹ with standard methods and benchmarks.

Inductively Coupled Plasma (ICP). Elemental concentrations in supernatant from the filtered acid digestion of the mineralized surface deposits from the Jackpile Mine samples and the batch experiments were measured using a PerkinElmer Optima 5300DV Inductively Coupled Plasma-Optical Emission Spectrometer (ICP-OES). Trace elemental concentrations were measured using a PerkinElmer NexION 300D (Dynamic Reaction Cell) Inductively Coupled Plasma-Mass Spectrometer (ICP-MS). Both ICPs are calibrated with a 5-point calibration standards and QC samples were analyzed periodically to ensure quality results.

Solid Phase Extraction and Recoveries of DOC and soluble U from SPE. Solid phase extraction (SPE) was conducted on the supernatant prior FTICR-MS analysis, as the presence of dissolved salts negatively impacts the ESI-FTMS response. SPE is used to minimize matrix effects and to eliminate any remaining salts in the supernatant, which would otherwise suppress the ion generation within the electrospray and negatively impact the ESI-FTMS response. We conducted SPE on supernatant samples using Varian Mega Bond Elut PPL SPE cartridges filled with 6 g of a functionalized styrene-divinylbenzene polymer (PPL) sorbent. We chose PPL cartridges for our

study because PPL material offered the best properties for the highest DOM recoveries, extracted a more representative proportion of DOM.³² PPL cartridges recovery presents advantageous characteristics for subsequent FT-ICR MS analysis as it minimizes too strong and too weak DOM-sorbent interactions.³³⁻³⁶ The cartridges were conditioned by gravity fed using 3 mL of methanol followed by 3 mL of high purity grade water at the corresponding pH. Then, 10 mL of sample were then added followed by 6 mL of high purity grade water. After the cartridge was dried, 5 mL of methanol was used to elute the DOM to be analyzed by FTICR-MS.

We quantified the DOC and soluble U recovery of the SPE process to have a basis of how representative the purified DOC and U is in relation to the concentrations after the reaction time was completed. We collected three samples during the SPE process: No SPE, Rinse and Recovery. No SPE samples corresponds to the samples before they passed through the SPE cartridges to determine the DOC and U concentrations after the reaction time was completed and before the SPE process. Rinse corresponds to the DOC or U concentrations flushed from the resin by the rinsing solution (10 mL sample + 3 mL high purity grade water). Recovery corresponds to the DOC and U concentrations recovered from the SPE cartridge with 5 mL of MeOH.

Table S1. Batch reactors setup for U-NOM precipitation experiments

ID	Reaction	U (μM)	NOM (mgL^{-1})	HNO_3 (%)	FTICR	XPS	XAS	Purpose
U-NOM	U+ NOM	100	0.2	4%	Yes	Yes	Yes	Reaction to evaluate the effect of U on the organic functional chemistry of DOM at environmentally relevant pH
Control NOM	NOM	100	0.2	0%	Yes	Yes	No	Control to evaluate the effect of pH on the functional chemistry of DOM in the absence of U
Control HNO_3	NOM + HNO_3	100	0.2	4%	Yes	No	No	Control to evaluate the effect of HNO_3 on the functional chemistry of DOM in the absence of U
Control U	U	100	0	4%	No	No	No	Control to evaluate the soluble concentration of U in the absence of NOM.

Table S2. p-values (Shapiro-Wilken Test for Normality)

Normality Test - Soluble U (mM)				Normality Test - DOC (ppm)			
Reactor	pH 2	pH 4	pH 7	Reactor	pH 2	pH 4	pH 7
U	1.00	0.78	0.78	NOM	0.14	0.63	0.25
NOM+U	0.46	0.08	0.19	NOM+U	0.96	0.28	0.96

Table S3. ANOVA Tests

Anova: All pH values - NOM - UNOM (DOC ppm)

Response: pH 2, pH 4 and pH 7

	Df	Sum Sq	Mean Sq	F value	Pr(>F)
NOM	1	30.98	30.98	53.11	3.40E-04
U_NOM	1	3.51	3.51	6.02	0.049
Residuals	6	3.50	0.58		

Anova: All pH values - U – UNOM (Soluble U μM)

Response: pH 2, pH 4 and pH 7

	Df	Sum Sq	Mean Sq	F value	Pr(>F)
U	1	63.58	63.58	78.00	2.50E-07
U_NOM	1	0.19	0.19	0.23	0.64
Residuals	15	12.23	0.82		

Anova: All pH values in U-NOM

Response: pH 2, pH 4 and pH 7

	Df	Sum Sq	Mean Sq	F value	Pr(>F)
COH	1	23.00	23.00	35.05	0.001960 **
COOH	1	11.52	11.52	17.56	0.008572 **
CO	1	0.19	0.19	0.29	0.61
Residuals	5				

Signif. codes: 0 '***' 0.001 '**' 0.01 '*' 0.05 '.' 0.1 ' ' 1

Anova: All pH values in NOM (COOH)

Response: pH 2, pH 4 and pH 7

	Df	Sum Sq	Mean Sq	F value	Pr(>F)
COH	1	0.02	0.02	0.01	0.94322
COOH	1	0.13	0.13	0.03	0.861
CO	1	18.64	18.64	4.85	0.07884 .
Residuals	5				

Signif. codes: 0 '***' 0.001 '**' 0.01 '*' 0.05 '.' 0.1 ' ' 1

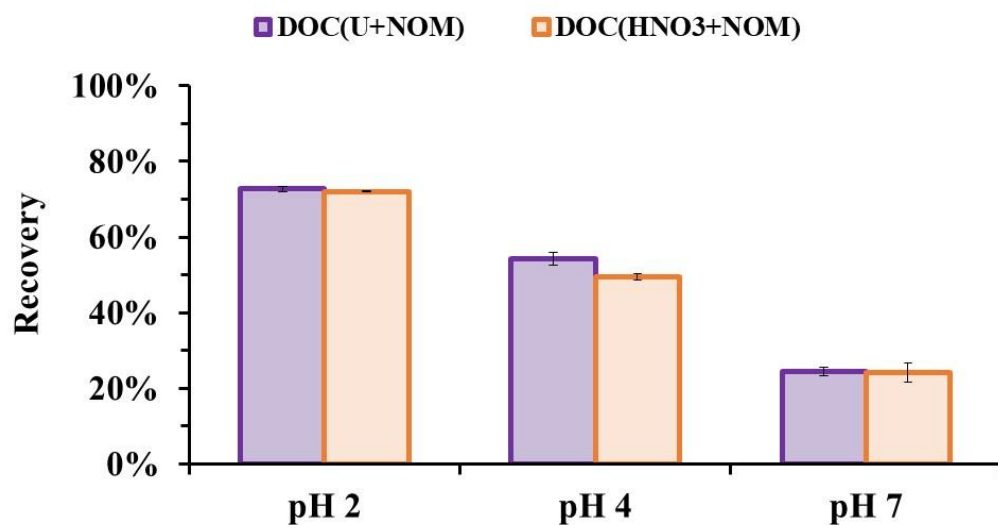


Figure S1. Dissolved organic carbon (DOC) recovery of salt phase extraction (SPE) from batch control reactor HNO₃ (orange) and from batch reactors containing NOM and U in 4% NO₃ (purple)

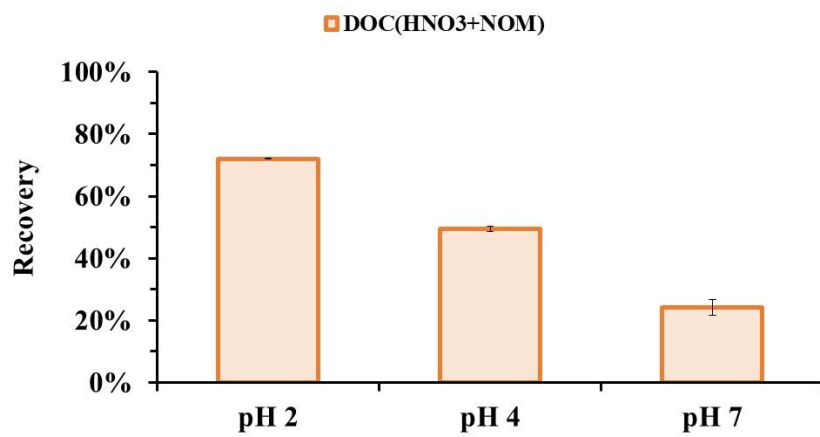


Figure S2. Dissolved organic carbon (DOC) recovery of salt phase extraction (SPE) from batch control reactor HNO₃.

References.

1. Ravel, B.; Newville, M., Athena, Artemis, Hephaestus: data analysis for X-ray absorption spectroscopy using IFEFFIT. *J. of Synchrotron Radiat.* **2005**, *12*, 537-541.